Experimental Gerontology 44 (2009) 161–169

Contents lists available at ScienceDirect

Experimental Gerontology

journal homepage: www.elsevier.com/locate/expgero

Age-related changes in GAD levels in the central auditory system of the rat

Jana Burianova, Ladislav Ouda *, Oliver Profant, Josef Syka

Department of Auditory Neuroscience, Institute of Experimental Medicine, Academy of Sciences of the Czech Republic, Videnska 1083, 142 20 Prague, Czech Republic

ARTICLE INFO

Article history:
Received 27 June 2008
Received in revised form 22 September 2008
Accepted 29 September 2008
Available online 4 October 2008

Keywords:
GAD
GABA
Aging
Inferior colliculus
Auditory cortex
Rat
Western blot

ABSTRACT

Changes in the levels of gamma-aminobutyric acid (GABA) are known to occur in different parts of the brain during aging. In our study we attempted to define the effect that aging has on glutamate decarboxylase (GAD), the key enzyme in the synthesis of GABA, in the central parts of the auditory system. Age-related changes in GAD65 and GAD67 levels were investigated using immunohistochemistry and Western blotting in the inferior colliculus (IC), the auditory cortex (AC) and the visual cortex in Long-Evans rats. The results show that aging is associated with a decrease in the numbers of GAD65- and 67-immunoreactive neurons and the optical density of their somas in both the IC and AC. Western blot analysis revealed a pronounced age-related decline in the levels of GAD65 and 67 proteins in both the IC and AC. For comparison, in the visual cortex the decrease in both proteins was less pronounced than in the IC and AC. A similar pattern of age-related changes was found in Fischer 344 rats, a strain that manifests a rapid loss of hearing function with aging. The observed age-related decline in the levels of GAD65 and 67 may contribute significantly to the deterioration of hearing function that accompanies aging in mammals, including man.

© 2008 Elsevier Inc. All rights reserved.

1. Introduction

Auditory function in mammals is known to be significantly affected by aging, ultimately resulting in presbycusis (for review see Syka, 2002; Gates and Mills, 2005; Ohlemiller and Frisina, 2008). In the human population, a loss of speech understanding with aging constitutes an important health and social impairment (Frisina and Frisina, 1997; Mazelová et al., 2003; Gordon-Salant et al., 2007). Pathological changes in presbycusis occur both in the inner ear and in the central auditory system. The peripheral component of presbycusis, which comprises mainly alterations of the inner and outer hair cells and/or stria vascularis, is relatively well understood (Schuknecht and Gacek, 1993; Parham, 1997; Spongr et al., 1997; Harding et al., 2005; Buckiova et al., 2007). The central component of presbycusis is thought to be associated with age-related alterations in the processing of the temporal parameters of complex acoustical stimuli occurring within the central auditory system. Inhibitory systems in the brain are apparently strongly involved in the temporal processing of acoustical stimuli with the aim of sharpening responses to rapid complex sounds (Walton et al., 1997; Strouse et al., 1998; Krishna and Semple, 2000; Liang et al., 2002; Tremblay et al., 2002; Ostroff et al., 2003; Mazelová et al., 2003). Since gamma-aminobutyric acid (GABA) is a major inhibitory neurotransmitter in the central auditory system (Markram et al., 2004), a decrease in GABA inhibition may significantly contribute to hearing deterioration with aging.

Recently, growing evidence has accumulated about the role of GABA-expressing neurons in inhibitory networks in different parts of the brain (Caspary et al., 1995; Gupta et al., 2000; Buzsáki et al., 2007). The distribution of GABA-immunoreactive (-ir) neurons and inputs in the auditory cortex has been described in detail for cats and monkeys and implies that GABA-ir neurons are present in the AC in relatively large numbers, approximately 20–25% of the total population of neurons (Hendry et al., 1987; Prieto et al., 1994a,b). In the IC, a similar portion, 20–30% of the total number of neurons, was found to be GABA-ir in cats and rats (Oliver et al., 1994; Merchán et al., 2005). GABA is synthesized by the decarboxylation of glutamate, and the reaction is catalysed by the key rate-limiting enzyme glutamate decarboxylase (GAD). In the mammalian brain, two GAD isoforms of 65,000 and 67,000 molecular weight (GAD 65 and GAD 67) are present (Erlander et al., 1991). Most GABA-expressing neurons contain both isoforms, with GAD 65 being more prevalent in axonal terminals and membranes preferentially synthesizing GABA for vesicular release, while GAD 67 is distributed throughout the neuron including the soma, preferentially synthesizing non-vesicular cytoplasmic GABA (Erlander and Tobin, 1991; Feldblum et al., 1993, 1995; Esclapez et al., 1994; Hendrickson et al., 1994). The two GAD isoforms might be differently involved in the spatial and temporal processing and/or coding of information by GABA-expressing neurons (for review see Soghomonian and Martin, 1998; Wei and Wu, 2008).

* Corresponding author. Tel.: +420 241062690; fax: +420 241062787.
E-mail address: ouda@biomed.cas.cz (L. Ouda).

0531-5565/$ - see front matter © 2008 Elsevier Inc. All rights reserved.
doi:10.1016/j.exger.2008.09.012

Several lines of evidence suggest a decreasing function of GABA-mediated inhibition within the central auditory pathway in aged animals. For example, single unit recordings illustrate the presence of a less precise processing of complex sounds and extended excitatory areas in the IC (Palombi and Caspary, 1996; Walton et al., 1998, 2002; Simon et al., 2004). Age-related alterations in the fine-tuned receptive fields and a relative increase in poorly tuned receptive fields could influence the processing of sounds in the central auditory system (Turner et al., 2005a,b). The results of measurements of GABA or GAD levels and GABA receptor subunit levels and binding intensity correspond with the electrophysiological reports. In Fischer 344 rats, a significant age-related decrease in the number of GABA immunoreactive cells was found in the central nucleus of the IC (CIC) combined with a decrease in the enzymatic activity of GAD and in the release of GABA (Caspary et al., 1990, 1995; Raza et al., 1994). In addition, a decline in the number of GABA-ergic synaptic terminals and synapses of GABA-ir neurons was observed in the CIC with no detectable neuronal losses (Helfert et al., 1999). Also GABA-A and GABA-B receptor binding intensity was reported to decline, and the protein levels of the receptor subunits were found to be altered during aging in the IC of Sprague–Dawley and Fischer 344 rats (Gutiérrez et al., 1994; Milbrandt et al., 1994, 1997; Caspary et al., 1999; Schmidt et al., 2008). Decreases in the levels of GAD65 and GAD67 mRNAs and in the optical density of GAD67-immunoreactive cells were observed in the auditory cortex of old Fischer 344/Brown Norway rat (Ling et al., 2005).

However, it is not well known whether the age-related decline in the GABA system is activity-dependent and primarily follows the deterioration of the sensory inputs with aging or whether it rather results from changes occurring within the central auditory system with aging (for review see Caspary et al., 2008). In addition, no clear evidence of inter-strain differences in these changes has been reported, in contrast to the findings in calcium binding proteins that are well known to colocalize in neurons with GABA (Kosaka et al., 1987; Kawaguchi and Kubota, 1998). In this case, a significant strain-specificity in their age-related expression was shown for calretinin and parvalbumin (Zettel et al., 1997, 2001; Ouda et al., 2008).

In our study we attempted to evaluate the age-related changes in both GAD isoforms in the central auditory system in Long-Evans rats, a strain with a very limited age-related loss of hearing function (Syka et al., 1996; Popelar et al., 2006). Immunohistochemistry and Western blot protein analysis were used to compare GAD 65 and 67 expression in the inferior colliculus (IC) and auditory cortex (AC) in young and old rats. In addition, the same analysis was also performed on a representative sample of Fischer 344 rats, a strain with pronounced hearing deterioration with aging, with the aim of studying possible inter-strain differences.

2. Materials and methods

2.1. Animals

Thirty rats, strain Long-Evans (15 young animals 3–5 months old and 15 aged animals 30–35 months old), and 12 rats of the strain Fischer 344 (7 young animals 3–5 months old and 5 aged animals 24 months old) were used in the experiments. The Long-Evans rats were obtained from a local facility and, starting at 2 months of age, were reared and aged (aging group) in-house, under known rearing conditions and with a known health history. Fischer 344 rats were purchased at 2 months of age from Charles River Deutschland (Sulzfeld, Germany) and then reared in-house under the same conditions. No signs of middle ear infection were present in any animal during their stay in the animal facility. The care and use of the animals and all experimental procedures were performed in compliance with the guidelines of the Ethical Committee, Institute of Experimental Medicine, Academy of Sciences of the Czech Republic, and the Declaration of Helsinki.

2.2. GAD67 immunohistochemistry

Long-Evans rats, 3–5 ($n = 5$) and 30–35 ($n = 5$) months old, and Fischer 344 rats, 3–5 ($n = 5$) and 24 ($n = 3$) months old, were placed under deep anesthesia (ketamine 35 mg/kg + xylazine 6 mg/kg, i.m.) then transcardially perfused with saline followed by 4% paraformaldehyde fixative in 0.1 M phosphate buffer (pH 7.4). Brains were removed within 15 min of perfusion, postfixed 1 h at 4 °C (same fixative) and then cryoprotected with 30% sucrose in phosphate buffer overnight. Coronal sections (40 μm thick) were cut with a freezing microtome.

Free-floating sections were preblocked in normal serum for 1 h and then incubated at 4 °C with anti-GAD67 (mouse monoclonal, Chemicon, 1:2000) diluted in PBS containing 1% normal serum. After 24 h, sections were incubated with a biotinylated secondary antibody (Vector, 1:200) for 45 min and then with peroxidase-labeled ABC reagent (Vector). The antibody labeling was visualized by incubating the sections for 3 min in 0.05% diaminobenzidine (DAB) with 0.01% hydrogen peroxide. Sections were mounted on slides, dehydrated and coverslipped.

2.3. GAD65 immunohistochemistry

Long-Evans rats, 3–5 ($n = 4$) and 30–35 ($n = 4$) months old, were subjected to the same procedure leading to the preparation of histological sections as in the case of rats for GAD 67 staining.

Free-floating sections were preblocked in normal serum for 1 h and then incubated at 4 °C with anti-GAD65 (rabbit polyclonal, Chemicon, 1:750) diluted in PBS containing 1% normal serum. After 72 h, sections were incubated with a biotinylated secondary antibody (Biosource, 1:200) for 1 h and then with peroxidase-labeled ABC reagent (Vector). The antibody labeling was visualized by incubating the sections for 3 min in 0.05% diaminobenzidine (DAB) with 0.01% hydrogen peroxide. Sections were mounted on slides, dehydrated and coverslipped.

2.4. Western blot protein analysis

Long-Evans rats, 3–5 ($n = 6$) and 30–35 ($n = 6$) months old, and Fischer 344 rats, 4 ($n = 2$) and 24 ($n = 2$) months old, were used in the analysis. Anesthetized rats (ketamine 35 mg/kg + xylazine 6 mg/kg, i.m) were decapitated, their brains quickly extracted and rinsed in ice-cold physiological solution, and the inferior colliculi (ICs) and auditory (ACs) and visual cortices (VCs) were rapidly removed bilaterally. The samples included the whole IC, the Te1 + Te3 (Zilles, 1985) areas of the AC and the V1 + V2 areas of the VC (Paxinos and Watson, 1998). All samples were immediately put into dry ice after extraction and stored frozen at −80 °C until processed.

For the analysis, ICs, ACs and VCs were homogenized by a Potter–Elvehjem homogenizer in 0.05 M Tris–NaCl (pH 7.4) buffer with protease inhibitors (Sigma). The homogenate was centrifuged at 10,000g for 10 min at 4 °C. To ensure similar protein loading, the total protein concentration of these extracts was determined by using the Bradford method with BSA as the standard. Samples (cytosolic fraction) were incubated in boiling water for 10 min at 80 °C in sodium dodecyl sulfate–polyacrylamide gel electrophoresis buffer containing 10% glycerol, 2% SDS, 0.05% bromphenol blue and 4 M dithiotreitol. Samples were then subjected to Tris/Tricine/SDS–PAGE on a 3% bis-acrylamide polyacrylamide gel at 30 mA/gel for 150 min on a Mini-Protean II apparatus (Bio-Rad). After electrophoresis, the resolved proteins were transferred (Bio-Rad Mini Protean II transblot apparatus at 350 mA for 60 min at 4 °C in 25 mM

Tris, 192 mM glycine, 20% methanol, 0.1% SDS) to a nitrocellulose membrane (Amersham, Biosciences). Membranes were incubated in 5% non-fat dry milk in 10% Tris-buffered saline with 0.05% Tween 20 (TBST) for 60 min at room temperature to block non-specific protein binding. After being washed in TBST buffer (three times quickly, 3 × 5 min each), the membranes were probed with GAD 67-specific (mouse monoclonal, Chemicon, 1:5000 in TBST), GAD 65-specific (rabbit polyclonal, Chemicon, 1:1200 in TBST) or actin-specific (mouse monoclonal, Chemicon, 1:10,000 in TBST) primary antisera overnight at 4 °C. The membranes were washed again and incubated with goat anti-mouse IgG or anti-rabbit IgG antibody conjugated with horse radish peroxidase (Upstate, 1:7500; Chemicon, 1:3333 in TBST) for 2 h at room temperature. Before enhanced chemiluminescence (ECL), the membranes were washed as described above and stored in TBST for at least 2 h. For ECL, substrates A (Luminol solution) and B (H_2O_2 solution) were prepared, mixed 40:1 (Amersham Biosciences) just before use, and poured on the membranes. The specific signals were detected on autoradiographic film (Kodak MXB). Films were developed at room temperature, stopped, fixed, washed under running cold water and air-dried. Scanning (Canon CanoScan 8400F) and ImageQuant software were used for quantifying the relative abundance of GAD and actin in individual samples. The amount of protein applied to the gel varied for each isoform and fraction to achieve linearity with the intensity × area (volume) of the band on the Western blot. To ensure the specificity of GAD67, GAD65 and actin immunoreactive proteins, prestained molecular weight protein standards were used (Invitrogen). The levels of GAD65 and GAD67 were calculated as the ratio of the optical density of the antibody of interest to the optical density of the antibody directed against β-actin.

2.5. Immunohistochemistry – stereological quantification

GAD65 and 67 immunoreactivity was examined in all sections containing the inferior colliculus, auditory and visual cortices, delineated according to anatomical atlases (Zilles, 1985; Paxinos and Watson, 1998) and with the help of Nissl-stained sections (topographical borders of cortical areas) (Fig. 1A and B). For the IC, sections were sampled from bregma −8.0 to −9.2 mm. Sections containing the auditory cortex were sampled from bregma −4.2 to −6.0 mm (Zilles, 1985), identified by measuring 2.0–2.5 mm from the rhinal fissure for Te3 and 3.5–4.0 mm for Te1. As an auxiliary criterion, the line going through the dorsal margin of the diencephalon indicated the control dorsal (upper) border of the auditory cortex. For the visual cortex (V1, V2 – Paxinos and Watson, 1998), sections were sampled from bregma −5.0 to −8.0 mm. To estimate the total number of GAD65 and 67-ir neurons, an unbiased stereological method, the optical fractionator, was used (West et al., 1991; for review see Mayhew and Gunderesen, 1996). The optical fractionator method is unaffected by tissue shrinkage, and therefore it was not necessary to measure this variable. Measurements were determined using bright-field microscopy (Leica DMRXA microscope) connected to a video camera, which transmitted the microscopic image to a monitor (Optronics, 1600 × 1200 px) coupled with Neurolucida software (MicroBrightField). Two sets of motors were connected to the microscope to move the section a known distance in the *x*- and *y*-directions. The *z*-direction was measured using a microcator. A 10× objective lens was used to delineate the regions of interest and the starting position of the counting frame. We adapted the Neurolucida-generated grid superimposed on the screen with the use of a random number table to establish the random starting position of the counting frame in the area of interest.

A 100× oil-immersion objective was used and the appropriate counting frame superimposed on the screen. The counting frames used to obtain the sampling had the same size (3880 μm^2). The upper and lower surfaces of the sections were examined to determine if the margins of the tissue sections were depleted of neuronal nuclei, as suggested by Andersen and Gundersen (1999). The height of the optical dissector was constant at 5 μm, and the first and last 5 μm of the section thickness was omitted from the analysis. Approximately 200 neurons per animal were counted in each examined structure. Each neuron in the counting frame was counted when its distinct nucleus came to maximum focus. At maximum focus, the cell body was outlined by a cursor on the computer screen, and the morphological parameters and optical density were measured automatically using Neurolucida software.

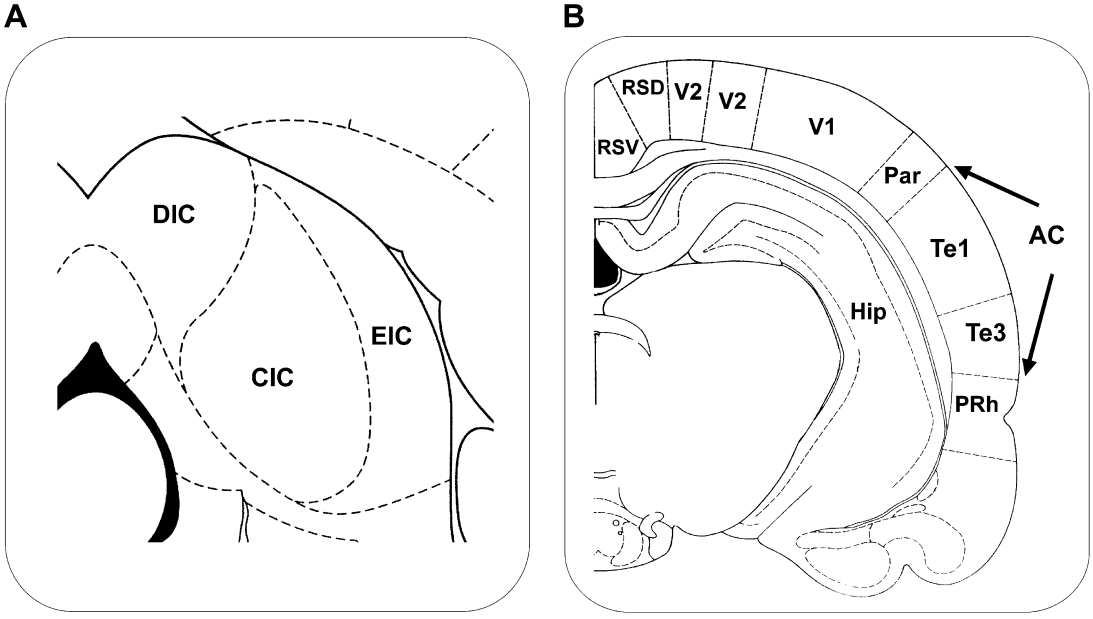

Fig. 1. Topographical overview of the IC (A), AC and VC (B) and their subdivisions. Drawings adapted from Paxinos and Watson (1998) and Zilles (1985); (A) bregma −8.8 mm; (B) bregma −5.0 mm. Par, parietal cortex; Hip, hippocampus; PRh, perirhinal cortex; V1,2, visual cortex 1,2; RSD, RSV, retrosplenial cortex, dorsal and ventral.

Only positive somas that exceeded 5 μm in diameter and with a distinct nucleus were counted and used for analysis.

Variation in the background immunostaining affects the real values of the optical density of the neuronal soma. In studies of aging, there are not specific "indifferent reference structures" available in the brain for normalization, hence we calculated the normalized value of the optical density in each section as the ratio between the average optical density of the analyzed GAD-ir neurons in the section and the average optical density of a corresponding number of immunonegative cells in the same section (compare Ling et al., 2005). In most cases the immunopositivity of the neurons was explicit; in a few disputable cases, a selected neuron was omitted from the analysis as "non-GAD-ir" unless the measured optical density of its soma was higher than double the average optical density of immunonegative cells in the same section.

2.6. Statistical analysis

The results of the statistical analysis were expressed as means ± S.E.M. The significance of the differences between young and old groups of rats was assessed by the non-parametric two-tailed Mann–Whitney test with the use of GraphPad Prisma software (version 4.0) for both immunohistochemistry and Western blots. The significance of differences in Western blot protein analysis among protein levels and among the magnitudes of changes in different brain structures (IC vs. AC vs. VC) in young and in old rats was assessed by a one-way ANOVA test and Bonferroni's multiple comparison test with the use of GraphPad Prisma software (version 4.0). P values of 0.05 or less were considered statistically significant. For each statistical test, each examined animal was represented by one number to ensure the maximal independence of the data entering the tests.

3. Results

3.1. GAD65 and 67 changes with aging in the Long-Evans strain

3.1.1. Inferior colliculus

GAD65 and 67-ir neurons were distributed in both young and old animals throughout all three subdivisions of the IC. In the central nucleus of the IC, cell bodies of variable sizes and shapes prevailed, with a large variation in the intensity of immunostaining. The majority of GAD-ir neurons in the external cortex of the IC (EIC) were large spindle and multipolar cells or smaller oval neurons, in both the 2nd and 3rd layers of the EIC (for details see Oliver et al., 1994). Only a few small immunoreactive neurons were present in the dorsal cortex of the IC (Fig. 2A and B).

Significant age-related changes in GAD immunoreactivity were found in the CIC and EIC (Fig. 3A–D). In the CIC, the optical density of GAD65 and 67-ir neuronal somas decreased by 23% ($P = 0.028$, $U = 0$) and 25% ($P = 0.008$, $U = 0$), respectively. The number of GAD65 and 67-ir cells decreased slightly by 17% ($P = 0.028$, $U = 0$) and 9% (N.S.), respectively. In the EIC only in GAD67-ir somas the optical density decreased significantly by 14% ($P = 0.032$, $U = 2$), while the number of GAD65 and 67-ir did not differ between old and young animals. No significant age-related changes in the volume of GAD-ir somas were found in the IC with aging.

Western blot analysis demonstrated a significant age-related decline in the levels of GAD65 and GAD67 proteins in the whole IC of old rats in comparison with young animals of 51% and 49%, respectively (both $P = 0.002$, $U = 0$) (Fig. 4). The analyzed samples included all three subdivisions of the IC. A remarkable finding of the additional statistical analysis, in both young and old animals, the levels of GAD65 and GAD67 proteins in the IC were almost three times higher compared to the levels in both the auditory and visual cortices (both proteins $P < 0.001$, Bonferroni's multiple comparison test).

3.1.2. Auditory cortex

Independently of age, GAD65 and 67-ir cells were scattered throughout all layers, with slightly higher numbers observed in the superficial cortical layers (I–IV) than in the deeper layers (V–VI) (for description see Prieto et al., 1994a,b). The neuropil staining followed the same pattern with greater positivity in the superficial layers (II–IV) (Fig. 2C and D).

The results of immunohistochemical staining indicated a significant decrease in the optical density of GAD65 and 67-ir somas in old animals of 21% ($P = 0.028$, $U = 0$) and 22% ($P = 0.016$, $U = 1$), respectively (Fig. 3A–D). The number of GAD65-ir neurons did not change in old rats in comparison with young animals (only a slight decrease of 7%, N.S.), while the number of GAD67-ir neurons decreased more markedly by 13% ($P = 0.032$, $U = 2$). No layer-specificity or inter-areal differences (Te1 vs. Te3) of these changes were observed; similarly, the average volume of GAD-ir somas did not change with aging.

Western blot protein analysis revealed a significant age-related decrease in the levels of GAD65 and GAD67 of 43% and 52%, respectively (both $P = 0.002$, $U = 0$) (Fig. 4). The analyzed samples included the Te1 + Te3 areas. Differences in GAD65 and 67 protein levels between the auditory and visual cortices were non-significant in young animals. In old rats, GAD67 protein levels in the auditory cortex were lower than in the visual cortex ($P < 0.05$, Bonferroni's multiple comparison test), whereas for GAD65 protein levels, the difference between the auditory and visual cortices was still non-significant. The declines found in all three examined brain regions are apparent on representative blots shown in Fig. 5.

3.1.3. Visual cortex

GAD65 and 67 immunoreactive neurons were present in all cortical layers of the visual cortex; their distribution and neuropil staining followed a similar pattern as in the auditory cortex.

The optical density was found to decrease by 11% for GAD65-ir somas (N.S.) and 18% for GAD67-ir somas ($P = 0.016$, $U = 1.5$) (Fig. 3A–D). In contrast, the numbers of GAD65 and 67-ir neurons did not change with aging (the decrease was in the range of 5%, N.S). As in the AC, no significant changes in the average volumes of immunoreactive somas or layer-specificity were found with aging.

In Western blot analysis, decreases in the levels of GAD65 and GAD67 proteins were found in the visual cortex as well: a decrease of 22% for GAD65 ($P = 0.041$, $U = 5$) and 20% for GAD67 ($P = 0.028$, $U = 2$) (Fig. 4). However, the decrease was less apparent compared to both the auditory cortex and the IC ($P < 0.01$, Bonferroni's multiple comparison test), while a comparison between decreases in the IC and AC showed no difference. These results held true for both GAD65 and GAD67.

3.2. GAD65 and 67 changes with aging in the Fischer 344 strain

In principle, the age-related changes in Fischer 344 rats followed the same pattern as the age-related changes in the Long-Evans animals; however, the relatively low number of animals of this strain used in our study precluded a detailed statistical evaluation of the results. Using immunohistochemistry, only differences in GAD67 staining were studied: the optical density of GAD67-ir neuronal somas decreased by 21% ($P = 0.035$, $U = 0$), 13%, 14% and 15% in the CIC, EIC, AC and VC, respectively, while the number of GAD67-ir cells decreased by 6%, 10%, 10% and 6% in the same structures (Fig. 3E–F).

Both GAD65 and GAD67 proteins were examined by Western blot protein analysis. In the IC, GAD65 protein levels decreased

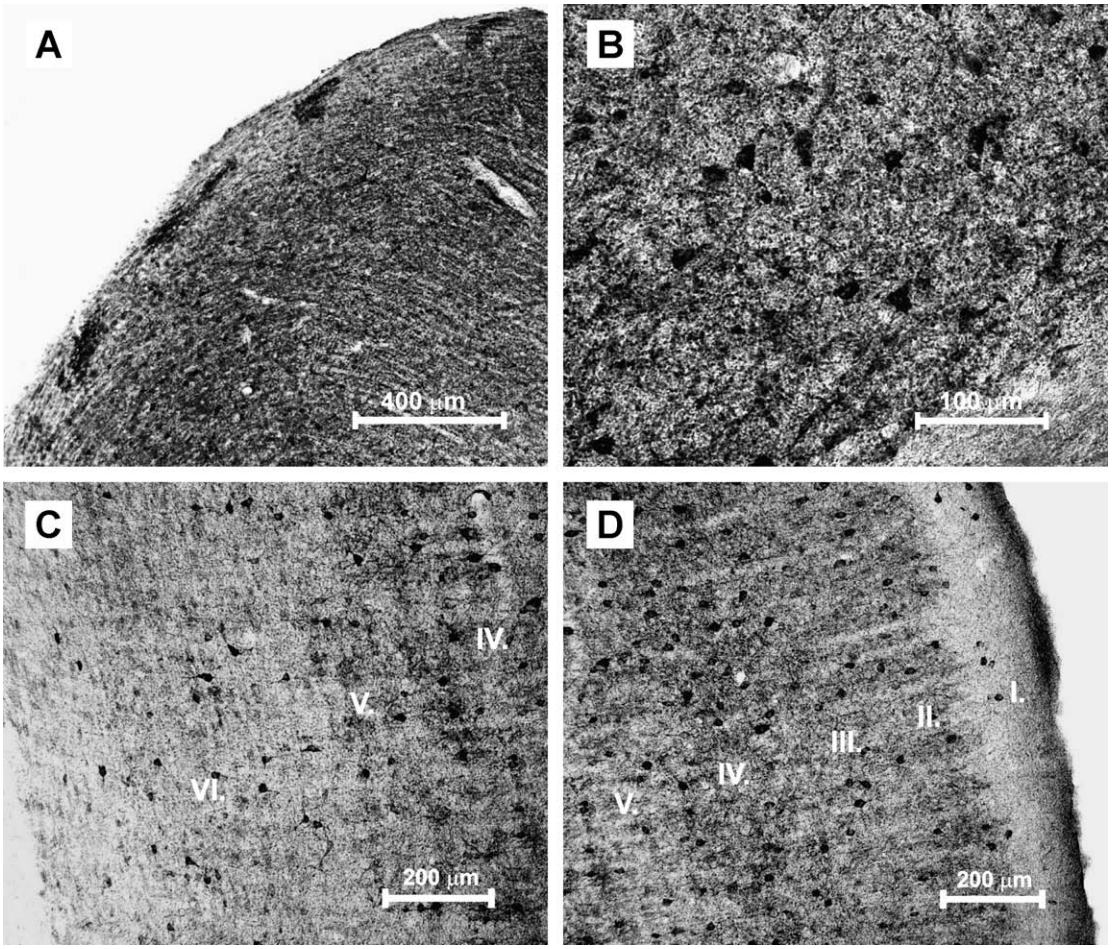

Fig. 2. Illustration of GAD67 immunoreactivity in the EIC (A), CIC (B) and in the deep and superficial layers of the AC (C and D) of young Long-Evans rats.

by 46% and GAD67 levels by 44% (Fig. 4). The decline of GAD65 protein levels in the AC was 34% and that of GAD67 was 49%; in the VC decreases of 19% in GAD65 protein levels and 20% in GAD67 levels were observed. In young and old Fischer 344 animals, the relative ratios between GAD65 and GAD67 protein levels in the IC, AC and VC followed a very similar pattern as that seen in young and old Long-Evans rats. However, due to the limited number of animals, the data did not show statistically significant differences ($P < 0.05$ only when GAD65 or 67 protein levels in the IC were compared with the levels in the AC and VC cortices, Bonferroni's test).

4. Discussion

Our results demonstrate significant age-related changes in GAD65 and 67 immunoreactivity in the inferior colliculus and auditory cortex of the rat auditory system, which comprise decreases in the number and optical density of GAD65 and 67-ir neuronal somas and a decline in the levels of GAD65 and 67 proteins. The obtained data demonstrate a rather uniform character of the changes. First, the age-related changes in both GAD65 and 67 proteins shared very similar patterns. Second, the results obtained with immunohistochemical techniques were in good agreement with the results acquired with Western blotting. Third, similar tendencies in the changes were present in both the IC and AC. In summary, the decrease in GAD expression with aging occurs similarly at both the subcortical and cortical levels of the rat central auditory system and involves both GAD isoforms.

The overall reductions in the levels of GAD65 and 67 proteins reported in the present work are in accordance with previous publications that reported an age-related decline in GABA and GAD levels in the IC and AC. In the IC, the number of GABA immunoreactive cells was described to be decreased in the central nucleus of the IC (CIC) in old rats. This decrease was associated with a decrease in enzymatic activity, the levels of GABA and the release of GABA (Caspary et al., 1990, 1995; Raza et al., 1994; Gutiérrez et al., 1994). No changes in the optical density of GABA or GAD stained cells in the IC with aging have yet been reported, but such a decline, comparable to our results, was observed in the auditory cortex of old Fischer 344/Brown Norway F1 hybrid rats (Ling et al., 2005). In addition, the authors also reported a decline in GAD65 and 67 mRNA labeling in the auditory cortex, consistent with the decreased optical density of GAD67-ir neurons. No cortical layer specificity for the reported changes was found in their study, which is in agreement with our results. A decline in the optical density of neuronal somas may reflect either a decrease in the expression of the protein or changes in the volume of the cell (for example, Krzywkowski et al., 1995). Since there were no significant changes in the average volume of GAD-ir somas in the present work, the results support the diminished expression of the proteins in this case. This is in agreement with the decreased levels of GAD proteins found in our Western blotting analysis.

The observed decreased number of GAD-ir (GAD65 and GAD67) neurons in the IC and AC in the present paper cannot be explained simply by a non-selective neuronal loss because in our previous experiments, we did not find any reduction in the total number

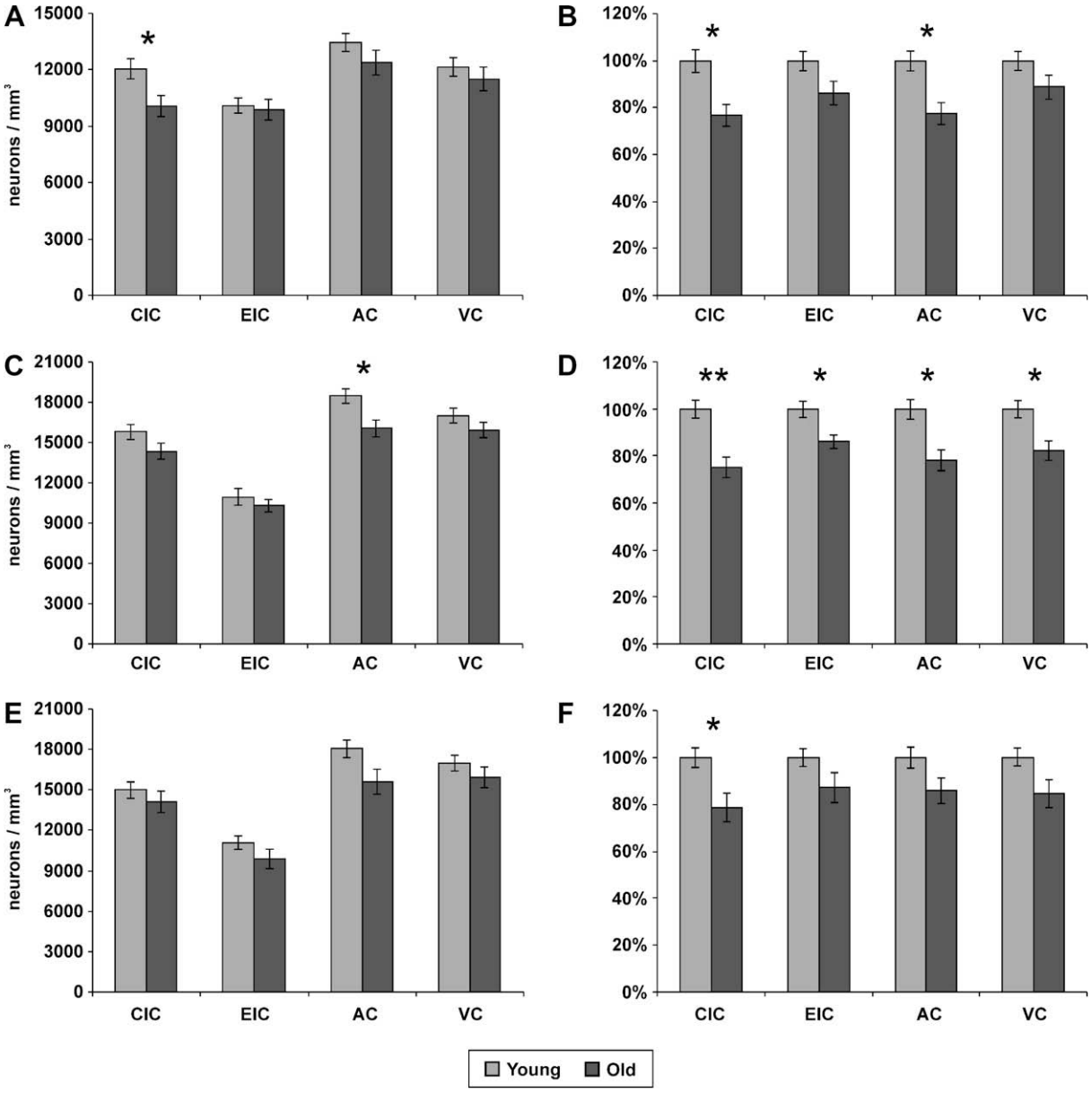

Fig. 3. Results of the quantitative evaluation of GAD65 and 67 immunoreactivity in Long-Evans and Fischer 344 rats. Light columns represent young animals, dark columns old animals. The error bars represent S.E.M. The optical density of neuronal somas is expressed as 100% for young animals. (A and B) Number and optical density of GAD65-immunoreactive neurons in the CIC, EIC, AC and VC of young ($n = 4$) and old ($n = 4$) Long-Evans rats. (C and D) Number and optical density of GAD67-immunoreactive neurons in the CIC, EIC, AC and VC of young ($n = 5$) and old ($n = 5$) Long-Evans rats. (E and F) Number and optical density of GAD67-immunoreactive neurons in the CIC, EIC, AC and VC of young ($n = 5$) and old ($n = 3$) Fischer 344 rats ($^{*}P < 0.05$, $^{**}P < 0.01$).

of neurons in old Long-Evans and Fischer 344 rats on Nissl-stained sections (Ouda et al., 2008). This finding is in agreement with the data of other authors, who reported no significant changes accompanying aging in the total number of neurons in the inferior colliculus, hippocampus or cortex in rats (Helfert et al., 1999; Poe et al., 2001; Merrill et al., 2001; Stanley and Shetty, 2004). In our experiments, the decrease in the optical density of GAD-immunoreactive somas rather suggests the diminished expression of the protein, beyond the level detectable by immunohistochemical methods, as the major reason for the reduced number of GAD-ir neurons.

An interesting finding in our experiments is the striking difference in the regional levels of GAD found with Western blotting. The approximately 3-fold higher levels of GAD65 and 67 in the IC in comparison with the auditory and visual cortices are in good agreement with previously reported ratios of both isoform levels in the midbrain and thalamus on one side and the neocortex on the other side (Sheikh et al., 1999). The functional implication of these differences remains to be determined. In our immunohistochemical analysis, no significant indication of striking differences between the IC and cortex was observed. Nevertheless, our immunohistochemical method was not designed to evaluate dendritic branching or GAD-ir puncta, which could contain a significant proportion of GAD. The fundamental role of inhibition in the IC is well known, including the strong representation of GABA terminals, which also implies the presence of high GAD levels in the IC (Gerken, 1996; Pollak et al., 2002; Frisina, 2001; Batra and Fitzpatrick, 2002; Merchán et al., 2005).

In addition to the Long-Evans strain, a relatively small but representative sample of young and old Fischer 344 rats was exam-

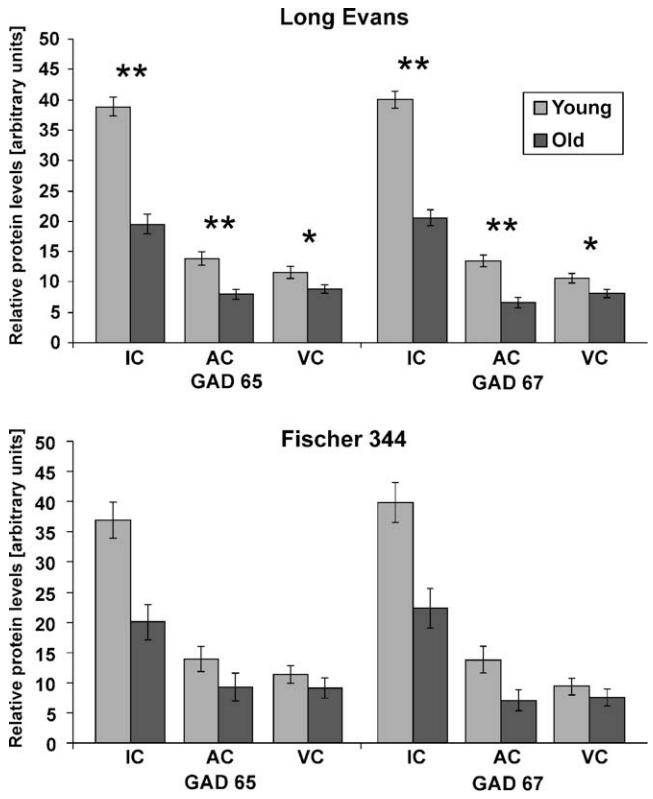

Fig. 4. Results of Western blot GAD65 and GAD67 protein analysis in young (6 for Long-Evans and 2 for Fischer 344) and old (6 for Long-Evans and 2 for Fischer 344) animals of both examined strains. The error bars represent S.E.M. Arbitrary units were calculated as the ratio of the optical density of the examined protein and actin (in scanned films analyzed using ImageQuant software) ($^{*}P < 0.05$, $^{**}P < 0.01$).

ined in the present work. Long-Evans and Fischer 344 represent two rat strains with a variety of morphological, physiological and behavioral differences. For example, similarly to other inbred strains (Wistar, Sprague–Dawley and Dark-Agouti), Fischer 344 rats display large cognitive deficits in different tests of spatial memory in contrast to wild rats and Long-Evans rats (Harker and Whishaw, 2002). A faster and more pronounced deterioration of hearing function with aging was found in the Fischer 344 strain in comparison with Long-Evans rats, resulting in larger hearing threshold shifts, a diminution of distortion product otoacoustic emissions and a decrease in middle-ear compliance (Popelar et al., 2003, 2006). In addition, the deterioration of the stria vascularis and ligamentum spirale was observed in aged Fischer 344 rats (Buckiova et al., 2006, 2007). Age-related sensory deficits in this strain are also present in visual function due to retinal degeneration (Di Loreto et al., 1994). In spite of this, we observed very similar age-related changes in GAD65 and 67 protein levels and in the immunohistochemical results in Fischer 344 rats and Long-Evans rats. Taking into account the similar effects of aging on GAD levels described in the Fischer 344/Brown Norway hybrid rats (Ling et al., 2005), it might be suggested that age-related changes in GAD proteins in the IC and AC share a uniform tendency, which is not dependent on the rat strain. A similar situation exists in another species, in mice: hearing function in the CBA/CaJ strain of mice deteriorates very slowly as in the Long-Evans strain of rats, whereas the C57BL/6J strain is known to undergo rapid deterioration with early deafness (Parham, 1997; Spongr et al., 1997). In spite of these differences in age-related defects of auditory function, which are mostly caused by pathologies in the inner ear, significant age-related alterations of the inhibitory function in the central auditory system were reported in both strains of mice (Walton et al., 1998, 2002; Felix and Portfors, 2007). Therefore, we may tentatively suggest that the age-related decline in GAD expression in the IC and AC demonstrated in our experiments does not depend primarily on peripheral deafferentation but is, at least partially, of central origin.

The present results are to some extent different from our previous findings concerning age-related changes in parvalbumin immunoreactivity in the IC and AC of Long-Evans and Fischer 344 rats (Ouda et al., 2008). Specifically, there was no reduction in parvalbumin immunoreactivity in old Long-Evans rats, while there was a pronounced decline in the number of parvalbumin-ir cells in the AC of old Fischer 344 rats. Since parvalbumin-expressing cells in the central nervous system form a subpopulation of GABA-expressing neurons (Kosaka et al., 1987; Freund and Buzsaki, 1996; Kawaguchi and Kubota, 1998), it could be expected that the changes in parvalbumin and GAD expression with aging would have a more similar character. However, different age-related changes in the immunoreactivity of parvalbumin and the expression of GABA (GAD) were reported, for example, in the rat septum, hippocampus and sensorimotor cortex (Krzywkowski et al., 1995; Vela et al., 2003; Potier et al., 2006; Shi et al., 2006).

Age-related alteration in GABA inhibition was a feature also present in the visual cortex. Our observation of decreased GAD65 and 67 immunoreactivity and protein levels in the visual cortex is in agreement with Hua et al. (2008), who found a reduction in the number of GABA-ir neurons in the primary visual cortex of the cat with aging while no changes in the total number of neurons were observed. In addition, a decreased function of the GABA sys-

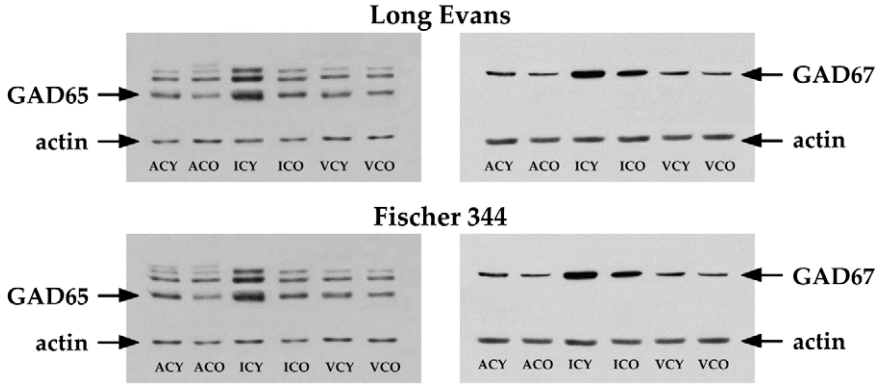

Fig. 5. Representative films of the Western blot analysis of GAD 65 (left panel) and 67 (right panels) protein isoforms developed with the enhanced luminescence method. Actin, used as an internal control, was detected at a position corresponding to a molecular weight of 42 kDa. Note the partial non-specific labeling on the left panel (non-labeled upper stripes) using polyclonal antibody (for GAD 65). The abbreviations are: AC, auditory cortex; IC, inferior colliculus; VC, visual cortex; Y, young and O, old animals.

tem was reported in the primary visual cortex of aged monkeys (Schmolesky et al., 2000; Leventhal et al., 2003). Western blot protein analysis in our experiments showed a statistically less pronounced decline in GAD65 and GAD67 levels with aging in the VC compared to the AC, which may signal different GABA-related aging processes in the two cortical sensory areas. A decreased function of the GABA inhibitory system with aging was also documented in the rat hippocampus (Shetty and Turner, 1998; Stanley and Shetty, 2004; Shi et al., 2004; Ling et al., 2005), while no reduction in the number of GABA neurons or GAD immunoreactivity was found in the septum, sensorimotor cortex or parietal cortex (Krzywkowski et al., 1995; Poe et al., 2001; Ling et al., 2005; Shi et al., 2006). Therefore, it is evident that aging is not necessarily accompanied with a homogenous decline of GABA levels in all brain regions.

The alteration of GABA-mediated inhibition in the central auditory pathway may have functional implications. The decreased inhibition may result in a broadening of the excitatory areas and thus in the poorer tuning of the neuronal receptive fields, which is in agreement with existing electrophysiological reports (Palombi and Caspary, 1996; Walton et al., 2002; Turner et al., 2005a,b). The reduction of fine-tuned receptive fields results in poorer discrimination of the temporal parameters of sounds (Narayan et al., 2005). The reduced temporal acuity limits the gap detection thresholds and gap duration difference limen, which are believed to be essential for the successful processing of complex sounds including language (Gordon-Salant and Fitzgibbons, 1993; Grose et al., 2006; Gordon-Salant et al., 2007). With aging, the gap detection thresholds significantly increase and gap duration difference limen worsens (Rybalko et al., 2008) These data support the conclusion that the age-related decline of GABA levels could contribute significantly to the deterioration of hearing function associated with aging in mammals, including presbycusis in man.

Acknowledgements

The authors wish to thank Mrs. J. Janouskova and Mr. J. Setnicka for their technical assistance. This study was supported by the Grant Agency of the Czech Republic (309/07/1336), by the Grant Agency of the Ministry of Health of the Czech Republic (NR8113-4), and by AV0Z50390512 and LC 554.

References

Andersen, B.B., Gundersen, H.J.G., 1999. Pronounced loss of cell nuclei and anisotropic deformation of thick sections. J. Microsc. 196, 69–73.
Batra, R., Fitzpatrick, D.C., 2002. Monaural and binaural processing in the ventral nucleus of the lateral lemniscus: a major source of inhibition to the inferior colliculus. Hear. Res. 168, 90–97.
Buckiova, D., Popelar, J., Syka, J., 2006. Collagen changes in the cochlea of aged Fischer 344 rats. Exp. Gerontol. 41, 296–302.
Buckiova, D., Popelar, J., Syka, J., 2007. Aging cochleas in the F344 rat: morphological and functional changes. Exp. Gerontol. 42, 629–638.
Buzsáki, G., Kaila, K., Raichle, M., 2007. Inhibition and brain work. Neuron 56, 771–783.
Caspary, D.M., Raza, A., Lawhorn Armour, B.A., Pippin, J., Arneric, S.P., 1990. Immunocytochemical and neurochemical evidence for age-related loss of GABA in the inferior colliculus: implications for neural presbycusis. J. Neurosci. 10, 2363–2372.
Caspary, D.M., Milbrandt, J.C., Helfert, R.H., 1995. Central auditory aging: GABA changes in the inferior colliculus. Exp. Gerontol. 30, 349–360.
Caspary, D.M., Holder, T.M., Hughes, L.F., Milbrandt, J.C., McKernan, R.M., Naritoku, D.K., 1999. Age-related changes in GABAA receptor subunit composition and function in rat auditory system. Neuroscience 93, 307–312.
Caspary, D.M., Ling, L., Turner, J.G., Hughes, L.F., 2008. Inhibitory neurotransmission, plasticity and aging in the mammalian central auditory system. J. Exp. Biol. 211, 1781–1791.
Di Loreto Jr., D., Cox, C., Grover, D.A., Lazar, E., del Cerro, C., del Cerro, M., 1994. The influences of age, retinal topography, and gender on retinal degeneration in the Fischer 344 rat. Brain Res. 647, 181–191.
Erlander, M.G., Tillakaratne, N.J.K., Feldblum, S., Patel, N., Tobin, A.J., 1991. Two genes encode distinct glutamate decarboxylase. Neuron 7, 91–100.
Erlander, M.G., Tobin, A.J., 1991. The structural and functional heterogeneity of glutamic acid decarboxylase: a review. Neurochem. Res. 16, 215–226.
Esclapez, M., Tillakaratne, N.J., Kaufman, D.L., Tobin, A.J., Houser, C.R., 1994. Comparative localization of two forms of glutamic acid decarboxylase and their mRNAs in rat brain supports the concept of functional differences between the forms. J. Neurosci. 14, 1834–1855.
Feldblum, S., Erlander, M.G., Tobin, A.J., 1993. Different distributions of GAD65 and GAD67 mRNAs suggest that the two glutamate decarboxylases play distinctive functional roles. J. Neurosci. Res. 34, 689–706.
Feldblum, S., Dumoulin, A., Anoal, M., Sandillon, F., Privat, A., 1995. Comparative distribution of GAD65 and GAD67 mRNAs and proteins in the rat spinal cord supports a differential regulation of these two glutamate decarboxylases in vivo. J. Neurosci. Res. 42, 742–757.
Frisina, R.D., 2001. Subcortical neural coding mechanisms for auditory temporal processing. Hear. Res. 158, 1–27.
Frisina, D.R., Frisina, R.D., 1997. Speech recognition in noise and presbycusis: relations to possible neural mechanisms. Hear. Res. 106, 95–104.
Felix 2nd, R.A., Portfors, C.V., 2007. Excitatory, inhibitory and facilitatory frequency response areas in the inferior colliculus of hearing impaired mice. Hear. Res. 228, 212–229.
Freund, T.F., Buzsaki, G., 1996. Interneurons of the hippocampus. Hippocampus 6, 347–470.
Gates, G.A., Mills, J.H., 2005. Presbycusis. Lancet 366, 1111–1120.
Gerken, G.M., 1996. Central tinnitus and lateral inhibition: an auditory brainstem model. Hear. Res. 97, 75–83.
Gordon-Salant, S., Fitzgibbons, P.J., 1993. Temporal factors and speech recognition performance in young and elderly listeners. J. Speech Hear. Res. 36, 1276–1285.
Gordon-Salant, S., Fitzgibbons, P.J., Friedman, S.A., 2007. Recognition of time-compressed and natural speech with selective temporal enhancements by young and elderly listeners. J. Speech Lang. Hear. Res. 50, 1181–1193.
Grose, J.H., Hall 3rd, J.W., Buss, E., 2006. Temporal processing deficits in the pre-senescent auditory system. J. Acoust. Soc. Am. 119, 2305–2315.
Gupta, A., Wang, Y., Markram, H., 2000. Organizing principles for a diversity of GABAergic interneurons and synapses in the neocortex. Science 287, 273–278.
Gutiérrez, A., Khan, Z.U., Morris, S.J., De Blas, A.L., 1994. Age-related decrease of GABAA receptor subunits and glutamic acid decarboxylase in the rat inferior colliculus. J. Neurosci. 14, 7469–7477.
Harker, K.T., Whishaw, I.Q., 2002. Place and matching-to-place spatial learning affected by rat inbreeding (Dark-Agouti, Fischer 344) and albinism (Wistar, Sprague–Dawley) but not domestication (wild rat vs. Long-Evans, Fischer-Norway). Behav. Brain. Res. 134, 467–477.
Harding, G.W., Bohne, B.A., Vos, J.D., 2005. The effect of an age-related hearing loss gene (Ahl) on noise-induced hearing loss and cochlear damage from low-frequency noise. Hear. Res. 204, 90–100.
Helfert, R.H., Sommer, T.J., Meeks, J., Hofstetter, P., Hughes, L.F., 1999. Age-related synaptic changes in the central nucleus of the inferior colliculus of Fischer-344 rats. J. Comp. Neurol. 406, 285–298.
Hendry, S.H., Schwark, H.D., Jones, E.G., Yan, J., 1987. Numbers and proportions of GABA-immunoreactive neurons in different areas of monkey cerebral cortex. J. Neurosci. 7, 1503–1519.
Hendrickson, A.E., Tillakaratne, N.J., Mehra, R.D., Esclapez, M., Erickson, A., Vician, L., Tobin, A.J., 1994. Differential localization of two glutamic acid decarboxylases (GAD65 and GAD67) in adult monkey visual cortex. J. Comp. Neurol. 343, 566–581.
Hua, T., Kao, C., Sun, Q., Li, X., Zhou, Y., 2008. Decreased proportion of GABA neurons accompanies age-related degradation of neuronal function in cat striate cortex. Brain Res. Bull. 75, 119–125.
Kawaguchi, Y., Kubota, Y., 1998. Neurochemical features and synaptic connections of large physiologically-identified GABAergic cells in the rat frontal cortex. Neuroscience 85, 677–701.
Kosaka, T., Katsumaru, H., Hama, K., Wu, J.Y., Heizmann, C.W., 1987. GABAergic neurons containing the Ca^{2+} binding protein parvalbumin in the rat hippocampus and dentate gyrus. Brain Res. 419, 119–130.
Krishna, B.S., Semple, M.N., 2000. Auditory temporal processing: responses to sinusoidally amplitude-modulated tones in the inferior colliculus. J. Neurophysiol. 84, 255–273.
Krzywkowski, P., De Bilbao, F., Senut, M.C., Lamour, Y., 1995. Age-related changes in parvalbumin- and GABA-immunoreactive cells in the rat septum. Neurobiol. Aging 16, 29–40.
Leventhal, A.G., Wang, Y., Pu, M., Zhou, Y., Ma, Y., 2003. GABA and its agonists improved visual cortical function in senescent monkeys. Science 300, 812–815.
Liang, L., Lu, T., Wang, X., 2002. Neural representations of sinusoidal amplitude and frequency modulations in the primary auditory cortex of awake primates. J. Neurophysiol. 87, 2237–2261.
Ling, L.L., Hughes, L.F., Caspary, D.M., 2005. Age-related loss of the GABA synthetic enzyme glutamic acid decarboxylase in rat primary auditory cortex. Neuroscience 132, 1103–1113.
Markram, H., Toledo-Rodriguez, M., Wang, Y., Gupta, A., Silberberg, G., Wu, C., 2004. Interneurons of the neocortical inhibitory system. Nat. Rev. Neurosci. 5, 793–807.
Mayhew, T.M., Gunderesen, H.J.G., 1996. 'If you assume, you can make an ass out of u and me': a decade of the dissector for stereological counting of particles in 3D space. J. Anat. 188, 1–15.
Mazelová, J., Popelar, J., Syka, J., 2003. Auditory function in presbycusis: peripheral vs. central changes. Exp. Gerontol. 38, 87–94.

Merchán, M., Aguilar, L.A., Lopez-Poveda, E.A., Malmierca, M.S., 2005. The inferior colliculus of the rat: quantitative immunocytochemical study of GABA and glycine. Neuroscience 136, 907–925.
Merrill, D.A., Chiba, A.A., Tuszynski, M.H., 2001. Conservation of neuronal number and size in the entorhinal cortex of behaviorally characterized aged rats. J. Comp. Neurol. 438, 445–456.
Milbrandt, J.C., Albin, R.L., Caspary, D.M., 1994. Age-related decrease in GABAB receptor binding in the Fischer 344 rat inferior colliculus. Neurobiol. Aging 15, 699–703.
Milbrandt, J.C., Hunter, C., Caspary, D.M., 1997. Alterations of GABAA receptor subunit mRNA levels in the aging Fisher 344 rat inferior colliculus neurons. J. Comp. Neurol. 379, 455–465.
Narayan, R., Ergün, A., Sen, K., 2005. Delayed inhibition in cortical receptive fields and the discrimination of complex stimuli. J. Neurophysiol. 94, 2970–2975.
Ohlemiller, K.K., Frisina, R.D., 2008. Clinical characterization of age-related hearing loss and its neural and molecular bases. In: Schacht, J., Popper, A., Fay, R. (Eds.), Auditory Trauma, Protection and Treatment. Springer-Verlag, New York, pp. 145–194.
Oliver, D.L., Winer, J.A., Beckius, G.E., Saint Marie, R.L., 1994. Morphology of GABAergic neurons in the inferior colliculus of the cat. J. Comp. Neurol. 340, 27–42.
Ostroff, J.M., McDonald, K.L., Schneider, B.A., Alain, C., 2003. Aging and the processing of sound duration in human auditory cortex. Hear. Res. 181, 1–7.
Ouda, L., Druga, R., Syka, J., 2008. Changes in parvalbumin immunoreactivity with aging in the central auditory system of the rat. Exp. Gerontol. 43, 782–789.
Palombi, P.S., Caspary, D.M., 1996. Physiology of the aged Fischer 344 rat inferior colliculus: responses to contralateral monaural stimuli. J. Neurophysiol. 76, 3114–3125.
Parham, K., 1997. Distortion product otoacoustic emissions in the C57BL/6J mouse model of age-related hearing loss. Hear. Res. 112, 216–234.
Paxinos, G., Watson, C., 1998. The Rat Brain, fourth ed. Academic Press, New York.
Poe, B.H., Linville, C., Brunso-Bechtold, J., 2001. Age-related decline of presumptive inhibitory synapses in the sensorimotor cortex as revealed by the physical dissector. J. Comp. Neurol. 439, 65–72.
Pollak, G.D., Burger, R.M., Park, T.J., Klug, A., Bauer, E.E., 2002. Roles of inhibition for transforming binaural properties in the brainstem auditory system. Hear. Res. 168, 60–78.
Popelar, J., Groh, D., Mazelova, J., Syka, J., 2003. Cochlear function in young and adult Fischer 344 rats. Hear. Res. 186, 75–84.
Popelar, J., Groh, D., Pelánová, J., Canlon, B., Syka, J., 2006. Age-related changes in cochlear and brainstem auditory functions in Fischer 344 rats. Neurobiol. Aging 27, 490–500.
Potier, B., Jouvenceau, A., Epelbaum, J., Dutar, P., 2006. Age-related alterations of GABAergic input to CA1 pyramidal neurons and its control by nicotinic acetylcholine receptors in rat hippocampus. Neuroscience 142, 187–201.
Prieto, J.J., Peterson, B.A., Winer, J.A., 1994a. Morphology and spatial distribution of GABAergic neurons in cat primary auditory cortex (AI). J. Comp. Neurol. 344, 349–382.
Prieto, J.J., Peterson, B.A., Winer, J.A., 1994b. Laminar distribution and neuronal targets of GABAergic axon terminals in cat primary auditory cortex (AI). J. Comp. Neurol. 344, 383–402.
Raza, A., Milbrandt, J.C., Arneric, S.P., Caspary, D.M., 1994. Age-related changes in brainstem auditory neurotransmitters: measures of GABA and acetylcholine function. Hear. Res. 77, 221–230.
Rybalko, N., Suta, D., Pelanova, J., Syka, J. 2008. Age-related deterioration of hearing in rats, FENS Abstr., vol. 4, 188.22.
Sheikh, S.N., Martin, S.B., Martin, D.L., 1999. Regional distribution and relative amounts of glutamate decarboxylase isoforms in rat and mouse brain. Neurochem. Int. 35, 73–80.
Schmidt, S., Redecker, C., Bruehl, C., Witte, O.W., 2008. Age-related decline of functional inhibition in rat cortex. Neurobiol. Aging. doi:10.1016/j.neurobiolaging.2008.04.006.
Schmolesky, M.T., Wang, Y., Pu, M., Leventhal, A.G., 2000. Degradation of stimulus selectivity of visual cortical cells in senescent rhesus monkeys. Nat. Neurosci. 3, 384–390.
Schuknecht, H.F., Gacek, M.R., 1993. Cochlear pathology in presbycusis. Ann. Otol. Rhinol. Laryngol. 102, 1–16.
Shetty, A.K., Turner, D.A., 1998. Hippocampal interneurons expressing glutamic acid decarboxylase and calcium-binding proteins decrease with aging in Fischer 344 rats. J. Comp. Neurol. 394, 252–269.
Shi, L., Argenta, A.E., Winseck, A.K., Brunso-Bechtold, J.K., 2004. Stereological quantification of GAD-67-immunoreactive neurons and boutons in the hippocampus of middle-aged and old Fischer 344 × Brown Norway rats. J. Comp. Neurol. 478, 282–291.
Shi, L., Pang, H., Linville, M.C., Bartley, A.N., Argenta, A.E., Brunso-Bechtold, J.K., 2006. Maintenance of inhibitory interneurons and boutons in sensorimotor cortex between middle and old age in Fischer 344 × Brown Norway rats. J. Chem. Neuroanat. 32, 46–53.
Simon, H., Frisina, R.D., Walton, J.P., 2004. Age reduces response latency of mouse inferior colliculus neurons to AM sounds. J. Acoust. Soc. Am. 116, 469–477.
Soghomonian, J.J., Martin, D.L., 1998. Two isoforms of glutamate decarboxylase: why? Trends Pharmacol. Sci. 19, 500–505.
Spongr, V.P., Flood, D.G., Frisina, R.D., Salvi, R.J., 1997. Quantitative measures of hair cell loss in CBA and C57BL/6 mice throughout their life spans. J. Acoust. Soc. Am. 101, 3546–3553.
Stanley, D.P., Shetty, A.K., 2004. Aging in the rat hippocampus is associated with widespread reductions in the number of glutamate decarboxylase-67 positive interneurons but not interneuron degeneration. J. Neurochem. 89, 204–216.
Strouse, A., Ashmead, D.H., Ohde, R.N., Grantham, D.W., 1998. Temporal processing in the aging auditory system. J. Acoust. Soc. Am. 104, 2385–2399.
Syka, J., Rybalko, N., Brozek, G., Jilek, M., 1996. Auditory frequency and intensity discrimination in pigmented rats. Hear. Res. 100, 107–113.
Syka, J., 2002. Plastic changes in the central auditory system after hearing loss, restoration of function, and during learning. Physiol. Rev. 82, 601–636.
Tremblay, K.L., Piskosz, M., Souza, P., 2002. Aging alters the neural representation of speech cues. Neuroreport 13, 1865–1870.
Turner, J.G., Hughes, L.F., Caspary, D.M., 2005a. Effects of aging on receptive fields in rat primary auditory cortex layer V neurons. J. Neurophysiol. 94, 2738–2747.
Turner, J.G., Hughes, L.F., Caspary, D.M., 2005b. Divergent response properties of layer-V neurons in rat primary auditory cortex. Hear. Res. 202, 129–140.
Vela, J., Gutierrez, A., Vitorica, J., Ruano, D., 2003. Rat hippocampal GABAergic molecular markers are differentially affected by ageing. J. Neurochem. 85, 368–377.
Walton, J.P., Frisina, R.D., Ison, J.E., O'Neill, W.E., 1997. Neural correlates of behavioral gap detection in the inferior colliculus of the young CBA mouse. J. Comp. Physiol. A 181, 161–176.
Walton, J.P., Frisina, R.D., O'Neill, W.E., 1998. Age-related alteration in processing of temporal sound features in the auditory midbrain of the CBA mouse. J. Neurosci. 18, 2764–2776.
Walton, J.P., Simon, H., Frisina, R.D., 2002. Age-related alterations in the neural coding of envelope periodicities. J. Neurophysiol. 88, 565–578.
Wei, J., Wu, J.Y., 2008. Post-translational regulation of L-glutamic acid decarboxylase in the brain. Neurochem. Res. 33, 1459–1465.
West, M.J., Slomianka, L., Gundersen, H.J., 1991. Unbiased stereological estimation of the total number of neurons in the subdivisions of the rat hippocampus using the optical fractionator. Anat. Rec. 231, 482–497.
Zettel, M.L., Frisina, R.D., Haider, S.E., O'Neill, W.E., 1997. Age-related changes in calbindin D-28k and calretinin immunoreactivity in the inferior colliculus of CBA/CaJ and C57Bl/6 mice. J. Comp. Neurol. 386, 92–110.
Zettel, M.L., O'Neill, W.E., Trang, T.T., Frisina, R.D., 2001. Early bilateral deafening prevents calretinin up-regulation in the dorsal cortex of the inferior colliculus of aged CBA/CaJ mice. Hear. Res. 158, 131–138.
Zilles, K., 1985. The Cortex of the Rat, A Stereotaxic Atlas. Springer-Verlag, Berlin.

Experimental Gerontology 47 (2012) 497–506

Contents lists available at SciVerse ScienceDirect

Experimental Gerontology

journal homepage: www.elsevier.com/locate/expgero

Age-related changes in calbindin and calretinin immunoreactivity in the central auditory system of the rat

Ladislav Ouda *, Jana Burianova, Josef Syka

Department of Auditory Neuroscience, Institute of Experimental Medicine, Academy of Sciences of the Czech Republic, Prague, Czech Republic

ARTICLE INFO

Article history:
Received 26 January 2012
Received in revised form 22 March 2012
Accepted 10 April 2012
Available online 20 April 2012

Section Editor: Christian Humpel

Keywords:
Calbindin
Calretinin
Aging
Inferior colliculus
Medial geniculate body
Auditory cortex

ABSTRACT

Age-related changes in the levels of major intracellular calcium buffers are known to occur in different parts of the mammalian brain, including the central auditory pathway. In the present study, we evaluate with immunohistochemistry and the western blot technique the effect that aging has on the calbindin- and calretinin-expressing system of neurons in the higher structures of the central auditory pathway, in the inferior colliculus (IC), medial geniculate body (MGB) and auditory cortex (AC) of two rat strains, the slowly aging Long-Evans and the fast aging Fischer 344. Interestingly, the age-related changes demonstrated a similar character regardless of the rat strain. In the IC of young animals, the majority of calbindin and calretinin immuno-reactive (CB and CR-ir) cells were found in the dorsal and external cortices and only sparse positive cells were present in the central nucleus of the IC. With aging, the number of CB-ir and CR-ir neurons decreased significantly in both the dorsal and external cortices. Furthermore, these declines were accompanied by an age-related reduction in the mean volumes of CB- and CR-ir neuronal somas. In the MGB of young rats, CB-ir neurons were present in abundant numbers in both the dorsal and ventral subdivisions, while CR-ir neurons were practically absent in this structure. With aging, the number and mean volume of CB-ir cells in the ventral subdivision of the MGB were significantly decreased. In comparison with the IC and MGB, age-related numerical and volumetric declines of both CB-ir and CR-ir neurons in the AC were less pronounced. Western blot protein analysis revealed a pronounced age-related decline in the levels of calbindin in both strains and in all examined brain regions. In contrast, the decline in calretinin levels with aging was less prominent, with a significant decline only in the IC of both strains. The observed age-related changes in the calbindin- and calretinin-expressing systems may contribute significantly to the deterioration of hearing function known as central presbycusis.

© 2012 Elsevier Inc. All rights reserved.

1. Introduction

The calcium binding proteins (CBPs), calbindin (CB), parvalbumin (PV) and calretinin (CR), are among the major fast cytoplasmic calcium buffers in the central nervous system and thus protect neurons from insults that induce an elevation of intracellular Ca^{2+} (Baimbridge et al., 1992; Elston and González-Albo, 2003). The disruption of neuronal calcium homeostasis and consequent molecular events affect neuronal viability and synaptic plasticity and may represent early steps in the development of neuronal degeneration (Foster, 2007). Changes in calcium homeostasis in the brain during aging are thought to be tightly linked to a decline in neuronal performance (Khachaturian, 1989; Verkhratsky and Toescu, 1998).

The calcium binding proteins are widely expressed in different brain regions; however, their expression in the mammalian neocortex and hippocampus is predominantly localized in GABAergic inhibitory neurons. In contrast to excitatory pyramidal neurons, the inhibitory neurons are typically local circuit neurons, variable in their morphology, types of their responses to sensory stimuli and their expression of different biochemical markers (Freund and Buzsáki, 1996; Markram et al., 2004; Wang et al., 2002). The distribution of CB-immunoreactive (CB-ir) and parvalbumin-immunoreactive (PV-ir) neurons in the central nervous system of the rat was first described in a summary by Celio (1990). Their distribution seems to be complementary to some extent with a slightly higher occurrence of PV in the primary and CB in the non-primary auditory or visual regions, as also described in mice (Cruikshank et al., 2001), monkeys (Jones, 2003) and humans (Tardif et al., 2003). Interestingly, the mutual colocalization of CB, PV and CR in one neuron is very rare, and they mainly represent three distinct neuronal populations (Demeulemeester et al., 1989; Gonchar and Burkhalter, 1997; Gonchar et al., 2007; Jinno and Kosaka, 2002; Kubota et al., 1994).

Age-related changes in the expression of CBPs in the brain have been described in both animal and human studies. A significant loss of CB-ir neurons, but only small changes in the occurrence of PV-ir neurons, was observed in the aged rabbit hippocampus (De Jong et al., 1996). In the brain of hamsters, calretinin and parvalbumin mRNA expression remained unchanged during aging, while calbindin-D28k mRNA

* Corresponding author at: Institute of Experimental Medicine, Academy of Sciences of the Czech Republic, Vídeňská 1083, 142 20 Prague, Czech Republic. Tel.: +420 241062690; fax: +420 241062787.
E-mail address: ouda@biomed.cas.cz (L. Ouda).

0531-5565/$ – see front matter © 2012 Elsevier Inc. All rights reserved.
doi:10.1016/j.exger.2012.04.003

expression diminished (Kishimoto et al., 1998). In rats, Krzywkowski et al. (1995) found a reduction in the somatic cross-sectional areas and a decrease in the numerical density of PV-ir neurons in the cingulate cortex. In the same species, Hwang et al. (2003) reported an age-related decline in the number of PV-ir neurons together with other morphological changes in the olfactory bulb. Furthermore, Shetty and Turner (1998) reported a parallel decline in the number of CB-, PV- and CR-ir neurons in the hippocampus of aged Fischer 344 rats. In human studies, a reduction in CBPs has been reported in different human psychiatric and neurological diseases (Mikkonen et al., 1999; Woo and Lu, 2006). On the other hand, even in men with no sign of such an illness, Bu et al. (2003) reported an overall age-related decrease in the numerical density of calbindin- and calretinin-positive neurons in most of the cortical regions, including the auditory cortex (AC), while parvalbumin immunoreactivity remained virtually unchanged.

In the auditory pathway, age-related changes in the levels of the calcium binding proteins have been demonstrated in mice and rats. In the cochlear nuclei, the changes were reported for all three calcium binding proteins in different mouse strains (Idrizbegovic et al., 2001, 2004, 2006). Significant strain-dependent differences were found in the superior olivary complex and inferior colliculus (IC) of the CBA/CaJ and C57/BL/6J mouse strains: an age-related decline in calbindin-immunoreactivity was found in the medial nucleus of the trapezoid body only in C57 mice, not in CBA mice (O'Neill et al., 1997). With aging, both strains show a decline in the number of calbindin-ir neurons in the IC, whereas calretinin-ir neurons increase with age only in the IC of CBA mice, not in C57 mice (Zettel et al, 1997). In addition, this up-regulation of calretinin was shown to be dependent on preserved sound-evoked activity, since in CBA mice bilaterally deafened in youth, the increase with age does not occur (Zettel et al., 2001). Significant strain-specific changes were found in parvalbumin immunoreactivity with aging in the IC and AC of Long-Evans rats, an outbred strain with normal aging and preserved hearing function up to late senescence, and in Fischer 344 rats, an inbred fast aging strain with early and severe hearing deterioration. While in the Long-Evans rats rather mild age-related changes occurred, a significant decline in the number of cortical PV-ir neurons was observed in Fischer 344 rats (Ouda et al., 2008).

In the present study, Long-Evans and Fischer 344 rats were studied in order to determine the strain-specificity of age-related changes in calbindin- and calretinin-expressing neurons in the inferior colliculus (IC), medial geniculate body (MGB) and auditory cortex (AC). The major outcome of this study is that significant changes in calbindin- and calretinin-expressing neurons occurred with aging in both strains, but they are likely not strain-dependent.

2. Materials and methods

2.1. Animals

Thirty-six rats of the Long-Evans (18 animals) and Fischer 344 (18 animals) strains were used in the experiments. The Long-Evans rats were obtained from a local facility and, starting at 2 months of age, were reared and aged (aging group) in-house, under known rearing conditions and with a known health history. Fischer 344 rats were purchased at 2 months of age from Charles River Deutschland (Sulzfeld, Germany) and then reared in-house under the same conditions. No signs of middle ear infection were present in any animal during their stay in the animal facility. The care and use of the animals and all experimental procedures were performed in compliance with the guidelines of the Ethical Committee, Institute of Experimental Medicine, Academy of Sciences of the Czech Republic, and the Declaration of Helsinki.

2.2. Immunohistochemistry

Long-Evans rats, 3–5 (n = 5) and 28–33 (n = 5) months old, and Fischer 344 rats, 3–5 (n = 5) and 18–24 (n = 5) months old, were placed under deep anesthesia (ketamine 35 mg/kg + xylazine 6 mg/kg, i.m.), then transcardially perfused with saline followed by 4% paraformaldehyde fixative in 0.1 M phosphate buffer (pH 7.4). Brains were removed within 15 min of perfusion, postfixed 1 h at 4 °C (same fixative) and then cryoprotected with 30% sucrose in phosphate buffer overnight. Coronal sections (40 μm thick) were cut with a freezing microtome and stained for either calbindin or calretinin.

Free-floating sections were preblocked in normal serum for 1 h and then incubated at 4 °C with anti-calbindin (rabbit polyclonal, Chemicon, 1:1000) or anti-calretinin (rabbit polyclonal, Millipore, 1:5000) diluted in PBS containing 1% normal serum. After 48 h, sections were incubated with a biotinylated secondary antibody, anti-rabbit IgG (Vector, 1:200), for 1 h and then with peroxidase-labeled ABC reagent (1:100, Vector) for 1 h. The antibody labeling was visualized by incubating the sections for 5 min in 0.02% diaminobenzidine (DAB) with 0.01% hydrogen peroxide. Sections were mounted on slides, dehydrated and coverslipped.

2.3. Stereological quantification

Calbindin (CB) immunoreactivity was examined in all sections containing the inferior colliculus, medial geniculate body and auditory cortex, delineated according to anatomical atlases (Paxinos and Watson, 1998; Zilles, 1985) and with the help of Nissl-stained sections (topographical borders of cortical areas) (Fig. 1A,B,C). Sections for the auditory cortex were sampled from bregma −4.2 mm to bregma −5.8 mm (Zilles, 1985), identified by measuring 2.0–2.5 mm from the rhinal fissure for Te3 and 3.5–4.0 mm for Te1. As an auxiliary criterion, the line going through the dorsal margin of the diencephalon indicated the control dorsal (upper) border of the auditory cortex. For the IC, sections were sampled from bregma −8.0 to −9.2 mm, for the MGB from bregma −5.0 to −6.2 mm and for the visual cortex (V1, V2 - Paxinos and Watson, 1998) from bregma −5.0 mm to −8.0 mm.

To estimate the total number of CB- and CR-ir neurons, an unbiased stereological method, the optical fractionator, was used (West et al., 1991; for review see Mayhew and Gundersen, 1996). Measurements were performed using bright-field microscopy (Leica DMRXA microscope) connected to a video camera, which transmitted the microscopic image to a monitor (Optronics, 1600 × 1200 px) coupled with Neurolucida software (MicroBrightField, Inc.). Two sets of motors were connected to the microscope to move the section on a known distance in the x- and y-directions. The z-direction was measured using a microcator. A 10× objective lens was used to delineate the regions of interest and the starting position of the counting frame. We adapted the Neurolucida-generated grid superimposed on the screen with the use of a random number table to establish the random starting position of the counting frame in the area of interest.

A 100× oil-immersion objective was used and the appropriate counting frame was superimposed on the screen. The counting frames used to obtain the sampling had the same size (3850 μm²–70 × 55 μm). The upper and lower surfaces of the sections were examined to determine if the margins of the tissue sections were depleted of neuronal nuclei, as suggested by Andersen and Gundersen (1999). The height of the optical dissector was constant at 10 μm, and the first and last 5 μm of the section thickness were omitted from the analysis. At least 200 neurons per animal were counted in each examined structure. Each neuron in the counting frame was counted when its distinct nucleus came to maximum focus. At maximum focus, the cell body was outlined by a cursor on the computer screen, and the cross-sectional area was measured automatically using Neurolucida software. The mean volume was consequently recalculated from the values of the cross-sectional areas. Only positive somas exceeding 5 μm in diameter and with a distinct nucleus were counted and used for analysis.

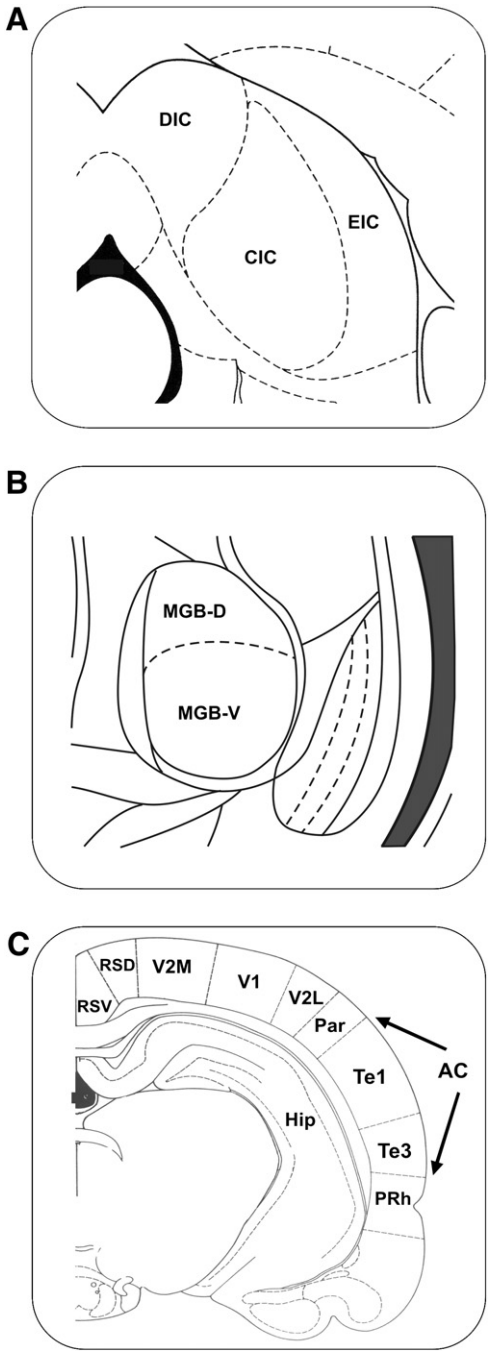

Fig. 1. Topographical overview of coronal sections including the IC, MGB and AC. Drawings adapted from Paxinos and Watson (1998) and Zilles (1985); (A) bregma −8.8 mm, (B) bregma −5.1 mm, (C) bregma −5.3 mm. CIC — central nucleus of the inferior colliculus; DIC — dorsal cortex of the IC; EIC — external cortex of the IC; MGB-V, D — ventral and dorsal divisions of the medial geniculate body; AC — auditory cortex, Te1 and Te3 areas, Par — parietal cortex; Hip — hippocampus; PRh — perirhinal cortex; V1,2 — visual cortex 1,2; RSD, RSV — retrosplenial cortex, dorsal and ventral.

2.4. Western blot protein analysis

Long-Evans rats, 3–6 (n = 4) and 30–33 (n = 4) months old, and Fischer 344 rats, 4 (n = 4) and 21–25 (n = 4) months old, were used in the analysis. Anesthetized rats (ketamine 35 mg/kg + xylazine 6 mg/kg, i.m.) were decapitated, their brains quickly extracted and rinsed in ice-cold physiological solution, and the inferior coliculli (ICs) and auditory (ACs) and visual cortices (VCs) were rapidly removed bilaterally. The samples included the whole IC, the Te1 + Te3 (Zilles, 1985) areas of the AC and the V1 + V2 areas of the VC (Paxinos and Watson, 1998). All samples were immediately put into dry ice after extraction and stored frozen at −80 °C until processed. In contrast to the IC or cortical areas, the medial geniculate body was practically impossible to extract quickly and precisely enough from the fresh brain tissue due to anatomical localization of this structure. Therefore, this structure was not included into the western blot protein analysis.

For the analysis, ICs, ACs and VCs were homogenized by a Potter-Elvehjem homogenizer in 0.05 M Tris-NaCl (pH 7.4) buffer with protease inhibitors (Sigma). The homogenate was centrifuged at 10 000 *g* for 10 min at 4 °C. To ensure similar protein loading, the total protein concentration of these extracts was determined by using the Bradford method with BSA as the standard. Samples (cytosolic fraction) were incubated in boiling water for 10 min at 80 °C in sodium dodecyl sulfate–polyacrylamide gel electrophoresis buffer containing 10% glycerol, 2% SDS, 0.05% bromphenol blue and 4 M dithiotreitol. Samples were then subjected to Tris/Tricine/SDS-PAGE electrophoresis on a 3% bis-acrylamide polyacrylamide gel at 30 mA/gel for 150 min on a Mini-Protean II apparatus (Bio-Rad). After electrophoresis, the resolved proteins were transferred (Bio-Rad Mini Protean II transblot apparatus at 350 mA for 60 min at 4 °C in 25 mM Tris, 192 mM glycine, 20% methanol, 0,1% SDS) to a nitrocellulose membrane (Amersham, Biosciences). Membranes were incubated in 5% non-fat dry milk in 10% Tris-buffered saline with 0.05% Tween 20 (TBST) for 60 min at room temperature to block nonspecific protein binding. After being washed in TBST buffer (3 times quickly, 3 × 5 min each), the membranes were probed with anti-calbindin (rabbit polyclonal, Chemicon, 1:500 in TBST), anti-calretinin (rabbit polyclonal, Millipore, 1:200 in TBST) and anti-actin (mouse monoclonal, Chemicon, 1:1000 in TBST) primary antisera overnight at 4 °C. The membranes were washed again and incubated with goat anti-mouse IgG or anti-rabbit IgG antibody conjugated with horseradish peroxidase (Upstate, 1:7500 in TBST) for 2 h at room temperature. Before enhanced chemiluminescence (ECL), the membranes were washed as described above and stored in TBST for at least 2 h. For ECL, substrates A (Luminol solution) and B (H_2O_2 solution) were prepared, mixed 2:1 (Sigma) just before use, and poured on the membranes. The specific signals were detected on autoradiographic film (Kodak MXB). Films were developed at room temperature, stopped, fixed, washed under running cold water and air-dried. Scanning (Canon CanoScan 9000F) and ImageQuant software were used for quantifying the relative abundance of calbindin, calretinin and actin in individual samples. The amount of protein applied to the gel varied for each isoform and fraction to achieve linearity with the intensity × area (volume) of the band on the western blot. To ensure the specificity of CB-, CR- and actin-immunoreactive proteins, prestained molecular weight protein standards were used (Sigma). The levels of calbindin and calretinin were calculated as the ratio of the optical density of the antibody of interest to the optical density of the antibody directed against β-actin.

2.5. Statistical analysis

The significance of the differences between young and old groups of rats was assessed by the non-parametric two-tailed Mann–Whitney test for the immunohistochemistry and by the one-way ANOVA test and Bonferroni's multiple comparison test for western blots, both with the use of GraphPad Prisma software (version 4.0). In addition, the significance of differences in western blot protein analysis among protein levels in different brain structures (IC vs. AC vs. VC) in young and old rats was also assessed by the one-way ANOVA test and Bonferroni's multiple comparison test. P values of 0.05 or less were considered statistically significant. For each statistical test, each examined animal was represented by one number to ensure the maximal independence of the data entering the tests.

3. Results

3.1. Calbindin

3.1.1. Inferior colliculus

CB-ir neurons were observed throughout all three subdivisions of the IC; however, the majority of CB-ir cells were found in the dorsal and external cortices (Fig. 2A,B), while only a few were present in the central nucleus of the IC. Significant age-related changes in CB immunoreactivity were found predominantly in the dorsal (DIC) and external cortices (EIC). With aging, the number of CB-neurons decreased significantly in the DIC and EIC cortices of both rat strains (by 21% and 16% in Long-Evans and by 18% and 13% in F344 rats, respectively, $P<0.05$, $P<0.01$ in the DIC of LE rats; Fig. 4A,B). The average volumes of CB-ir neuronal somas significantly decreased only in the dorsal cortex of the IC (by 18% in Long-Evans and 16% in F344 rats, respectively, $P<0.05$; Fig. 4C,D).

Western blot analysis revealed a significant age-related decline in the levels of calbindin in the whole IC of old rats of both species in comparison with young animals of 49% for LE and 45% for F344 (both $P<0.001$) (Fig. 6A). The analyzed samples included all three subdivisions of the IC.

3.1.2. Medial geniculate body

In the MGB, CB-ir neurons were present in both the dorsal and ventral subdivisions in a markedly higher numerical density compared to the IC and auditory cortex (Fig. 2C–E). In comparison with young rats, the number of CB-ir cells in the ventral subdivision was significantly decreased in both aged Long-Evans and F344 rats, by 18% and 23%, respectively (both $P<0.01$,Fig. 4A,B). Furthermore, in the dorsal subdivision of old F344 rats, the number of CB-ir neurons also decreased significantly (by 21%, $P<0.01$); Fig. 4A,B. Similarly, the average volume of CB-ir neuronal somas was smaller with aging in the ventral subdivisions of both rat strains and in the dorsal

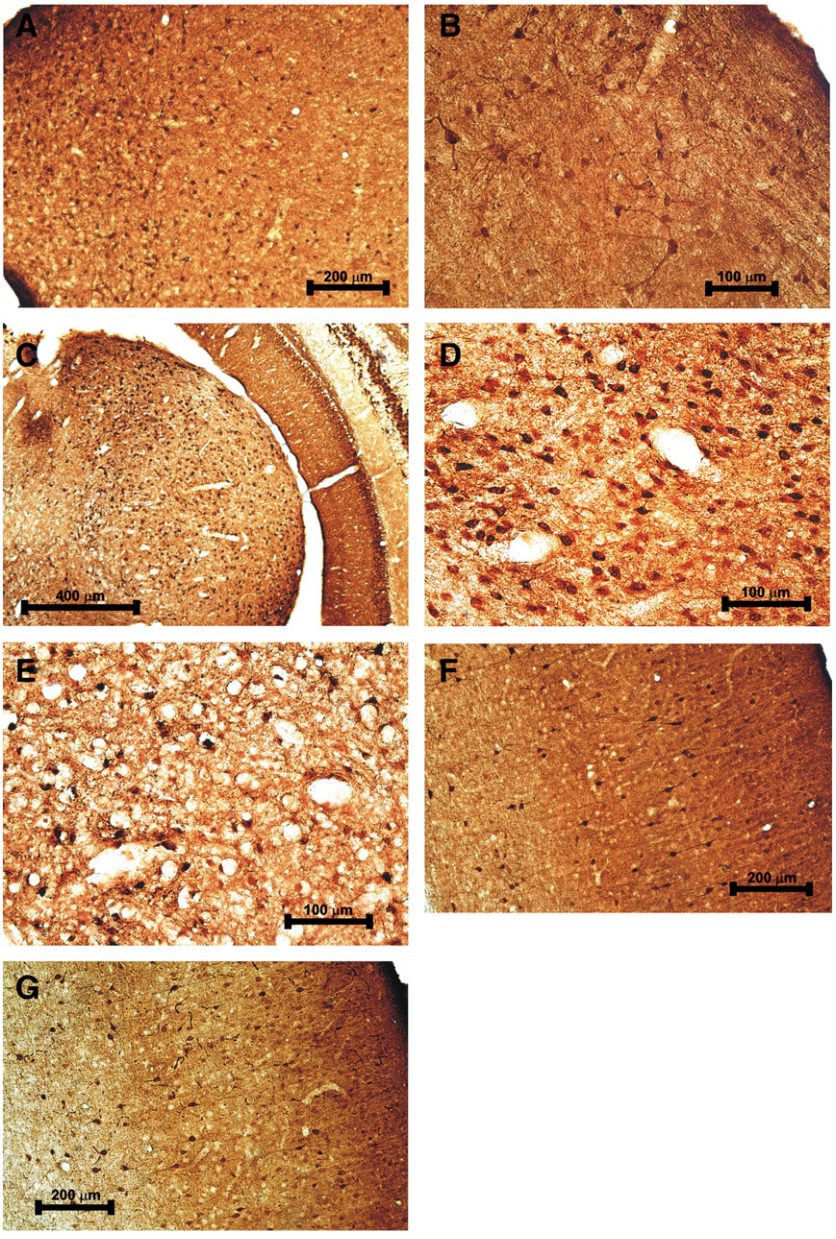

Fig. 2. Illustration of CB immunoreactivity in the dorsal (A) and external (B) cortices of the IC in young Long-Evans rats, in the MGB (C) of a young Fischer 344 rat, in detail in the ventral MGB of young (D) and old (E) Fischer 344 rats, and in the Te1 auditory cortical area in young (F) and old (G) Long-Evans rats.

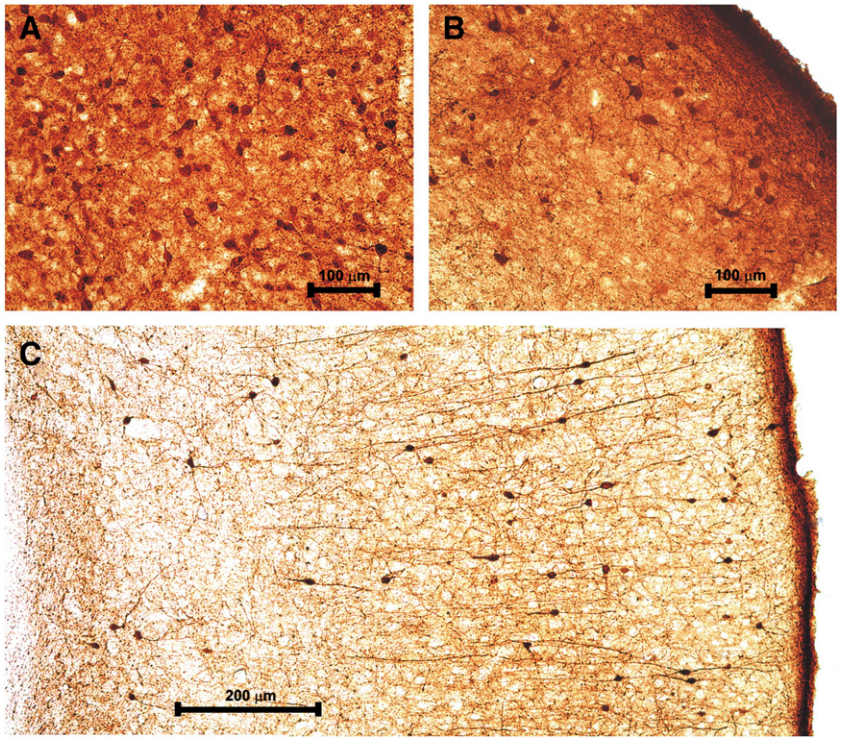

Fig. 3. Illustration of CR immunoreactivity in the dorsal (A) and external (B) cortices of the IC of a young adult Long-Evans rats, and in the Te1 auditory cortical area of a young Fischer 344 rat (C).

subdivision of F344 rats (all $P<0.05$; Fig.4C,D). The difference in the numerical density of immunoreactive neurons between young and old animals was visible to the naked eye in some cases (Fig. 2D,E). The smaller cross-sectional size of the medial division of the MGB and the low number of CB-ir neurons per section in this structure resulted in a considerably higher S.E.M. in comparison with all other analyzed structures, which would not allow us to conduct any meaningful statistical analysis, therefore we decided to omit the medial division from our calculations.

Due to methodological reasons, the MGB was not included into the western blot protein analysis (see Section 2.4).

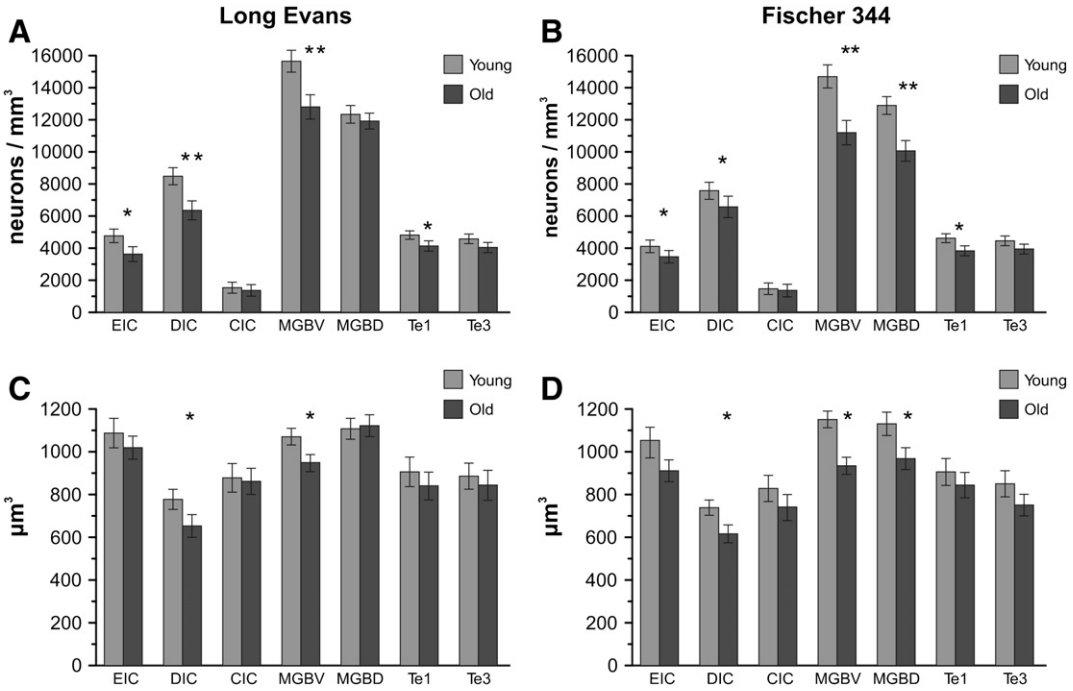

Fig. 4. Results of the quantitative evaluation of calbindin immunoreactivity in the external and dorsal cortices and central nucleus of the inferior colliculus, in the ventral and dorsal subdivisions of the medial geniculate body, and in the Te1 and Te3 auditory cortical areas of young and old Long-Evans (A,C) and Fischer 344 (B,D) rats. A,B — Numerical density of CB-ir neurons. C,D — Mean volumes of CB-ir neurons. The error bars represent S.E.M. (* — $P<0.05$, ** — $P<0.01$).

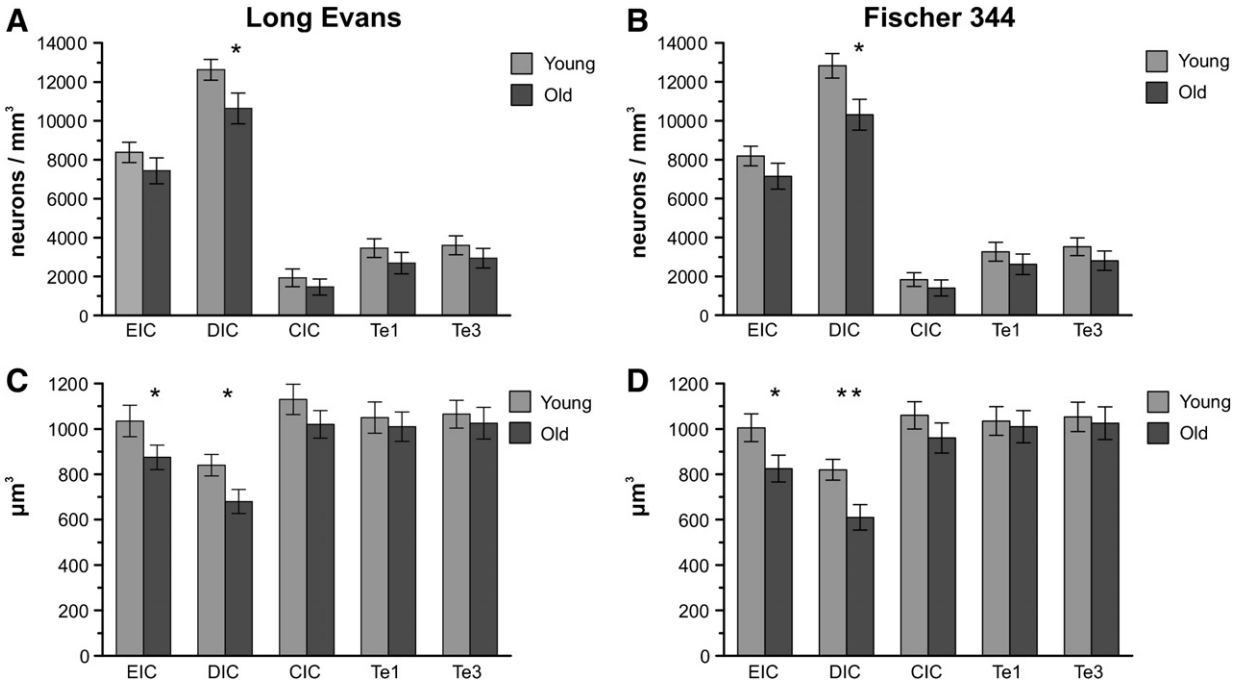

Fig. 5. Results of the quantitative evaluation of calretinin immunoreactivity in the external and dorsal cortices and central nucleus of the inferior colliculus, and in the Te1 and Te3 auditory cortical areas of young and old Long-Evans (A,C) and Fischer 344 (B,D) rats. A,B — Numerical density of CR-ir neurons. C,D — Mean volumes of CR-ir neurons. The error bars represent S.E.M. (* — P<0.05, ** — P<0.01).

3.1.3. Auditory cortex

The CB-ir cells in both LE and Fischer 344 rats were scattered throughout cortical layers II–VI in the Te1 and Te3 areas with a markedly higher numerical density and stronger neuropile immunostaining in the superficial layers (I–IV) than in the deep layers (V–VI). These features were present in both young and old animals (Fig. 2F, G). The neurons in the superficial layers were more weakly stained when compared with CB-ir cells in the deep layers, and in few cases their morphology was reminiscent of pyramidal neurons. In comparison with age-related changes in the IC and MGB, the numerical changes of CB-ir neurons in the AC were less pronounced (by 14% and 16% in LE and F344 rats, respectively). The decrease in the number of CB-ir neurons with aging in the Te1 area of old rats reached the level of statistical significance (P<0.05); Fig. 4A,B. On the other hand, the volumetric changes of CB-ir neuronal somas were rather small and non-significant.

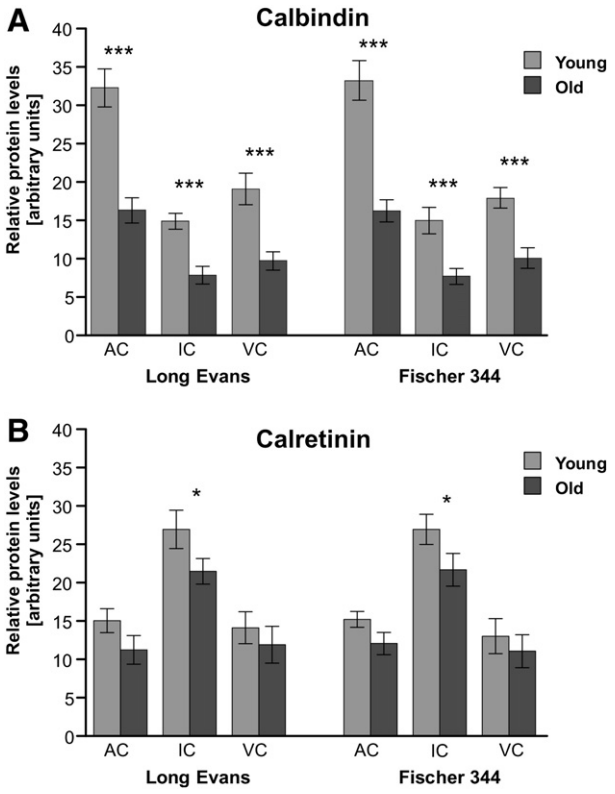

Fig. 6. Results of western blot protein analysis of calbindin (A) and calretinin (B) in young and old Long-Evans and Fischer 344 rats. Arbitrary units were calculated as the ratio between the optical density of the examined protein and the optical density of actin (in scanned films analyzed using ImageQuant software). The abbreviations are: AC — auditory cortex, IC — inferior colliculus, VC — visual cortex. The error bars represent S.E.M. (* — P<0.05, *** — P<0.001).

Nevertheless, western blot protein analysis revealed a significant age-related decrease in the total levels of calbindin of 54% for LE and 48% for F344 (both P<0.001) (Fig. 6A). The analyzed samples included both the Te1 and Te3 areas. A significant age-related decline in the protein levels of calbindin of 42% in LE and 50% in F344 rats was also observed in the visual cortex (both P<0.001) (Fig.6A). The age-related declines found in the subcortical and cortical auditory brain regions are clearly seen on the representative blots shown in Fig. 7.

Interestingly, the levels of calbindin, in both young and old animals, were approximately two times higher in the AC than in the IC and visual cortex (P<0.01, Bonferroni's multiple comparison test).

3.2. Calretinin

3.2.1. Inferior colliculus

CR-ir neurons were found throughout all three subdivisions of the IC; however, the majority of CR-ir cells were present in the dorsal and external cortices (Fig. 3A,B) and only a few were scattered in the central nucleus of the IC. Age-related changes were similar regardless of the examined strain and comprised a tendency towards a decline in the number of CR-ir neurons as well as a decrease in the mean volumes of the remaining CR-ir neuronal somas in all subdivisions of the IC. The number of CR-neurons decreased significantly in the dorsal cortex of the IC in both rat strains by 16% in Long-Evans and by 20%

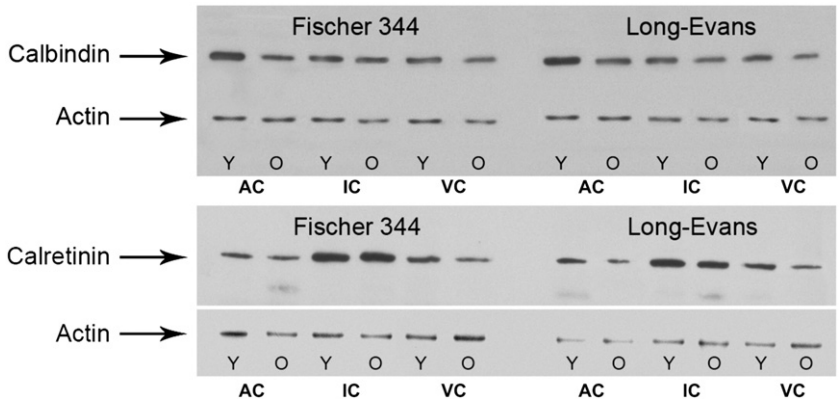

Fig. 7. Representative films of the western blot analysis of calbindin and calretinin protein isoforms developed with the enhanced luminescence method. Actin, used as an internal control, was detected at a position corresponding to a molecular weight of 42 kDa. The abbreviations are: AC — auditory cortex, IC – inferior colliculus, VC — visual cortex, Y — young and O — old animals.

in F344 rats (both $P<0.05$; Fig. 5A,B). In addition, the average volumes of CR-ir neuronal somas were significantly decreased in both the DIC and EIC cortices when compared with the situation in young animals, by 19% ($P<0.05$) and 15% ($P<0.05$) in Long-Evans and by 25% ($P<0.01$) and 18% ($P<0.05$) in F344 rats, respectively (Fig. 5C,D).

Western blot analysis demonstrated a significant age-related decline in the levels of calretinin in the IC of both rat strains, of 22% for the LE and 21% for the F344 strain (both $P<0.05$) (Fig. 6B). The analyzed samples included all three subdivisions of the IC. Interestingly, the levels of calretinin, in both young and old animals, were almost two times higher in the IC than in the cortical tissue (either AC or VC) ($P<0.01$, Bonferroni's multiple comparison test), as also visible on the representative blots in Fig. 7.

3.2.2. Medial geniculate body

Practically no calretinin-immunoreactive cells were present in any section containing the MGB in either young or old animals of either strain. In some cases, regardless of strain or age of animals, few CR-ir cells might have been situated within the outer superficial part of the dorsal MGB, however, the precise borders to the surrounding nuclei were not clear in these instances.

3.2.3. Auditory cortex

CR-ir neurons were present in all cortical layers regardless of the rat strain or the age of the examined animals; however, they were more prevalent in the superficial layers (II–III). In the Te3 auditory area, the number of CR-ir cells was slightly higher when compared to the Te1 auditory area in both examined strains, especially in the superficial layers, but the distribution of CR-ir neurons throughout the cortical layers was practically identical in both auditory cortical areas. The positive neurons with well-stained processes predominantly showed restricted horizontal and long vertical arborizations (Fig. 3C). With aging, the number of CR-ir neurons in the Te1 and Te3 areas decreased; however, the decline was non-significant in both LE and F344 rats. The difference in the mean volumes of CR-ir somas between young and old animals was negligible (Fig. 5C,D). Interestingly, when determined for particular cortical layers separately, the decrease in the number of CR-ir neurons was more pronounced in cortical layers I–III and VI, while in layers IV–V, the number of CR-ir cells was only very slightly decreased with aging.

In western blotting, only a non-significant decline in the levels of calretinin was associated with aging, as observed in both the auditory and visual cortices. In the AC, the percentage age-related decrease, 26% for LE and 20% for F344 rats, was greater when compared to the VC (16% for LE and 15% for F344 rats) and more similar to the findings in the IC. However, due to a greater variability among values in particular animals (calretinin protein levels in particular auditory cortices), the differences were in comparison with the situation in the IC non-significant (Fig. 6B).

4. Discussion

Our results demonstrated significant age-related changes in calbindin and calretinin immunoreactivity in the upper parts of the auditory pathway in two rat strains, which comprised a significant decrease in the number and volumes of immunoreactive neurons and decreased protein levels. The obtained data demonstrated a rather uniform character of the changes. First, the observed changes were relatively similar at both the subcortical and cortical levels of the rat central auditory system and also in the visual cortex. Second, age-related changes in both rat strains, Long-Evans and Fischer 344, shared very similar patterns. Third, the results obtained with immunohistochemical techniques were in principle in agreement with the results acquired with western blotting. In addition, the decline in calbindin levels was more pronounced in comparison with the changes in calretinin immunoreactivity.

Our findings of a significant decrease in calbindin protein levels and the number of CB-ir neurons with aging in the central auditory system and visual cortex are in agreement with previous reports that demonstrated a prevalent age-related decline in calbindin immunoreactivity in different brain regions. In the brain of hamsters, calretinin and parvalbumin mRNA expression remained unchanged during aging, while calbindin-D28k mRNA expression diminished (Kishimoto et al., 1998). Shetty and Turner (1998) reported a parallel decline in the number of CB-, PV- and CR-ir neurons in the hippocampus of old Fischer 344 rats. In the perirhinal cortex of Sprague–Dawley rats, a significant decline in the number of CB-ir neurons was found, while no changes in the number of CR-ir or PV-ir neurons were found (Moyer et al., 2011). The age-related loss of CB has been evaluated in the cerebellum as well as the olfactory bulb and nucleus basalis of Meynert (Geula et al., 2003; Iacopino and Christakos, 1990; Kishimoto et al., 1998).

It follows that age-related changes in calretinin expression are rather more complex and multivalent in comparison with age-related changes in calbindin. This has also been shown in the central auditory system where a similar complexity of changes has been demonstrated to some degree. In the cochlear nuclei of mice, the number of CB-ir cells did not changed with aging in BALB/c mice, while number of PV- and CR-ir neurons increased significantly (Idrizbegovic et al., 2006). Significant strain-dependent differences were found in the inferior colliculus of the CBA/CaJ and C57/BL/6J mouse strains: with aging, both strains showed a decline in the number of calbindin-ir neurons in the IC, whereas calretinin-ir neurons increased with age only in the IC of CBA mice (a mouse strain with preserved hearing function up to an advanced age), not in C57 mice (Zettel et al, 1997). The increase in the number of CR-ir neurons in the IC of CBA mice contrasts in some degree with our finding

of a decrease in the number of CR-ir neurons in the IC of Long-Evans rats. The reason for this difference is not clear; however, it may reflect interspecies differences as well as the discussed complexity of age-related changes in calretinin expression.

The Long-Evans and Fischer 344 rat strains involved in our experiment represent two strains with a variety of morphological, physiological and behavioral differences (Harker and Whishaw, 2002). While Long-Evans rats show preserved hearing function up to late senescence, Fischer 344 rats represent a fast aging strain with an early onset of severe hearing deterioration with aging (Popelar et al., 2003, 2006; for review see Syka, 2010). The age-related pathology linked to hearing deterioration in Fischer 344 rats includes changes in both the middle and inner ear (Buckiova et al., 2007; Popelar et al., 2006) and apparently also the disruption of prestin in the outer hair cells of old animals of this strain (Chen et al., 2009).

However, despite the differently preserved function of the peripheral part of the auditory system with aging, Long-Evans and Fischer 344 rats demonstrated almost identical age-related changes in calbindin and calretinin. In our previous experiments, we found analogous uniform age-related changes in glutamate decarboxylase (the key rate-limiting enzyme for the synthesis of GABA) in the central auditory system of both Long-Evans and Fischer 344 rats. Similarly as in the present results, the observed changes were expressed as a uniform homogenous decline in the number of glutamate decarboxylase positive neurons in the IC and AC accompanied by a notable decrease in protein levels in the IC, AC, and also VC of both strains as assessed by western blotting (Burianova et al., 2009). These findings suggest that certain age-related changes in the central auditory system may not be exclusively dependent on the loss of peripheral inputs but may represent, at least partially, a feature of the aging brain. On the other hand, in spite of the fact that parvalbumin-expressing neurons form a significant subpopulation of GABA-expressing cells in the IC and AC of the rat (Fredrich et al., 2009; Gonchar and Burkhalter, 1997), the age-related changes in the PV-ir neuronal population were rather mild in Long-Evans rats, while in old Fischer 344, the observed changes included large deficits in the local occurrence of PV-ir cells, especially in the AC (Ouda et al., 2008).

The expression of major intracellular calcium buffers – calbindin, calretinin and parvalbumin – in the higher levels of the central auditory system as well as in most cortical non-auditory areas is distinctive for the system of GABAergic neurons, with the partial exception of calbindin. Simultaneously, the mutual colocalization of CB, PV and CR in one neuron is very rare, and they mainly represent three distinct neuronal populations (Demeulemeester et al., 1989; Gonchar and Burkhalter, 1997; Gonchar et al., 2007; Jinno and Kosaka, 2006; Kubota et al., 1994). These neuronal populations also mostly represent different neuronal types with respect to morphology, synaptic connection, electrophysiological responses and function in neuronal networks (Markram et al., 2004), which may result in their different roles and different manifestations of changes, including the divergent strain-dependency of these changes, during aging.

As mentioned above, among the three major discussed CBPs, calbindin may not belong exclusively to the GABAergic neuronal population: especially some weakly stained CB-ir cells in the superficial cortical layers are known to be pyramidal neurons (De Felipe, 1997; Kubota et al., 1994; Van Brederode et al., 1991). This fact must be specifically recognized in the MGB, since in rodents, this auditory region contains only very few GABAergic neurons (Winer and Larue, 1996). In contrast, the presence of CB-ir neurons in the MGB is abundant, even in comparison with the IC and AC, therefore most of them are evidently non-GABAergic cells. On the other hand, only very few PV-ir and CR-ir neurons are present in the rat MGB, as shown in both the present study and also in our earlier work (Ouda et al., 2008). However, despite these facts, the age-related decline in the number of CB-ir neurons in our findings was uniform in all three examined auditory structures, the IC, MGB and AC.

An interesting finding in our experiments is the significant regional difference in the protein levels found with western blotting, which includes approximately two-fold higher levels of calbindin in the AC in comparison with the IC and visual cortex and almost two-fold higher levels of calretinin in the IC in comparison with the AC and VC. The background and functional implications of this variation remain to be determined. The regional differences in calretinin protein levels are in agreement with our previous finding of almost three-fold higher GAD protein levels in the IC when compared to the AC and VC (Burianova et al., 2009). On the other hand, higher levels of calbindin in the AC could simply reflect the amount of calbindin in neurons, including the intensely stained neuropile, in the superficial cortical layers. However, this reasoning does not apply for the comparison between the AC and VC.

When comparing our results obtained by immunohistochemistry with the results from western blotting, the age-related changes observed in immunohistochemistry were generally less pronounced. This finding could be, at least partially, attributed to a more complex interpretation of the immunohistochemical data. Not only changes in the total number of immunoreactive neurons, but also in the intensity of immunostaining (a variable, which is profoundly dependent on renormalization against the background staining) and the volumes of the stained neurons are necessary to take into account. Therefore, the changes in the total protein levels as indicated by immunohistochemistry are difficult to estimate, and a comparison with the results obtained by western blotting is not straightforward, as also shown for CBPs by other authors who used both immunohistochemistry and western blotting (Choi et al., 2010; Kim et al., 2010; Ng et al., 1996). However, a qualitative agreement between the results obtained by both techniques in our experiments is evident. For technical reasons, the medial geniculate body could not be included into the western blot protein analysis (see Section 2.4); therefore, we cannot determine whether the more pronounced decline in the number of CB-ir neurons found by immunohistochemistry in this structure, when compared to the IC and AC, would also be associated with a more pronounced decline in calbindin protein levels in western blot results.

In animal and human studies, increasing evidence has accumulated about the mutual links among intracellular calcium regulation, alterations in intracellular calcium binding protein levels and neurodegenerative and neuropsychiatric disorders (for review see Woo and Lu, 2006; Mattson, 2007). For example, in Alzheimer's disease mouse models, there was a loss of CB immunoreactivity in the hippocampus that correlated with hippocampal-dependent learning deficits (Palop et al., 2003, 2011). A reduction in CBPs has been also reported in humans diagnosed with Alzheimer's disease (Mikkonen et al., 1999). On the other hand, a decline in the number of CB-ir and CR-ir neurons has been observed in different brain neocortical areas, including the auditory cortex, in old individuals without any previous signs of psychiatric or neurological diseases (Bu et al., 2003). Since CBPs may play an important role in neuroprotection and neuronal performance (Foster, 2007; Mattson et al., 1991; Verkhratsky and Toescu, 1998), their decreased expression with aging may compromise neuronal function and, further, influence the viability of the neurons with increased susceptibility to various disorders.

The functional implication of the age-related decline in the expression of CB and CR in auditory processing could predominantly involve alterations in the GABA-mediated inhibitory system, which preferentially includes neuronal populations expressing CBPs, and consequently affect different populations of pyramidal neurons. Specifically, large pyramidal neurons in layer V, which exhibit sharp, “V/U” shaped receptive fields, are likely to have fewer inhibitory inputs on their somas (Hefti and Smith, 2000, 2003), synaptic connections typical for fast spiking PV-ir basket cells, and therefore may be under the influence of other GABAergic neurons with synaptic connections preferentially located on dendrites of pyramidal cells like the CB-ir and CR-ir neuronal populations (Freund and Buzsáki, 1996; Markram et al., 2004). Therefore,

age-related changes in the number and function of CB-ir and CR-ir neurons could contribute to the age-related decline in the performance of sharply tuned pyramidal neurons, since the number and reliability of "V/U" shaped receptive fields significantly decrease with aging and the neurons fire less onset responses (Turner et al., 2005a).

The compromised inhibition in the central auditory system may result in a broadening of the excitatory areas and thus in the poorer tuning of the neuronal receptive fields. The reduction of fine-tuned receptive fields consequently results in poorer discrimination of the temporal parameters of sounds (Narayan et al., 2005; Palombi and Caspary, 1996; Turner et al., 2005a, 2005b; Walton et al., 2002). The reduced temporal acuity limits the gap detection thresholds and gap duration difference limen, which are known to worsen with aging and are believed to be essential for the successful processing of complex sounds, including human language (Gordon-Salant et al., 2007; Grose et al., 2006; Mazelová et al., 2003; Suta et al., 2011). From this point of view, the age-related decline in CB and CR expression levels in the central auditory system could also contribute significantly to the deterioration of hearing function associated with aging in mammals, including presbycusis in man.

5. Conclusions

In summary, a significant loss of CBPs expression during normal aging could contribute to a cellular environment that makes neurons more susceptible to dysfunction and degeneration. The disruption of calcium homeostasis in neurons may consequently be involved in both the impairments that accompany normal aging and also in the pathologies associated with age-related disorders (Foster, 2007; Khachaturian, 1989; Mattson, 2007; Riascos et al., 2011). Therefore, our findings of age-related decline in calbindin- and calretinin expression in the central auditory pathway may contribute significantly to the deterioration of hearing function in mammals known as central presbycusis, especially the processing of complex sounds including human language. Since in the human population, a loss of speech understanding with aging constitutes an important health and social impairment (Gates and Mills, 2005; Syka, 2002), an understanding of the mechanisms underlying this deterioration is important for possible therapeutic intervention. Eventually, the age-related alterations in calcium binding proteins in the central auditory system as well as alterations in GABA-mediated transmission might present targets for future treatment in human presbycusis.

Acknowledgment

The authors wish to thank Mrs. J. Janouskova and Mr. J. Setnicka for their technical assistance. This study was supported by the Grant Agency of the Czech Republic P304/12/1342 and P304/12/G069.

References

Andersen, B.B., Gundersen, H.J.G., 1999. Pronounced loss of cell nuclei and anisotropic deformation of thick sections. J. Microsc. 196, 69–73.
Baimbridge, K.G., Celio, M.R., Rogers, J.H., 1992. Calcium-binding proteins in the nervous system. Trends Neurosci. 15, 303–308.
Bu, J., Sathyendra, V., Nagykery, N., Geula, C., 2003. Age-related changes in calbindin-D28k, calretinin, and parvalbumin-immunoreactive neurons in the human cerebral cortex. Exp. Neurol. 182, 220–231.
Buckiova, D., Popelar, J., Syka, J., 2007. Aging cochleas in the F344 rat: morphological and functional changes. Exp. Gerontol. 42, 629–638.
Burianova, J., Ouda, L., Profant, O., Syka, J., 2009. Age-related changes in GAD levels in the central auditory system of the rat. Exp. Gerontol. 44, 161–169.
Celio, M.R., 1990. Calbindin D-28k and parvalbumin in the rat nervous system. Neuroscience 35, 375–475.
Chen, G.D., Li, M., Tanaka, C., Bielefeld, E.C., Hu, B.H., Kermany, M.H., Salvi, R., Henderson, D., 2009. Aging outer hair cells (OHCs) in the Fischer 344 rat cochlea: function and morphology. Hear. Res. 248, 39–47.
Choi, J.H., Lee, C.H., Yoo, K.Y., Hwang, I.K., Lee, I.S., Lee, Y.L., Shin, H.C., Won, M.H., 2010. Age-related changes in calbindin-D28k, parvalbumin, and calretinin immunoreactivity in the dog main olfactory bulb. Cell. Mol. Neurobiol. 30, 1–12.
Cruikshank, S.J., Killackey, H.P., Metherate, R., 2001. Parvalbumin and calbindin are differentially distributed within primary and secondary subregions of the mouse auditory forebrain. Neuroscience 105, 553–569.
De Felipe, J., 1997. Types of neurons, synaptic connections and chemical characteristics of cells immunoreactive for calbindin-D28K, parvalbumin and calretinin in the neocortex. J. Chem. Neuroanat. 14, 1–19.
De Jong, G.I., Naber, P.A., Van der Zee, E.A., Thompson, L.T., Disterhoft, J.F., Luiten, P.G., 1996. Age-related loss of calcium binding proteins in rabbit hippocampus. Neurobiol. Aging 17, 459–465.
Demeulemeester, H., Vandesande, F., Orban, G.A., Heizmann, C.W., Pochet, R., 1989. Calbindin D-28K and parvalbumin immunoreactivity is confined to two separate neuronal subpopulations in the cat visual cortex, whereas partial coexistence is shown in the dorsal lateral geniculate nucleus. Neurosci. Lett. 99, 6–11.
Elston, G.N., González-Albo, M.C., 2003. Parvalbumin-, calbindin-, and calretinin-immunoreactive neurons in the prefrontal cortex of the owl monkey (Aotus trivirgatus): a standardized quantitative comparison with sensory and motor areas. Brain Behav. Evol. 62, 19–30.
Foster, T.C., 2007. Calcium homeostasis and modulation of synaptic plasticity in the aged brain. Aging Cell 6, 319–325.
Fredrich, M., Reisch, A., Illing, R.B., 2009. Neuronal subtype identity in the rat auditory brainstem as defined by molecular profile and axonal projection. Exp. Brain Res. 195, 241–260.
Freund, T.F., Buzsáki, G., 1996. Interneurons of the hippocampus. Hippocampus 6, 347–470.
Gates, G.A., Mills, J.H., 2005. Presbycusis. Lancet 366, 1111–1120.
Geula, C., Bu, J., Nagykery, N., Scinto, L.F., Chan, J., Joseph, J., Parker, R., Wu, C.K., 2003. Loss of calbindin-D28k from aging human cholinergic basal forebrain: relation to neuronal loss. J. Comp. Neurol. 455, 249–259.
Gonchar, Y., Burkhalter, A., 1997. Three distinct families of GABAergic neurons in rat visual cortex. Cereb. Cortex 7, 347–358.
Gonchar, Y., Wang, Q., Burkhalter, A., 2007. Multiple distinct subtypes of GABAergic neurons in mouse visual cortex identified by triple immunostaining. Front. Neuroanat. 1, 1–11.
Gordon-Salant, S., Fitzgibbons, P.J., Friedman, S.A., 2007. Recognition of time-compressed and natural speech with selective temporal enhancements by young and elderly listeners. J. Speech Lang. Hear. Res. 50, 1181–1193.
Grose, J.H., Hall III, J.W., Buss, E., 2006. Temporal processing deficits in the presenescent auditory system. J. Acoust. Soc. Am. 119, 2305–2315.
Harker, K.T., Whishaw, I.Q., 2002. Place and matching-to-place spatial learning affected by rat inbreeding (Dark-Agouti, Fischer 344) and albinism (Wistar, Sprague–Dawley) but not domestication (wild rat vs. Long-Evans, Fischer-Norway). Behav. Brain Res. 134, 467–477.
Hefti, B.J., Smith, P.H., 2000. Anatomy, physiology and synaptic responses of layer V cells in rat auditory cortex: characterization and study of inhibition through intracellular GABAA blockade. J. Neurophysiol. 83, 2626–2638.
Hefti, B.J., Smith, P.H., 2003. Distribution and kinetic properties of GABAergic inputs to layer V pyramidal cells in rat auditory cortex. J. Assoc. Res. Otolaryngol. 4, 106–121.
Hwang, I.K., Kim, D.S., Lee, H.Y., Lee, J.Y., Choi, G.P., Lee, D.I., Kim, J.D., Lee, Y.B., Sohn, H.S., Kang, T.C., Won, M.H., 2003. Age-related changes of parvalbumin immunoreactive neurons in the rat main olfactory bulb. Mol. Cells 16, 302–306.
Iacopino, A.M., Christakos, S., 1990. Specific reduction of calcium-binding protein (28-kilodalton calbindin-D) gene expression in aging and neurodegenerative diseases. Proc. Natl. Acad. Sci. U. S. A. 87, 4078–4082.
Idrizbegovic, E., Canlon, B., Bross, L.S., Willott, J.F., Bogdanovic, N., 2001. The total number of neurons and calcium binding protein positive neurons during aging in the cochlear nucleus of CBA/CaJ mice: a quantitative study. Hear. Res. 158, 102–115.
Idrizbegovic, E., Bogdanovic, N., Willott, J.F., Canlon, B., 2004. Age-related increases in calcium-binding protein immunoreactivity in the cochlear nucleus of hearing impaired C57BL/6J mice. Neurobiol. Aging 25, 1085–1093.
Idrizbegovic, E., Salman, H., Niu, X., Canlon, B., 2006. Presbyacusis and calcium-binding protein immunoreactivity in the cochlear nucleus of BALB/c mice. Hear. Res. 216–217, 198–206.
Jinno, S., Kosaka, T., 2002. Patterns of expression of calcium binding proteins and neuronal nitric oxide synthase in different populations of hippocampal GABAergic neurons in mice. J. Comp. Neurol. 449, 1–25.
Jinno, S., Kosaka, T., 2006. Cellular architecture of the mouse hippocampus: a quantitative aspect of chemically defined GABAergic neurons with stereology. Neurosci. Res. 56, 229–245.
Jones, E.G., 2003. Chemically defined parallel pathways in the monkey auditory system. Ann. N. Y. Acad. Sci. 999, 218–233.
Khachaturian, Z.S., 1989. The role of calcium regulation in brain aging: re-examination of a hypothesis. Aging 1, 17–34.
Kim, S.A., Jeon, J.H., Son, M.J., Cha, J., Chun, M.H., Kim, I.B., 2010. Changes in transcript and protein levels of calbindin D28k, calretinin and parvalbumin, and numbers of neuronal populations expressing these proteins in an ischemia model of rat retina. Anat. Cell Biol. 43, 218–229.
Kishimoto, J., Tsuchiya, T., Cox, H., Emson, P.C., Nakayama, Y., 1998. Age-related changes of calbindin-D28k, calretinin, and parvalbumin mRNAs in the hamster brain. Neurobiol. Aging 19, 77–82.
Krzywkowski, P., De Bilbao, F., Senut, M.C., Lamour, Y., 1995. Age-related changes in parvalbumin- and GABA-immunoreactive cells in the rat septum. Neurobiol. Aging 16, 29–40.
Kubota, Y., Hattori, R., Yui, Y., 1994. Three distinct subpopulations of GABA-ergic neurons in rat frontal agranular cortex. Brain Res. 649, 159–173.
Markram, H., Toledo-Rodriguez, M., Wang, Y., Gupta, A., Silberberg, G., Wu, C., 2004. Interneurons of the neocortical inhibitory system. Nat. Rev. Neurosci. 5, 793–807.
Mattson, M.P., 2007. Calcium and neurodegeneration. Aging Cell 6, 337–350.
Mattson, M.P., Rychlik, B., Chu, C., Christakos, S., 1991. Evidence for calcium-reducing and excito-protective roles for the calcium-binding protein calbindin-D28k in cultured hippocampal neurons. Neuron 6, 41–51.

Mayhew, T.M., Gundersen, H.J.G., 1996. 'If you assume, you can make an ass out of u and me': a decade of the disector for stereological counting of particles in 3D space. J. Anat. 188, 1–15.
Mazelová, J., Popelar, J., Syka, J., 2003. Auditory function in presbycusis: peripheral vs. central changes. Exp. Gerontol. 38, 87–94.
Mikkonen, M., Alafuzoff, I., Tapiola, T., Soininen, H., Miettinen, R., 1999. Subfield and layer-specific changes in parvalbumin, calretinin and calbindin-D28K immunoreactivity in the entorhinal cortex in Alzheimer's disease. Neuroscience 92, 515–532.
Moyer Jr., J.R., Furtak, S.C., McGann, J.P., Brown, T.H., 2011. Aging-related changes in calcium-binding proteins in rat perirhinal cortex. Neurobiol. Aging 32, 1693–1706.
Narayan, R., Ergün, A., Sen, K., 2005. Delayed inhibition in cortical receptive fields and the discrimination of complex stimuli. J. Neurophysiol. 94, 2970–2975.
Ng, M.C., Iacopino, A.M., Quintero, E.M., Marches, F., Sonsalla, P.K., Liang, C.L., Speciale, S.G., German, D.C., 1996. The neurotoxin MPTP increases calbindin-D28k levels in mouse midbrain dopaminergic neurons. Brain Res. Mol. Brain Res. 36, 329–336.
O'Neill, W.E., Zettel, M.L., Whittemore, K.R., Frisina, R.D., 1997. Calbindin D-28k immunoreactivity in the medial nucleus of the trapezoid body declines with age in C57BL/6, but not CBA/CaJ, mice. Hear. Res. 112, 158–166.
Ouda, L., Druga, R., Syka, J., 2008. Changes in parvalbumin immunoreactivity with aging in the central auditory system of the rat. Exp. Gerontol. 43, 782–789.
Palombi, P.S., Caspary, D.M., 1996. Physiology of the aged Fischer 344 rat inferior colliculus: responses to contralateral monaural stimuli. J. Neurophysiol. 76, 3114–3125.
Palop, J.J., Jones, B., Kekonius, L., Chin, J., Yu, G.Q., Raber, J., Masliah, E., Mucke, L., 2003. Neuronal depletion of calcium-dependent proteins in the dentate gyrus is tightly linked to Alzheimer's disease-related cognitive deficits. Proc. Natl. Acad. Sci. U. S. A. 100, 9572–9577.
Palop, J.J., Mucke, L., Roberson, E.D., 2011. Quantifying biomarkers of cognitive dysfunction and neuronal network hyperexcitability in mouse models of Alzheimer's disease: depletion of calcium-dependent proteins and inhibitory hippocampal remodeling. Methods Mol. Biol. 670, 245–262.
Paxinos, G., Watson, C., 1998. The Rat Brain in Stereotaxic Coordinates. Academic Press, New York.
Popelar, J., Groh, D., Mazelova, J., Syka, J., 2003. Cochlear function in young and adult Fischer 344 rats. Hear. Res. 186, 75–84.
Popelar, J., Groh, D., Pelanova, J., Canlon, B., Syka, J., 2006. Age-related changes in cochlear and brainstem auditory functions in Fischer 344 rats. Neurobiol. Aging 27, 490–500.
Riascos, D., De Leon, D., Baker-Nigh, A., Nicholas, A., Yukhananov, R., Bu, J., Wu, C.K., Geula, C., 2011. Age-related loss of calcium buffering and selective neuronal vulnerability in Alzheimer's disease. Acta Neuropathol. 122, 565–576.
Shetty, A.K., Turner, D.A., 1998. Hippocampal interneurons expressing glutamic acid decarboxylase and calcium-binding proteins decrease with aging in Fischer 344 rats. J. Comp. Neurol. 394, 252–269.
Suta, D., Rybalko, N., Pelánová, J., Popelář, J., Syka, J., 2011. Age-related changes in auditory temporal processing in the rat. Exp. Gerontol. 46, 739–746.
Syka, J., 2002. Plastic changes in the central auditory system after hearing loss, restoration of function, and during learning. Physiol. Rev. 82, 601–636.
Syka, J., 2010. The Fischer 344 rat as a model of presbycusis. Hear. Res. 264, 70–78.
Tardif, E., Chiry, O., Probst, A., Magistretti, P.J., Clarke, S., 2003. Patterns of calcium-binding proteins in human inferior colliculus: identification of subdivisions and evidence for putative parallel systems. Neuroscience 116, 1111–1121.
Turner, J.G., Hughes, L.F., Caspary, D.M., 2005a. Effects of aging on receptive fields in rat primary auditory cortex layer V neurons. J. Neurophysiol. 94, 2738–2747.
Turner, J.G., Hughes, L.F., Caspary, D.M., 2005b. Divergent response properties of layer-V neurons in rat primary auditory cortex. Hear. Res. 202, 129–140.
Van Brederode, J.F.M., Helliesen, M.K., Hendrickson, A.E., 1991. Distribution of CaBPs parvalbumin and calbindin-D28 in the sensorimotor cortex of the rat. Neuroscience 44, 157–171.
Verkhratsky, A., Toescu, E.C., 1998. Calcium and neuronal ageing. Trends Neurosci. 21, 2–7.
Walton, J.P., Simon, H., Frisina, R.D., 2002. Age-related alterations in the neural coding of envelope periodicities. J. Neurophysiol. 88, 565–578.
Wang, J., McFadden, S.L., Caspary, D., Salvi, R., 2002. Gamma-aminobutyric acid circuits shape response properties of auditory cortex neurons. Brain Res. Interact. 944, 219–231.
West, M.J., Slomianka, L., Gundersen, H.J., 1991. Unbiased stereological estimation of the total number of neurons in the subdivisions of the rat hippocampus using the optical fractionator. Anat. Rec. 231, 482–497.
Winer, J.A., Larue, D.T., 1996. Evolution of GABAergic circuitry in the mammalian medial geniculate body. Proc. Natl. Acad. Sci. U. S. A. 93, 3083–3087.
Woo, N.H., Lu, B., 2006. Regulation of cortical interneurons by neurotrophins: from development to cognitive disorders. Neuroscientist 12, 43–56.
Zettel, M.L., Frisina, R.D., Haider, S.E., O'Neill, W.E., 1997. Age-related changes in calbindin D-28k and calretinin immunoreactivity in the inferior colliculus of CBA/CaJ and C57Bl/6 mice. J. Comp. Neurol. 386, 92–110.
Zettel, M.L., O'Neill, W.E., Trang, T.T., Frisina, R.D., 2001. Early bilateral deafening prevents calretinin up-regulation in the dorsal cortex of the inferior colliculus of aged CBA/CaJ mice. Hear. Res. 158, 131–138.
Zilles, K., 1985. The Cortex of the Rat, A Stereotaxic Atlas. Springer-Verlag, Berlin.

Experimental Gerontology 47 (2012) 966–973

Contents lists available at SciVerse ScienceDirect

Experimental Gerontology

journal homepage: www.elsevier.com/locate/expgero

Age-related changes in the acoustic startle reflex in Fischer 344 and Long Evans rats

Natalia Rybalko [a,*], Zbyněk Bureš [a,b], Jana Burianová [a], Jiří Popelář [a], Paul W.F. Poon [c], Josef Syka [a]

[a] Institute of Experimental Medicine, Academy of Sciences of the Czech Republic, Prague, Czech Republic
[b] College of Polytechnics, Jihlava, Czech Republic
[c] Dept. of Physiology, Medical School, National Cheng Kung University, Tainan, Taiwan

ARTICLE INFO

Article history:
Received 2 April 2012
Received in revised form 20 July 2012
Accepted 5 September 2012
Available online 12 September 2012

Section Editor: Christian Humpel

Keywords:
Fischer 344 rat
Long Evans rat
Acoustic startle response
Prepulse inhibition
Presbycusis

ABSTRACT

The behavioral consequences of age-related changes in the auditory system were studied in Fischer 344 (F344) rats as a model of fast aging and in Long Evans (LE) rats as a model of normal aging. Hearing thresholds, the strength of the acoustic startle responses (ASRs) to noise and tonal stimuli, and the efficiency of the prepulse inhibition (PPI) of ASR were assessed in young-adult, middle-aged, and aged rats of both strains. Compared with LE rats, F344 rats showed larger age-related hearing threshold shifts, and the amplitudes of their startle responses were mostly lower. Both rat strains demonstrated a significant decrease of startle reactivity during aging. For tonal stimuli, this decrease occurred at an earlier age in the F344 rats: middle-aged F344 animals expressed similar startle reactivity as aged F344 animals, whereas middle-aged LE animals had similar startle reactivity as young-adult LE animals. For noise stimuli, on the other hand, a similar progression of age-related ASR changes was found in both strains. No significant relationship between the hearing thresholds and the ASR amplitudes was found within any age group. Auditory PPI was less efficient in F344 rats than in LE rats. An age-related reduction of the PPI of ASR was observed in rats of both strains; however, a significant reduction of PPI occurred only in aged rats. The results indicate that the ASR may serve as an indicator of central presbycusis.

© 2012 Elsevier Inc. All rights reserved.

1. Introduction

Hearing loss associated with the aging process (presbycusis) is the most common cause of chronic, permanent hearing disability in both animals and humans (Gates and Mills, 2005; Syka, 2002; Willott, 1991). Pathological changes occur in presbycusis in both the inner ear and in the central auditory system. The peripheral component of presbycusis, which comprises mainly alterations of the inner and outer hair cells and/or the stria vascularis, is relatively well understood (Harding et al., 2005; Parham, 1997; Schuknecht and Gacek, 1993; Spongr et al., 1997). The central component of presbycusis is thought to be especially associated with age-related decline in the processing of complex acoustical stimuli including human speech (Gordon-Salant, 2005; Willott, 1991). In the human population, a loss of speech understanding with aging constitutes an important health and social impairment (Frisina and Frisina, 1997; Gordon-Salant et al., 2007; Mazelová et al., 2003).

Rodents with a life span of two to three years represent a suitable laboratory model to study the processes associated with the age-related deterioration of the auditory system. In our previous studies (for review see Syka, 2010) two rat strains were used as models of normal and fast aging: Long Evans (LE) rats — an outbred strain with normal aging and preserved hearing function up to late senescence, and Fischer 344 (F344) rats — an inbred strain with a frequent occurrence of pathologies, including an early deterioration of hearing function. Age-related alterations in the function of the inner ear in F344 rats, including pathology of the hair cells, stria vascularis and ligamentum spirale, have been described in detail and compared systematically with the age-related changes in LE rats (Buckiová et al., 2006, 2007; Popelář et al., 2003, 2006). Age-related changes in the function of the inner ear were found to be accompanied in both strains by pathologies in the central part of the auditory system, which comprised a significant decline in glutamic acid decarboxylase (GAD) levels and changes in the occurrence of parvalbumin-immunoreactive neurons (Burianová et al., 2009; Ouda et al., 2008). Another of our recent studies also demonstrated the existence of age-related changes in the temporal processing of acoustical signals in LE rats (Šuta et al., 2011).

In the present study, we decided to use the same model of fast aging F344 rats and normally aging LE rats for assessing the influence of aging on behavioral reactions to auditory stimuli. Therefore, the acoustic startle reflex (ASR) (a transient motor response to an intense unexpected stimulus) was used as an indicator of the behavioral responsiveness to sound stimuli. As the ASR is an unconditioned reflex reaction, there is no need for animal training, and the ASR can be measured at any age. The structural basis of the ASR is represented by a short neural circuit comprising the cochlear nucleus, the caudal pontine reticular nucleus and spinal motor neurons (Davis et al.,

Abbreviations: F344, Fischer 344; LE, Long Evans; ASR, acoustic startle response; PPI, prepulse inhibition; ABRs, auditory brainstem responses; WN, white noise.

* Corresponding author at: Institute of Experimental Medicine, Academy of Sciences of the Czech Republic, Vídeňská 1083, 142 20 Prague 4, Czech Republic. Tel.: +420 24106 2689; fax: +420 24106 2787.
E-mail address: rybalko@biomed.cas.cz (N. Rybalko).

0531-5565/$ – see front matter © 2012 Elsevier Inc. All rights reserved.
http://dx.doi.org/10.1016/j.exger.2012.09.001

1982; Koch, 1999). In spite of its relative simplicity, the ASR shows several forms of behavioral plasticity (habituation, facilitation and prepulse inhibition) that are functionally significant and reflect the processing of acoustic information at higher levels of the auditory system than the ASR itself (Ison and Hammond, 1971; Koch, 1999; Young and Fechter, 1983).

The ASR may be used to assess behavioral responses only to louder auditory stimuli (higher than approximately 70 dB SPL). To determine the auditory function in the range of intensities below the startling threshold, the measurement of the prepulse inhibition (PPI) of ASR is widely used in both human and animal studies. In the PPI procedure, the startle reaction is inhibited by a low-level sound that shortly precedes the intense startle stimulus. Animal studies have shown that auditory PPI is associated with the function of the cochlear nucleus, the inferior and superior colliculi and the pedunculopontine tegmental nucleus (Koch, 1999). The efficacy of the PPI undergoes a considerable modulating influence of the hippocampus, amygdala and the medial prefrontal cortex (Swerdlow et al., 2001). The PPI of ASR, which represents a basic inhibitory process regulating sensory inputs (Geyer and Braff, 1987; Swerdlow et al., 2001), may be used for estimating the age-related changes in inhibitory function.

The aim of the present study was to evaluate age-related changes in auditory behavior in rat strains with fast and normal aging and to estimate the behavioral correlates of auditory system aging in animals with the presence or absence of hearing loss. The hearing threshold in rats was assessed by recording of auditory brainstem responses (ABR). The strength of the acoustic startle response and the efficiency of the prepulse inhibition of ASR to noise and tonal stimuli were measured and compared in young-adult (approximately 3 months old), middle-aged (approximately 12 months old), and aged (older than 23 months) animals of the F 344 and LE rat strains.

2. Methods

Behavioral and electrophysiological testing of hearing function in Fischer 344 and Long Evans female rats of different ages was performed in this study using measurement of the ASR and its suppression by acoustic prepulse stimuli and the assessment of the rat's hearing threshold on the basis of the recording of ABR.

2.1. Subjects

The measurements were performed in three age groups: young-adult rats (3–5 months old: 10 rats of the F344 strain, mean body weight 198 ± 15 g, and 9 rats of the LE strain, mean body weight 246 ± 14 g), middle-aged rats (12–14 months old: 6 rats of the F344 strain, mean body weight 277 ± 13 g, and 5 rats of the LE strain, mean body weight 334 ± 14 g) and aged rats (24–26 months old: 7 rats of the F344 strain, mean body weight 291 ± 18 g, and 24–34 months old, n = 9 rats of the LE strain, mean body weight 338 ± 9 g). The range of animal ages in the aged F344 group was narrower than in LE rats due to differences in their lifespan (the life span for F344 rats is about 6–8 months shorter than for LE rats (Sass et al., 1975; Hoffman, 1979). For this reason, the aged LE group was divided into two subgroups that were evaluated separately: group LE-A1 with 24–26-month-old rats (n = 5, mean body weight 339 ± 14 g), and group LE-A2 with 29–34-month-old rats (n = 4 mean body weight 337 ± 37 g). This allowed us to compare both age-matched F344 and LE rats, and also the oldest animals of both strains. Animals in all age groups were in good health conditions; the testing period for each rat did not exceed three weeks. In each rat the normal otoscopic status of the outer ear canal and middle ear was controlled periodically using HEINE mini 2000 otoscope to exclude a middle ear infection.

Fischer 344 rats were purchased from Charles River Deutschland (Sulzfeld, Germany), while Long Evans rats were obtained from a local facility. All animals were housed in age-matched groups of two or three per cage under standard laboratory conditions in a constant environment and a 12/12 h normal light/dark cycle; food and water were available ad libitum. The care and use of animals and all experimental procedures were performed in compliance with the guidelines of the Ethical Committee of the Institute of Experimental Medicine, Academy of Sciences of the Czech Republic, and followed the guidelines of the EU Directive 2010/63/EU for animal experiments.

2.2. Apparatus and procedures

All behavioral tests were performed in a sound attenuated chamber (Coulbourn Habitest, model E10-21) located in a soundproof room. During the testing procedure, the rat was confined to a small wire mesh cage (160 × 85 × 90 mm) on a motion-sensitive platform. The animal's reflex movements were detected and transduced by a piezoelectric accelerometer. The amplified voltage signal was acquired and processed using a TDT system III with Enhanced Real-Time Processor RP2.1 (Tucker Davis Technologies, Florida, USA) and custom-made software in the Matlab environment (The MathWorks, Inc.). The startle responses were evaluated in a 100 ms window beginning at the onset of the startle stimulus. The magnitude of the ASR was given by the maximal peak-to-peak amplitude of transient voltage occurring in the response window. Acoustic startle stimuli (tone pips or noise bursts) and prepulse stimuli (tone pips) were generated by the TDT system and presented via a loudspeaker (SEAS, 29AF/W) placed 12 cm above the platform inside the chamber. Stimulus presentation and data acquisition were controlled by a custom-made application in the Matlab environment. Calibration of the apparatus was performed for frequencies between 1 kHz and 32 kHz by a 1/4 in. Brüel & Kjaer 4939 microphone connected to a Brüel & Kjaer ZC 0020 preamplifier and a B&K 2231 sound level meter. The calibrating microphone was positioned in the location of the animal's head in the test cage.

The ASRs to 4, 8, and 16 kHz tone pips and white noise (WN) bursts (50 ms duration, 5 ms rise/fall times, varying intensity levels) were recorded. Each test session contained 7 trial types presented in a random order: a baseline trial (–10 dB SPL stimulus intensity) and 7 startle stimuli of different intensities (60, 70, 80, 90, 100, 110, and 120 dB SPL). Each trial type was presented ten times. The inter-trial interval varied from 15 to 30 s. The mean ASR amplitude of each trial type was calculated as the average of all the ASR amplitudes for that given trial type with the highest and lowest ASR amplitudes excluded. A trial was considered to have evoked a startle reaction if the mean ASR amplitude for that trial exceeded the average amplitude of the baseline trial (0.03 ± 0.008 V) by more than twice the standard deviation (i.e., it was more than approximately 0.05 V). Thereafter, the ASR threshold was determined as the minimum intensity at which there was a startle reaction for at least 50% of the trials.

In the prepulse inhibition procedure, 3 different trial types were used: a baseline trial without any stimulus, an acoustic startle pulse alone (white noise at 115 dB SPL, 50 ms, 5 ms rise/fall times), and a combination of the startle pulse and prepulse tone pips (50 ms duration, 5 ms rise/fall time) at frequencies of 4, 8, and 16 kHz at 75 dB SPL. The inter-stimulus interval between the prepulse and the startle stimulus was set to 50 ms. Each of the trial types was presented ten times. The inter-trial interval varied from 15 to 30 s. The efficacy of the PPI of ASR was expressed as:

$$\mathrm{PPI} = [1 - (\text{amplitude of ASR suppressed by prepulse tone} / \text{amplitude of ASR alone})] \times 100\%.$$

Thus, a PPI of 100% corresponds to complete suppression of the ASR, and higher percentages indicate stronger PPI.

To assess the hearing thresholds in rats, ABRs to tonal stimuli were recorded in anesthetized rats with an intramuscular injection of 38 mg/kg body weight of ketamine (Calypsol, Gedeon Richter Ltd.)

and 5 mg/kg body weight of xylazine (Sedazine, Fort Dodge) using three stainless-steel needle electrodes, placed subcutaneously over the vertex (positive) and the right and left mastoids (negative and ground electrodes) of the animal. The signal from the electrodes was amplified by a TDT RA4LI and RA16PA amplifier (filters 300 Hz–3 kHz) and processed with a TDT data acquisition system (RX5-2 Pentusa Base Station, Tucker-Davis Technologies, Gainesville, FL; 16-bit A/D converter, sampling rate 25 kHz) using BioSig software. Acoustic stimuli for the ABR recordings were generated by a TDT RP2.1 Enhanced Real-Time Processor and presented with a repetition rate of 11 Hz in free-field conditions via two loudspeakers (Jamo woofer and SEAS T25CF 002 tweeter) placed 70 cm in front of the animal's head. Tone bursts (burst duration 3 ms, 1 ms rise/fall times) in one-octave steps, ranging from 2 to 32 kHz were used. The acoustic system was calibrated with a B&K 4939 microphone, a ZC0020 preamplifier, and a B&K 2231 sound level meter. The microphone was placed in the position of the animal's head and facing the speakers. The hearing threshold at each frequency was determined visually by reducing the stimulus intensity from the suprathreshold level in 5 dB steps to obtain a visually just-detectable response in the expected time window of the recorded signal. As a rule, responses to 250 acoustical stimuli were averaged.

2.3. Statistical analysis

Most of the parameters of interest: ABR thresholds, ASR thresholds, ASR amplitudes, and PPI of ASR, were evaluated in two ways: across-strain comparisons between age-matched animal groups (comparing, for example, young-adult F344 and young-adult LE rats), and age-related dependence within each rat strain (comparing, for example, young-adult and middle-age F344 rats). This approach allowed us to lower the number of free variables in each test and hence to use two-dimensional tests instead of three-dimensional ones, and to focus more precisely on the selected parameter by omitting the data that did not carry any relevant information. All tests employed two-way repeated-measures ANOVA with the Bonferroni posthoc test. The repeated-measures matching reflected the fact that each tested animal provided parameter values at all tested spectral contents: tones at 2, 4, 8, 16 and 32 kHz in the case of ABR thresholds, white noise and tones at 4, 8 and 16 kHz in the case of ASR thresholds and amplitudes, and tones at 4, 8 and 16 kHz in the case of PPI of ASR. The first type of analysis used three tests (one for each age group: young-adult, middle-age, aged), the grouping variables were stimulus spectral content and rat strain. In the second type of analysis, two tests were performed (one for each strain), the grouping variables were stimulus spectral content and age. Despite the fact that the ASR reactivity was measured at several levels of the startle stimulus, the statistical evaluation of ASR amplitudes was carried out at a single stimulus intensity, 120 dB SPL.

To test whether there was any dependence of the ASR amplitude on the hearing threshold, linear regression analysis was used, with an additional F-test to determine whether the slope of the linear fit was significantly different from zero.

3. Results

3.1. ABR hearing thresholds

An estimation of hearing sensitivity based on ABR recording was conducted in each rat. The mean ABR thresholds evaluated for both strains in the individual age groups are shown in Fig. 1.

Comparing the hearing thresholds between the two strains, we found that ABR thresholds in young-adult F344 rats tended to be slightly higher than in age-matched LE rats (see also Table 5, test ABR-Y); the differences were significant only at 32 kHz ($p<0.01$). In the middle-aged group, F344 rats already had significantly higher ABR thresholds than age-matched LE rats in the whole frequency range (see also Table 5, test ABR-M). A comparison of the hearing thresholds in the aged group revealed a similar impairment in both strains (animal groups F344 aged, LE-A1 and LE-A2); significantly higher ABR thresholds in F344 rats were present only at 32 kHz (see also Table 5, test ABR-A).

Comparing the age-related threshold elevations within each strain, the results show that for frequencies 16–32 kHz, the hearing thresholds were already significantly elevated in the middle-aged F344 rats; further deterioration of the hearing thresholds across the whole frequency range occurred during the second year of life (see also Table 5, test ABR-F344). In contrast to the F344 strain, the hearing thresholds in middle-aged LE rats were similar to those of young-adult LE rats (see also Table 5, test ABR-LE). A slight, but not significant increase of the hearing threshold relative to that of the young-adult animals was observed in the 24-26-month-old LE rats (aged group LE-A1, see also the Methods section), while a significant elevation of the hearing threshold relative to that of the young-adult animals was found only in the oldest LE rats (aged group LE-A2, 29–34 months old).

3.2. Acoustic startle response

The results of the experiments showed that the acoustic startle reactivity was different in F344 and LE rats; in addition, different age-related changes in the ASR amplitude were observed in each strain.

Comparing the ASR thresholds in age-matched F344 and LE rats, the mean values were similar in young-adult (see also Table 5, test ASRt-Y), middle-age (see also Table 5, test ASRt-M), and in aged animals (animal groups F344 aged, LE-A1 and LE-A2; see also Table 5, test ASRt-A). The

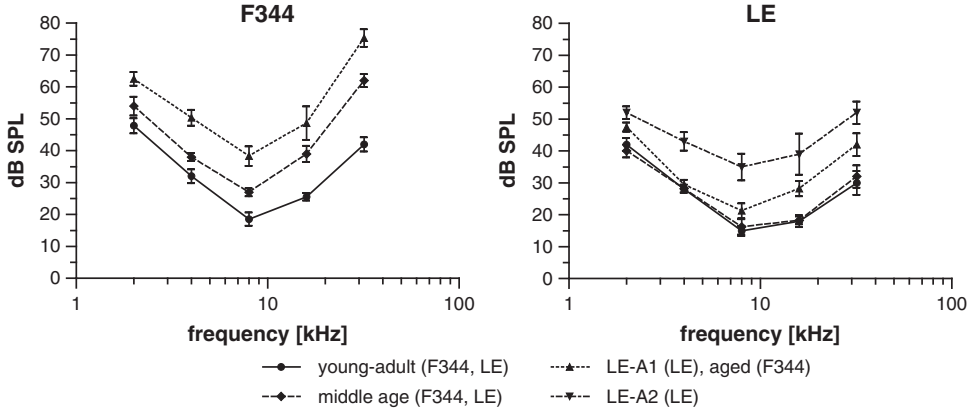

Fig. 1. Average hearing thresholds (mean ± SEM) in young-adult, middle-aged, and aged F344 and LE rats. Aged LE rats were divided into two subgroups: LE-A1 (24–26-month-old rats) and LE-A2 (29–34-month-old rats), see the Methods section.

ASR thresholds in both strains ranged between 75 and 90 dB SPL for 4–16 kHz tones with a shift toward larger values at higher frequencies, and 70–75 dB SPL for white noise. There was a trend of higher ASR thresholds in the aged rats, especially at higher frequencies. The differences in comparison with young-adult rats were not significant in F344 rats (see also Table 5, test ASRt-F344); in LE rats, there was a significant increase of ASR threshold in the oldest animals compared with young-adult rats at 8 and 16 kHz (see also Table 5, test ASRt-LE).

Fig. 2 shows average amplitude-intensity ASR functions for young-adult, middle-aged, and aged rats of the F344 and LE strains obtained for noise-bursts and tone-pips of various frequencies (4, 8, 16 kHz). Due to monotonic course of ASR amplitude-intensity functions and similar ASR changes at different intensities the statistical evaluation of the startle reactivity was performed at a single stimulus intensity, 120 dB SPL, that evoked usually a maximal ASR amplitude (Tables 1 and 2).

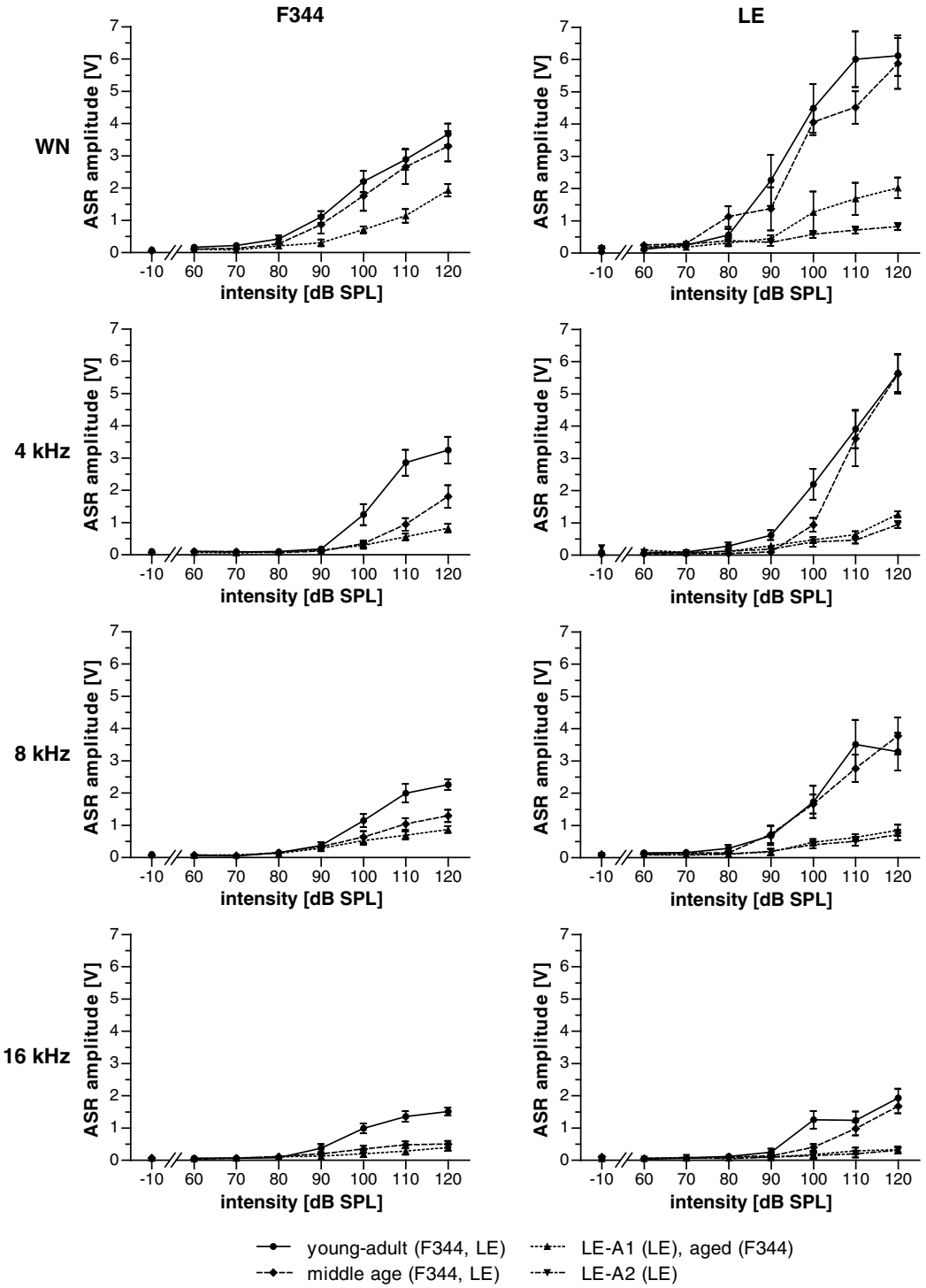

Fig. 2. Amplitude-intensity ASR functions (mean ± SEM) for young-adult, middle-aged, and aged F344 and LE rats obtained for white noise (WN) and tone pips of 4, 8, and 16 kHz. Aged LE rats were divided into two subgroups: LE-A1 (24–26-month-old rats) and LE-A2 (29–34-month-old rats), see the Methods section.

Table 1
Summary of the dependence of ASR amplitude on the rat strain (mean ± SEM, two-way repeated-measures ANOVAs with Bonferroni post-hoc tests, statistical significance expressed with symbols: ns — not significant, * — $p<0.05$, ** — $p<0.01$, and *** — $p<0.001$). Aged LE rats were divided into two subgroups: LE-A1 (24–26-month-old rats) and LE-A2 (29–34-month-old rats), see the Methods section.

	Young-adult		Middle-aged		Aged		
	F344	LE	F344	LE	F344	LE-A1	LE-A2
WN	3.7 ± 0.3 ***	6.2 ± 0.6	3.3 ± 0.5 ***	5.9 ± 0.9	1.9 ± 0.2 ns	2.0 ± 0.4	0.8 ± 0.1
4 kHz	3.2 ± 0.4 ***	5.6 ± 0.6	1.8 ± 0.4 ***	5.6 ± 0.7	0.8 ± 0.1 ns	1.3 ± 0.1	0.9 ± 0.1
8 kHz	2.3 ± 0.2 ns	3.3 ± 0.6	1.3 ± 0.2 ***	3.8 ± 0.6	0.9 ± 0.1 ns	0.8 ± 0.2	0.7 ± 0.2
16 kHz	1.5 ± 0.1 ns	1.9 ± 0.3	0.5 ± 0.1 ns	1.7 ± 0.2	0.4 ± 0.04 ns	0.3 ± 0.04	0.3 ± 0.1

Comparing the two strains of rats, the amplitudes of the startle responses were generally lower in the F344 rats (Fig. 2, Table 1). The difference was more pronounced for noise-bursts and low frequency tones and was manifested especially in young-adult and middle-aged animals: white noise and 4 kHz tones elicited approximately two-fold smaller ASR amplitudes in young-adult and middle-aged F344 rats in comparison with age-matched LE rats. In young-adult rats, the amplitude differences between the F344 and LE rats were significant only for noise bursts and tones at 4 kHz (see also Table 5, test ASRa-Y); in middle-aged rats, significantly lower ASR amplitudes were observed in F344 rats for noise bursts and tones at 4 to 8 kHz (see also Table 5, test ASRa-M). In the aged rats, the ASR amplitudes were similar in both strains (animal groups F344 aged, LE-A1 and LE-A2) irrespective of the stimulus (see also Fig. 2, Table 1) (see also Table 5, test ASRa-A).

During aging, the rats of both strains demonstrated a decrease in their startle reactivity; however, the age-related decrease in ASR amplitudes occurred at an earlier age in F344 rats compared with the LE rats (Table 2). In F344 rats, the age-related decrease in the amplitude of the ASR to tonal stimuli was already evident at 12–14 months of age: for tone-pips of all frequencies, the ASR amplitudes were significantly lower in the middle-aged F344 rats compared with the young-adult F344 rats (see also Table 5, test ASRa-F). Importantly, there was no significant difference between the ASR amplitudes of middle-aged and aged F344 rats for tonal stimuli. In contrast to the tonal stimuli, white noise stimuli elicited similar ASR strengths in young-adult and middle-aged F344 rats and significantly larger ASR amplitudes in middle-aged F344 rats compared with aged F344 rats. In LE rats, on the other hand, there was no significant difference between the ASR amplitudes of middle-aged and young-adult animals; furthermore, aged LE rats of both subgroups had significantly smaller ASR amplitudes than middle-aged LE rats for all stimuli except for the 16 kHz tone (see also Table 5, test ASRa-L). In summary, in F344 rats, middle-aged animals tended to have similar startle reactivity as aged animals, whereas in LE rats, middle-aged animals had similar startle reactivity as young-adult animals.

In the rats of both strains, the strength of the ASR exhibited a substantial dependence on the spectral content of the stimulus (see, e.g., Fig. 2). Generally, broad-band noise and low frequency tones evoked considerably higher ASR amplitudes than high frequency tones. The ASRs to tonal stimuli exhibited a similar frequency-related behavior in both rat strains: the ASRs to 4 kHz and 8 kHz tones were significantly different only in young-adult animals, the ASRs to 4 kHz and 16 kHz tones were significantly different in young-adult and middle-age groups, the ASRs to 8 kHz and 16 kHz tones were not significantly different in any age group. On the other hand, the ASR reactions to a broad-band noise relative to tonal stimuli were different in the two strains. In the LE rats, there was no significant difference between ASRs to white noise and to 4 kHz tones in any age group. Noise bursts only elicited significantly higher ASR amplitudes than 8 kHz tones in young-adult group and than 16 kHz tones in young-adult and middle-age groups (see also Table 5, test ASRa-L). In the F344 rats, however, noise bursts evoked significantly higher responses than all tonal stimuli in all age groups, except for the 4 kHz tone in young-adult group (see also Table 5, test ASRa-F).

As the average ABR thresholds elevated with aging and the average ASR amplitudes decreased with aging, we tested the possibility that these two parameters are correlated. In each age group in each rat strain, a linear regression fit was used to quantify the dependence of the ASR amplitude on hearing loss in individual animals. No statistical deviation of the linear fit from zero slopes was found, leading to the conclusion that there is no significant dependence of the ASR amplitude on hearing loss. In other words, an elevated ABR threshold does not generally imply lower ASR amplitude.

3.3. Prepulse Inhibition of the acoustic startle response (PPI of ASR)

The results indicate that auditory PPI of ASR provided by a tone of 75 dB SPL was generally less efficient in F344 rats compared with LE rats (see Table 3); the differences were dependent on the rat's age and the stimulus frequency. In young-adult rats, significantly less suppression of the ASR was found in F344 rats compared with the LE rats at all tested frequencies (see also Table 5, test PPI-Y). In the middle-age group, significant differences between the two strains were found only at 4 kHz (see also Table 5, test PPI-M). In the aged group, no significant differences between the two strains were

Table 2
Statistical summary of the dependence of ASR on age (two-way repeated-measures ANOVAs with Bonferroni post-hoc tests, significant difference of means marked with < or > signs, statistical significance expressed with symbols: ns — not significant, * — $p<0.05$, ** — $p<0.01$, and *** — $p<0.001$). The rats' ages are denoted with the letters Y, M, and A, which correspond to the young-adult, middle-aged and aged groups, respectively. Aged LE rats were divided into two subgroups: LE-A1 (24–26-month-old rats) and LE-A2 (29–34-month-old rats), see the Methods section.

	F344 rats		LE rats		
	M vs. Y	M vs. A	M vs. Y	M vs. LE-A1	LE-A1 vs. LE-A2
WN	ns	**	ns	***	ns
4 kHz	**	ns	ns	***	ns
8 kHz	*	ns	ns	**	ns
16 kHz	*	ns	ns	ns	ns

Table 3
Summary of the dependence of the efficacy of PPI of ASR on the rat strain; the numerical values show the percentage by which an uninhibited ASR amplitude decreased as a result of PPI (mean ± SEM, two-way repeated-measures ANOVAs with Bonferroni post-hoc tests, statistical significance expressed with symbols: ns — not significant, * — $p<0.05$, ** — $p<0.01$, and *** — $p<0.001$). Aged LE rats were divided into two subgroups: LE-A1 (24–26-month-old rats) and LE-A2 (29–34-month-old rats), see the Methods section.

	Young-adult		Middle-age		Aged		
	F344	LE	F344	LE	F344	LE-A1	LE-A2
4 kHz	71.5 ± 1.5 ***	84.7 ± 1.5	69.7 ± 2.2 *	83.8 ± 1.1	59.1 ± 3.9 ns	70.8 ± 2.6	65.6 ± 1.9
8 kHz	75.7 ± 0.8 ***	85.6 ± 0.8	72.6 ± 1.9 ns	84.9 ± 0.7	62.7 ± 3.8 ns	72.6 ± 4.5	62.9 ± 4.7
16 kHz	76.3 ± 1.8 *	82.1 ± 2.1	71.8 ± 5.9 ns	78.7 ± 4.8	64.7 ± 3.7 ns	69.8 ± 1.9	57.7 ± 2.7

Table 4
Statistical summary of the dependence of the efficacy of the PPI of ASR on age (symbols: ns — not significant, * — $p<0.05$, ** — $p<0.01$, and *** — $p<0.001$). The rats' ages are denoted with the letters Y, M and A, which correspond to the young-adult, middle-aged and aged groups, respectively. Aged LE rats were divided into two subgroups: two-way repeated-measures ANOVAs with Bonferroni post-hoc tests, significant difference of means marked with < or > signs, statistical significance expressed with LE-A1 (24–26-month-old rats) and LE-A2 (29–34-month-old rats), see the Methods section.

	F344 rats			LE rats		
	Y vs. M	M vs. A	Y vs. A	M vs. Y	M vs. LE-A1	LE-A1 vs. LE-A2
4 kHz	ns	ns	*	ns	**	ns
8 kHz	ns	ns	*	ns	**	ns
16 kHz	ns	ns	ns	ns	ns	*

found (animal groups F344 aged, LE-A1 and LE-A2; see also Table 5, test PPI-A).

Analogously to the ASR, a reduction in the efficacy of the PPI of ASR with aging was observed in rats of both strains (see Tables 3 and 4). In the F344 rats, the age-related changes in the PPI were statistically significant only when comparing the young-adult and aged groups (see also Table 5, test PPI-F). In LE rats, a significant decrease of the PPI was also found only in aged rats; a further decrease of the PPI of ASR was observed in the oldest LE animals (29–34-month-old LE rats), which was significant at 16 kHz (see also Table 5, test PPI-L).

4. Discussion

The results of the present study show that the acoustic startle reactivity and its age-related changes are different between the fast aging F344 strain of rats and the normal aging LE strain. First of all, F344 rats exhibit smaller ASR amplitudes than LE rats in almost all cases of acoustical stimulation, and the ASR amplitudes in F344 rats decrease with aging faster than in LE rats. Also, the prepulse inhibition is less expressed in F344 rats than in LE rats; however, the relative decrease of the PPI with age progresses in both strains at a similar rate, with a significantly reduced PPI occurring only in aged animals.

Differences between individual strains of rats and mice in terms of ASR and PPI have been described in several previous papers (Błaszczyk and Tajchert, 1996; Glowa and Hansen, 1994; McCaughran et al., 1999; Ouagazzal et al., 2006; Swerdlow et al., 2004; Van den Buuse et al., 2003; Varty and Higgins, 1994). A review of the differences in ASR amplitudes was presented by Glowa and Hansen (1994) when comparing the ASR to 110-dB (A) acoustic startle stimulus in forty-six rat strains. Their data corresponds with our results showing that the amplitude of the ASR in the LE strain is significantly larger than the amplitude of the ASR in F344 rats. There might be several reasons for the differences in ASR amplitudes between the Fischer 344 and the LE rat strains. Webb et al. (2003) observed that Fischer 344 rats are different in several aspects of their morphology, sensory and locomotor abilities compared to Lewis, Long Evans, Sprague–Dawley and Wistar rats. According to their data, Fischer 344 rats are smaller in physical stature, have an increased abduction of their distal hindlimbs, and are more sensitive to mechanical stimulation of their hindlimbs than other strains. The acoustic startle response, although its pathway is relatively simple, may be influenced by these facts, occurring in either the afferent or the efferent part of the response pathway. Interestingly, our data are analogous to the results of Ison and Allen (2003), who reported a lower asymptotic level of acoustic startle reactivity prior to the onset of hearing loss in young C57BL/6 mice compared with CBA mice. These mouse strains are frequently analogously to Fischer 344 and Long Evans rats used as models of fast (C57BL/6) and normal (CBA) aging of the auditory system.

Our results show that the ASR depends on the frequency characteristics of the stimulus. In agreement with previous data (Błaszczyk and Tajchert, 1997; Pilz et al., 1987; Rybalko et al., 2011), the ASRs elicited by broad-band noise stimuli and low-frequency tones were characterized by larger amplitudes compared with those elicited by high-frequency tonal stimuli. The ASR amplitudes in both F344 and LE rats depend also on age: both strains were characterized by a decrease in ASR amplitude with aging, which is consistent with the results of previous studies in rodents (Ison et al., 1997; McFadden et al., 2010; Ouagazzal et al., 2006; Parham and Willott, 1988; Varty et al., 1998) and humans (Ellwanger et al., 2003; Ludewig et al., 2003). However, the decrease of startle reactivity to tones appeared at an earlier age in F344 rats than in LE rats. The finding that middle-aged F344 rats have similar startle reactivity as aged F344 rats, whereas middle-aged LE rats have similar startle reactivity as young-adult LE rats, indicates an earlier onset of presbycusis in F344 animals.

The dynamics of the age-related changes in ASR amplitude in F344 rats were different for tonal and white noise stimuli; in contrast to tonal stimuli, the age-related decrease of the ASR to white noise was manifested only in the aged group. Differences in the age-related change of the startle reaction to noise and tonal stimuli were also observed in mice with early onset hearing loss (Ison and Allen, 2003; McCaughran et al., 1999). The authors associated this phenomenon with central tonotopic reorganization resulting from age-related high-frequency hearing loss, which has behavioral consequences only for sinusoidal startle stimuli. Similarly, we assume that the reaction to noise stimuli may mask the age-related changes that could be detected when tonal startle stimuli are used.

A potential source of differences in the age-related changes of the ASR between F344 and LE rats may be the different time of onset and the severity of the cochlear damage associated with the age-related hearing loss. According to our data, the ABR audiograms in LE rats indicated only small, non-significant age-related hearing threshold elevations until the age of 24–26 months; the hearing thresholds

Table 5
Results of ANOVA tests performed in the study. All tests comprised a two-way repeated-measures ANOVA, hence two grouping variables with the corresponding parameters are listed for each test. The columns denoted Df, F value, and η_p^2 show degrees of freedom, F value along with the statistical significance of the associated F-test (ns — not significant, * — $p<0.05$, ** — $p<0.01$, and *** — $p<0.001$), and partial eta squared (a measure of effect size), respectively. The abbreviations ABR, ASRt, ASRa, and PPI denote tests on ABR hearing thresholds, ASR thresholds, ASR amplitudes at 120 dB SPL, and PPI of ASR, respectively. The letters Y, M, A, F, and L correspond to the tests in young-adult animals, middle-aged animals, aged animals, F344 rats, and Long-Evans rats, respectively. See also Section 2.3 Statistical analysis of the Methods section.

	Grouping variable 1				Grouping variable 2			
	Name	Df	F value	η_p^2	Name	Df	F value	η_p^2
ABR-Y	Strain	1	11.22**	0.07	frequency	4	85.69***	0.73
ABR-M	Strain	1	130.1***	0.31	frequency	4	69.11***	0.53
ABR-A	Strain	2	18.61***	0.29	frequency	4	52.91***	0.44
ABR-F344	Age	2	58.96***	0.30	frequency	4	109.5***	0.56
ABR-LE	Age	3	14.80***	0.30	frequency	4	87.28***	0.50
ASRt-Y	Strain	1	4.29 ns	0.02	frequency, WN	3	38.17***	0.66
ASRt-M	Strain	1	3.62 ns	0.03	frequency, WN	3	23.71***	0.63
ASRt-A	Strain	2	1.99 ns	0.03	frequency, WN	3	21.01***	0.54
ASRt-F344	Age	2	2.73 ns	0.03	frequency, WN	3	37.56***	0.59
ASRt-LE	Age	3	5.84**	0.08	frequency, WN	3	37.98***	0.53
ASRa-Y	Strain	1	22.77***	0.16	frequency, WN	3	26.19***	0.42
ASRa-M	Strain	1	55.42***	0.35	frequency, WN	3	20.18***	0.38
ASRa-A	strain	2	7.28**	0.07	frequency, WN	3	29.07***	0.48
ASRa-F344	Age	2	38.66***	0.29	frequency, WN	3	31.70***	0.35
ASRa-LE	Age	3	38.82***	0.44	frequency, WN	3	17.64***	0.17
PPI-Y	Strain	1	41.56***	0.65	frequency	2	1.87 ns	0.03
PPI-M	Strain	1	10.65*	0.35	frequency	2	0.61 ns	0.03
PPI-A	Strain	2	3.13 ns	0.24	frequency	2	0.14 ns	0.003
PPI-F344	Age	2	5.18*	0.30	frequency	2	3.01 ns	0.06
PPI-LE	Age	3	38.27***	0.74	frequency	2	3.63 *	0.04

increased significantly only in the oldest LE rats (29–34 months of age). In contrast to the LE rats, the age-related elevation of hearing thresholds in F344 rats began much earlier and was more pronounced: the hearing thresholds in middle-aged F344 rats (12–14 months of age) were comparable with those of the oldest LE rats (29–34 months of age). A similar relatively early age-related decline in hearing sensitivity in F344 rats has been reported by several authors (Backoff and Caspary, 1994; Popelář et al., 2003; 2006).

To determine whether the age-related changes in the ASR appear as a consequence of the age-related hearing loss, the dependence of the ASR amplitude on the age-related hearing loss was examined. Our findings indicate in several ways that the ASR amplitude is not directly related to hearing sensitivity. First, young adult rats of both strains had similar hearing sensitivity below 16 kHz, yet they had significantly different ASR amplitudes. Vice versa, at 24–26 months of age, the two strains were characterized by highly significant differences in hearing thresholds while having similar ASR amplitudes. Finally, no statistically significant relationship between the ASR amplitude and the ABR threshold was found in any age group in either strain. It can be concluded that the age-related hearing loss is not the determining factor of ASR attenuation with age. Moreover, an age-related or post-traumatic hearing loss may be associated with auditory recruitment or hyperacusis (Carlson and Willott, 1996; Ison and Allen, 2003; Ison et al., 2007; Popelář et al., 2008; Rybalko et al., 2011). The absence of a direct dependence of ASR amplitude on the hearing threshold in mice of the same age with different onset hearing loss was reported by McCaughran et al. (1999) and by Ouagazzal et al. (2006).

Several age-related changes may contribute to the observed decrease in the ASR amplitude with aging. The decline in the function of the inner ear is combined with the decrease in the function of the central part of the auditory system and with the impairment of the motor function. Impairment of the motor functions associated with aging is well known in rats. During aging, there is a gradual decline in muscle tone and locomotor activity (Altun et al., 2007; Campbell and Gaddy, 1987; Gage et al., 1984), which may also be different in different strains. Several facts demonstrate declining function of the central auditory system with aging, which may be strain dependent. For example, more marked decrease of ABR amplitudes was found in old F344 rats compared to age-matched LE rats (Popelář et al., 2006). In addition to more pronounced decrease in the ABR amplitudes, faster age-related change of inter-peak latencies (reflecting the central conduction time) was observed in old F344 rats in comparison with old LE rats (Popelář et al., 2006). In F344 rats, prolongation of inter-peak latencies was possible to observe already at 20 months of age, whereas in LE rats the inter-peak latencies started to be prolonged not earlier than at 30 months of age.

The ASR reactivity may be also influenced by cognitive, memory and selective attention deficits, which have been found during aging in behavioral studies on rats of different strains (Ando and Ohashi, 1991; Gage et al., 1984; Roux et al., 1994). Apparently, the age-related decrease of ASR amplitudes is closely related to neurochemical, neuroanatomical and metabolic changes observed in rats during aging (Hauger et al., 1983; Sapolsky et al., 1983; Yau, et al., 1995). It should be noted that in F344 rats, neurochemical changes in the central auditory system are observed already during the first year of life (Milbrandt and Caspary, 1995; Milbrandt et al., 1994).

An additional factor that could also influence the strain- and age-related differences in ASR amplitudes is differences in body weight (Błaszczyk and Tajchert, 1996). We observed that the mean body weight for F344 rats (for each age group) was about 50 g less in comparison with LE rats of the same age group, which might have an influence on the smaller ASR amplitudes in F344 rats. However, the finding that the age-related changes in ASR amplitude and body weight move in opposite directions (middle-aged rats have a greater body weight compared with young-adult rats while they have a lower ASR amplitude) indicates that body weight is not the determining factor underlying the changes in ASR amplitude with aging.

Differences between the F344 and LE strains are also apparent when evaluating the PPI of ASR. To eliminate possible differences in the audibility of prepulse stimuli in different rats that had different hearing thresholds, prepulse tones of 75 dB SPL (about 5 dB less than the ASR threshold) were used in our study. The phenomenon of prepulse inhibition is considered as a form of sensorimotor gating, which reflects a basic inhibitory process that regulates sensory input to the brain (Geyer and Braff, 1987; Swerdlow et al., 2004). In previous studies it was shown that the expression of PPI might be different in different rodent strains (Ouagazzal et al., 2006; Paylor and Crawley, 1997; Swerdlow et al., 2004; Varty and Higgins, 1994). The authors assumed that the strain differences in PPI, like the strain differences in the ASR, are determined by the genetic background (Geyer et al., 2002; Ouagazzal et al., 2006). Our results show that PPI in F344 rats is less efficient than in LE rats. In contrast to our observations, however, Swerdlow et al. (2004) reported that the efficiency of the PPI of ASR is higher in F344 rats than in LE rats. Such a discrepancy between results is difficult to explain solely by differences in the experimental procedures (e.g., the spectral characteristics of the prepulse and startling stimuli, prepulse intensity, session design, etc.).

In both rat strains, a reduction of PPI efficiency with aging was present. However, in contrast to the age-related changes of the ASR, the age-related changes of the PPI of ASR exhibited a similar progression in both strains, i.e., the decrease of inhibitory efficacy was significant only in aged rats. This is in agreement with our previous findings that in both F344 and LE rats the levels of the key enzyme in the synthesis of GABA, GAD65 and 67, decrease in the auditory system with aging (Burianová et al., 2009). The available published data concerning age-related changes in PPI are contradictory. The common assumption that normal aging must be accompanied by a global decline in inhibitory function (Woodruff-Pak, 1997) has not been satisfactorily confirmed. Several authors have reported the absence of age-related changes in PPI in humans (Harbin and Berg, 1983; Ludewig et al., 2003). At the same time, according to Ellwanger et al. (2003), PPI in humans demonstrates an inverted U-shaped function with age (the greatest PPI at intermediate ages). Similarly to our results, Varty et al. (1998) reported that auditory PPI was reduced in aged F344 rats (22 months of age) compared to mature and young rats. However, an analogous study in CBA/J mice failed to find a significant effect of age on PPI (Ison et al., 1997).

5. Conclusions

Our data show that Fischer 344 rats, as a model of fast aging, exhibit a different course of age-related changes in the ASR compared with Long Evans rats as a model of normal aging. Besides differences in the age-related changes, the absolute values of most of the parameters were also different between the two strains. The deterioration of the hearing threshold and ASR reactivity occurs already in middle-aged F344 rats, whereas in the LE strain, middle-aged animals show no differences from young-adult animals. With respect to the prepulse inhibition of ASR, both strains exhibit similar trends of age-related changes despite the different efficiencies of the PPI. It is noteworthy that the age-related ASR changes in F344 rats depend on the frequency of the startling stimulus. In the case of pure tones, the decrease in ASR amplitudes is already significant in middle-aged animals, whereas for white noise, the decrease progresses more slowly and is significant only in aged animals. The results indicate that the evaluation of the ASR and its suppression by an acoustic prepulse may serve as an objective measure of age-related changes in auditory behavior; in particular, the ASR to tonal stimuli is a suitable indicator of central presbycusis.

Acknowledgments

This study was supported by the Grant Agency of the Czech Republic P303/11/J005, P304/12/G069 and P304/12/1342.

References

Altun, M., Bergman, E., Edström, E., Johnson, H., Ulfhake, B., 2007. Behavioral impairments of the aging rat. Physiol. Behav. 92, 911–923.
Ando, S., Ohashi, Y., 1991. Longitudinal study on age-related changes in working and reference memory in the rat. Neurosci. Lett. 128, 17–20.
Backoff, P.M., Caspary, D.M., 1994. Age-related changes in auditory brainstem responses in Fischer 344 rats: effects of rate and intensity. Hear. Res. 73, 163–172.
Błaszczyk, J.W., Tajchert, K., 1996. Sex and strain differences of acoustic startle reaction development in adolescent albino Wistar and hooded rats. Acta Neurobiol. Exp. (Wars) 56, 919–925.
Błaszczyk, J.W., Tajchert, K., 1997. Effect of acoustic stimulus characteristics on the startle response in hooded rats. Acta Neurobiol. Exp. (Wars) 57, 315–321.
Buckiová, D., Popelář, J., Syka, J., 2006. Collagen changes in the cochlea of aged Fischer 344 rats. Exp. Gerontol. 41, 296–302.
Buckiová, D., Popelář, J., Syka, J., 2007. Aging cochleas in the F344 rat: morphological and functional changes. Exp. Gerontol. 42, 629–638.
Burianová, J., Ouda, L., Profant, O., Syka, J., 2009. Age-related changes in GAD levels in the central auditory system of the rat. Exp. Gerontol. 44, 161–169.
Campbell, B.A., Gaddy, J.R., 1987. Rate of aging and dietary restriction: sensory and motor function in the Fischer 344 rat. J. Gerontol. 42, 154–159.
Carlson, S., Willott, J., 1996. The behavioral salience of tones as indicated by prepulse. inhibition of the startle response: relationship to hearing loss and central neural plasticity in C57BL/6J mice. Hear. Res. 99, 168–175.
Davis, M., Gendelman, D., Tischler, M., Gendelman, P., 1982. A primary acoustic startle circuit: lesion and stimulation studies. J. Neurosci. 6, 791–805.
Ellwanger, J., Geyer, M.A., Braff, D.L., 2003. The relationship of age to prepulse inhibition and habituation of the acoustic startle response. Biol. Psychol. 62, 175–195.
Frisina, D.R., Frisina, R.D., 1997. Speech recognition in noise and presbycusis: relations to possible neural mechanisms. Hear. Res. 106, 95–104.
Gage, F.H., Kelly, P.A.T., Bjorklund, A., 1984. Regional changes in brain glucose metabolism reflect cognitive impairments in aged rats. J. Neurosci. 4, 2856–2865.
Gates, G.A., Mills, J.H., 2005. Presbycusis. Lancet 366, 1111–1120.
Geyer, M.A., Braff, D.L., 1987. Startle habituation and sensorimotor gating in schizophrenia and related animal models. Schizophr. Bull. 13, 643–668.
Geyer, M.A., Mcllwain, K.L., Paylor, R., 2002. Mouse genetic models for prepulse inhibition: an early review. Mol. Psychiatry 7, 1039–1053.
Glowa, J.R., Hansen, C.T., 1994. Differences in response to an acoustic startle stimulus among forty-six rat strains. Behav. Genet. 24, 79–84.
Gordon-Salant, S., 2005. Hearing loss and aging: new research findings and clinical implications. J. Rehabil. Res. 42, 9–24.
Gordon-Salant, S., Fitzgibbons, P.J., Friedman, S.A., 2007. Recognition of time-compressed and natural speech with selective temporal enhancements by young and elderly listeners. J. Speech Lang. Hear. Res. 50, 1181–1193.
Harbin, T.J., Berg, W.K., 1983. The effects of age and prestimulus duration upon reflex inhibition. Psychophysiology 20, 603–610.
Harding, G.W., Bohne, B.A., Vos, J.D., 2005. The effect of an age-related hearing loss gene (Ahl) on noise-induced hearing loss and cochlear damage from low-frequency noise. Hear. Res. 204, 90–100.
Hauger, R.L., Thrivikraman, K.V., Plotsky, P.M., 1983. Age-related alterations of hypothalamic–pituitary–adrenal axis function in male Fischer 344 rats. Endocrinology 134, 1528–1536.
Hoffman, H.J., 1979. Survival distributions for selected laboratory rat strains and stocks. In: Gibson, D.C., Adelman, R.C., Finch, C. (Eds.), Development of the Rodent as a Model System for Aging, Book II, pp. 19–34.
Ison, J.R., Allen, P.D., 2003. Low-frequency tone pips elicit exaggerated startle reflexes in C57BL/6J mice with hearing loss. J. Assoc. Res. Otolaryngol. 4, 495–504.
Ison, J.R., Hammond, G.R., 1971. Modification of the startle reflex in the rat by changes in the auditory and visual environments. J. Comp. Physiol. Psychol. 75, 435–452.
Ison, J.R., Bowen, G.P., Pak, J., Gutierrez, E., 1997. Changes in the strength of prepulse inhibition with variation in the startle baseline associated with individual differences and with old age in rats and mice. Psychobiology 25, 266–274.
Ison, J.R., Allen, P.D., O'Neill, W.E., 2007. Age-related hearing loss in C57BL/6J mice has both frequency-specific and non-frequency-specific components that produce a hyperacusis-like exaggeration of the acoustic startle reflex. J. Assoc. Res. Otolaryngol. 8, 539–550.
McCaughran Jr., J., Bell, J., Hitzemann, R., 1999. On the relationships of high-frequency hearing loss and cochlear pathology to the acoustic startle response (ASR) and prepulse inhibition of the ASR in the BXD recombinant inbred series. Behav. Genet. 29, 21–30.
Koch, M., 1999. The neurobiology of startle. Prog. Neurobiol. 59, 107–128.
Ludewig, K., Ludewig, S., Seitz, A., Obrist, M., Geyer, M.A., Vollenweider, F.X., 2003. The acoustic startle reflex and its modulation: effects of age and gender in humans. Biol. Psychol. 63, 311–323.
Mazelová, J., Popelář, J., Syka, J., 2003. Auditory function in presbycusis: peripheral vs. central changes. Exp. Gerontol. 38, 87–94.
McFadden, S.L., Zulas, A.L., Morgan, R.E., 2010. Age-dependent effects of modafinil on acoustic startle and prepulse inhibition in rats. Behav. Brain Res. 208, 118–123.
Milbrandt, J.C., Caspary, D.M., 1995. Age-related reduction of [3H]strychnine binding sites in the cochlear nucleus of the Fischer 344 rat. Neuroscience 67, 713–719.
Milbrandt, J.C., Albin, R.L., Caspary, D.M., 1994. Age-related decrease in GABAB receptor binding in the Fischer 344 rat inferior colliculus. Neurobiol. Aging 15, 699–703.
Ouagazzal, A.M., Reiss, D., Romand, R., 2006. Effects of age-related hearing loss on startle reflex and prepulse inhibition in mice on pure and mixed C57BL and 129 genetic background. Behav. Brain Res. 172, 307–315.
Ouda, L., Druga, R., Syka, J., 2008. Changes in parvalbumin immunoreactivity with aging in the central auditory system of the rat. Exp. Gerontol. 43, 782–789.
Parham, K., 1997. Distortion product otoacoustic emissions in the C57BL/6J mouse model of age-related hearing loss. Hear. Res. 12, 216–234.
Parham, K., Willott, J.F., 1988. Acoustic startle response in young and aging C57BL/6J and CBA/J mice. Behav. Neurosci. 102, 881–886.
Paylor, R., Crawley, J.N., 1997. Inbred strain differences in prepulse inhibition of the mouse startle response. Psychopharmacology 132, 169–180.
Pilz, P.K., Schnitzler, H.U., Menne, D., 1987. Acoustic startle threshold of the albino rat (*Rattus norvegicus*). J. Comp. Psychol. 101, 67–72.
Popelář, J., Groh, D., Mazelová, J., Syka, J., 2003. Cochlear function in young and adult Fischer 344 rats. Hear. Res. 186, 75–84.
Popelář, J., Groh, D., Pelánová, J., Canlon, B., Syka, J., 2006. Age-related changes in cochlear and brainstem auditory functions in Fischer 344 rats. Neurobiol. Aging 27, 490–500.
Popelář, J., Grecová, J., Rybalko, N., Syka, J., 2008. Comparison of noise-induced changes of auditory brainstem and middle latency response amplitudes in rats. Hear. Res. 245, 82–91.
Roux, S., Hubert, I., Lenegre, A., Milinkevitch, D., Porsolt, R.D., 1994. Effect of piracetam on indices of cognitive function in a delay alternation task in young and aged rats. Pharmacol. Biochem. Behav. 49, 683–688.
Rybalko, N., Bureš, Z., Burianová, J., Popelář, J., Grécová, J., Syka, J., 2011. Noise exposure during early development influences the acoustic startle reflex in adult rats. Physiol. Behav. 102, 453–458.
Sapolsky, R.M., Krey, L.C., McEwen, B.S., 1983. Corticosterone receptors decline in a site-specific manner in the aged rat. Brain Res. 289, 235–240.
Sass, B., Rabstein, L.S., Madison, R., Nims, R.M., Peters, R.L., Kelloff, G.J., 1975. Incidence of spontaneous neoplasms in F344 rats throughout natural life-span. J. Natl. Cancer Inst. 54, 1449–1456.
Schuknecht, H.F., Gacek, M.R., 1993. Cochlear pathology in presbycusis. Ann. Otol. Rhinol. Laryngol. 102, 1–16.
Spongr, V.P., Flood, D.G., Frisina, R.D., Salvi, R.J., 1997. Quantitative measures of hair cell loss in CBA and C57BL/6 mice throughout their life spans. J. Acoust. Soc. Am. 101, 3546–3553.
Šuta, D., Rybalko, N., Pelánová, J., Popelář, J., Syka, J., 2011. Age-related changes in auditory temporal processing in the rat. Exp. Gerontol. 46, 739–746.
Swerdlow, N.R., Geyer, M.A., Braff, D.L., 2001. Neural circuit regulation of prepulse inhibition of startle in the rat: current knowledge and future challenges. Psychopharmacology 156, 194–215.
Swerdlow, N.R., Shoemaker, J.M., Crain, S., Goins, J., Onozuka, K., Auerbach, P.P., 2004. Sensitivity to drug effects on prepulse inhibition in inbred and outbred rat strains. Pharmacol. Biochem. Behav. 77, 291–302.
Syka, J., 2002. Plastic changes in the central auditory system after hearing loss, restoration of function, and during learning. Physiol. Rev. 82, 601–636.
Syka, J., 2010. The Fischer 344 rat as a model of presbycusis. Hear. Res. 264, 70–78.
Van den Buuse, M., Simpson, E.R., Jones, M.E., 2003. Prepulse inhibition of acoustic startle in aromatase knock-out mice: effects of age and gender. Genes Brain Behav. 2, 93–102.
Varty, G.B., Higgins, G.A., 1994. Differences between three rat strains insensitivity to prepulse inhibition of an acoustic startle response: influence of apomorphine and phencyclidine pretreatment. J. Psychopharmacol. 8, 148–156.
Varty, G.B., Hauger, R.L., Geyer, M.A., 1998. Aging effects on the startle response and startle plasticity in Fischer F344 rats. Neurobiol. Aging 19, 243–251.
Webb, A.A., Gowribai, K., Muir, G.D., 2003. Fischer (F-344) rats have different morphology, sensorimotor and locomotor abilities compared to Lewis, Long-Evans, Sprague–Dawley and Wistar rats. Behav. Brain Res. 144, 143–156.
Willott, J.F., 1991. Aging and the Auditory System. Singular, San Diego.
Woodruff-Pak, D.S., 1997. The Neuropsychology of Aging. Blackwell, Oxford.
Yau, J.L.W., Olsson, T., Morris, R.G.M., Meaney, M.J., Seckl, J.R., 1995. Glucocorticoids, hippocampal corticosteroid gene expression and antidepressant treatment: relationship with spatial learning in young and aged rats. Neuroscience 66, 571–581.
Young, J.S., Fechter, L.D., 1983. Reflex inhibition procedures for animal audiometry: a technique for assessing ototoxicity. J. Acoust. Soc. Am. 73, 1686–1693.

Physiology & Behavior 102 (2011) 453–458

Contents lists available at ScienceDirect

Physiology & Behavior

journal homepage: www.elsevier.com/locate/phb

Noise exposure during early development influences the acoustic startle reflex in adult rats

Natalia Rybalko [a,*], Zbyněk Bureš [a,b], Jana Burianová [a], Jiří Popelář [a], Jolana Grécová [a], Josef Syka [a]

[a] Institute of Experimental Medicine, Academy of Sciences of the Czech Republic, Prague, Czech Republic
[b] College of Polytechnics, Jihlava, Czech Republic

ARTICLE INFO

Article history:
Received 16 March 2010
Received in revised form 24 September 2010
Accepted 8 December 2010

Keywords:
Auditory system
Startle reflex
Prepulse inhibition
Behavioral
Noise exposure
Critical period
Development

ABSTRACT

Noise exposure during the critical period of postnatal development in rats results in anomalous processing of acoustic stimuli in the adult auditory system. In the present study, the behavioral consequences of an acute acoustic trauma in the critical period are assessed in adult rats using the acoustic startle reflex (ASR) and prepulse inhibition (PPI) of ASR. Rat pups (strain Long–Evans) were exposed to broad-band noise of 125 dB SPL for 8 min on postnatal day 14; at the age of 3–5 months, ASR and PPI of ASR were examined and compared with those obtained in age-matched controls. In addition, hearing thresholds were measured in all animals by means of auditory brainstem responses. The results show that although the hearing thresholds in both groups of animals were not different, a reduced strength of the startle reflex was observed in exposed rats compared with controls. The efficacy of PPI in exposed and control rats was also markedly different. In contrast to control rats, in which an increase in prepulse intensity was accompanied by a consistent increase in the efficacy of PPI, the PPI function in the exposed animals was characterized by a steep increase in inhibitory efficacy at low prepulse intensities of 20–30 dB SPL. A further increase of prepulse intensity up to 60–70 dB SPL caused only a small and insignificant change of PPI. Our findings demonstrate that brief noise exposure in rat pups results in altered behavioral responses to sounds in adulthood, indicating anomalies in intensity coding and loudness perception.

© 2010 Elsevier Inc. All rights reserved.

1. Introduction

The effect of early experience on the development of brain sensory functions is well known [1–3]. Numerous studies have demonstrated that alterations of cochlear output resulting from a transient or permanent hearing loss during a sensitive developmental period affect the development of the central auditory system [4–6]. Consequences of neonatal hearing loss leading to auditory deprivation during early ontogenesis depend on the maturity of auditory system at the time of traumatic exposure [7–9]. To study the effects of early deprivation on the formation of the auditory system, the rat often serves as a suitable animal model, as rat pups are born with an immature auditory system. The first reflex responses to acoustic stimuli in rats appear on postnatal day 10 (P10); later on, the auditory brainstem response (ABR) thresholds improve rapidly, approaching adult values between days 24 and 36. The maturation of the rat hearing function then proceeds up to the 4th–6th postnatal week [10–12]. Anomalous processing of auditory information in the higher parts of the auditory system (alterations in the frequency tuning and tonotopy) in rats exposed to sound in early ontogeny has been demonstrated in a number of electrophysiological studies [6,13–18]. In an immunohistochemical study of Pierson and Snyder-Keller [4], it was demonstrated that a brief acute acoustic trauma (125 dB SPL noise for 8 min) in rat pups on the 14th postnatal day leads to changes in the tonotopic pattern of pure tone responses in the inferior colliculus (IC) in adult rats. Diffuse non-structured patterns of Fos immunoreactivity were observed within the ventral portion of the IC (with normally structured pattern responses within the dorsal area), indicating the immature state of the high frequency tonotopic projections in the IC. In our previous electrophysiological experiments, we used the model of Pierson and Snyder-Keller (1994) and showed that an 8 minute exposure to 125 dB SPL on P14 in rats results in permanent alterations of frequency and intensity representation in the high-frequency IC neurons [17,18]. On the basis of these findings, we investigated whether the reported alterations of neuronal responsiveness are also accompanied by abnormal behavioral responses to sound. The acoustic startle reflex (ASR) was chosen as an indicator of the behavioral responsiveness to sound stimuli. The startle reflex – a transient motor response to an intense unexpected sensory stimulus – is a primitive behavior observed in all mammals. The structural basis of the startle reflex is represented by a short neural circuit comprising the posteroventral cochlear nucleus, one or more nuclei of the lateral lemniscus, the caudal pontine reticular

* Corresponding author. Institute of Experimental Medicine, Academy of Sciences of the Czech Republic, Videňská 1083, 142 20 Prague 4, Czech Republic. Tel.: +420 24106 2689; fax: +420 24106 2787.
E-mail address: rybalko@biomed.cas.cz (N. Rybalko).

0031-9384/$ – see front matter © 2010 Elsevier Inc. All rights reserved.
doi:10.1016/j.physbeh.2010.12.010

nucleus, spinal interneurons and spinal motor neurons [19,20]. In spite of its relative simplicity, the startle reflex shows several forms of behavioral plasticity including habituation, sensitization, and prepulse inhibition, and reveals remarkable sensitivity to a variety of experimental manipulations [20–23]. Investigations of the auditory function frequently employ the ASR and prepulse inhibition (PPI) of the ASR, i.e. the inhibition of the ASR induced by the presentation of an acoustic stimulus shortly preceding the startling sound. The PPI phenomenon is considered to be an example of sensori-motor gating, which reflects inhibitory processes that regulate sensory input to the brain. Results of animal studies have suggested that the effect of auditory prepulse stimulus on the startle circuit involves primarily the cochlear nucleus, the inferior and superior colliculus and the pedunculopontine tegmental nucleus [20,24]. PPI can be modulated by auditory cortex, thalamus, amygdala, hippocampus, striatum, ventral pallidum, and globus pallidum [24]. It was shown that evaluating the PPI of ASR is a simple yet efficient method for estimating supra-threshold auditory sensitivity [22,25,26].

With the aim of determining the behavioral consequences of acoustical trauma on the developing auditory system, the ASR and PPI of ASR were investigated in adult rats that were exposed to broad-band noise of 125 dB SPL for 8 min on P14. The obtained results were compared to those of age-matched controls. Hearing sensitivity in the exposed and control adult rats was assessed by means of auditory brainstem responses.

2. Materials and methods

2.1. Subjects

Fourteen female pigmented rats of the Long Evans strain with no primary pathology were used as experimental subjects. The animals were divided into two groups: 7 rat pups were briefly exposed to a broad-band noise of 125 dB SPL for 8 min on P14, the other 7 rats, used as controls, were manipulated similarly as the first group but without the noise exposure. All animals were housed under standard laboratory conditions in a constant environment and a 12/12 h normal light/dark cycle; food and water were available *ad libidum*. The rats were tested at 3–5 months of age in the daytime. The care and use of animals were approved by the Ethics Committee of the Institute of Experimental Medicine and followed the guidelines of the Declaration of Helsinki.

2.2. Noise exposure of rat pups

Awake rat pups at P14 were exposed individually to broad-band noise at 125 dB SPL for 8 min in a specially constructed anechoic box with inner dimensions 24×24×34 cm, supplied with a loudspeaker (B&C Speakers DE700) and coupled to a horn. The broad-band noise was generated with a RFT 03 004 white noise generator and amplified with a custom-made power amplifier. The sound field within the cage was measured with a B&K 4939 microphone, a ZC0020 preamplifier and a B&K 2231 Sound Level Meter. Measurements of sound intensity obtained at five points within the cage were found to vary by less than 1.5 dB. The frequency spectrum measured in the center of the exposure box is shown in Fig. 1. During the exposure to noise, the animal was placed in a round wire mesh cage (diameter 17 cm, height 10 cm, situated in the center of the exposure box) to prevent the animal from occluding the ear canal.

2.3. Apparatus and procedures

The ASR and PPI of ASR were measured in seven female rats (3–5 months, 250–350 g) exposed to broad-band noise on P14, and in seven age-matched control rats. Behavioral tests were performed in a sound attenuated chamber (Coulbourn Habitest, model E10-21) located in a soundproof room. During the testing procedure, the rat was confined to a small wire mesh cage (160×85×90 mm) on a motion-sensitive platform. The animal's reflex movements were detected and transduced by a piezoelectric accelerometer. The amplified voltage signal was acquired and processed using a TDT system III with Real-Time Processor RP 2 (Tucker Davis Technologies, Florida, USA) and custom-made software in a Matlab environment. The startle responses were evaluated in a 100 ms window beginning at the onset of the startle stimulus. The magnitude of ASR was given by the maximal peak-to-peak amplitude of transient voltage occurring in the response window. Acoustic startle stimuli (tone pips or noise bursts) and prepulse stimuli (tone pips) were generated by the TDT system and presented via loudspeaker (SEAS, 29AF/W) placed inside the chamber. Stimulus presentation and data acquisition were controlled by a custom-made application in a Matlab environment. Calibration of the apparatus was performed for frequencies between 1 kHz and 32 kHz by a 1/4 in. Brüel & Kjaer 4939 microphone connected to a Brüel & Kjaer ZC 0020 preamplifier and a B&K 2231 sound level meter. The calibrating microphone was positioned in the location of the animal's head in the test cage.

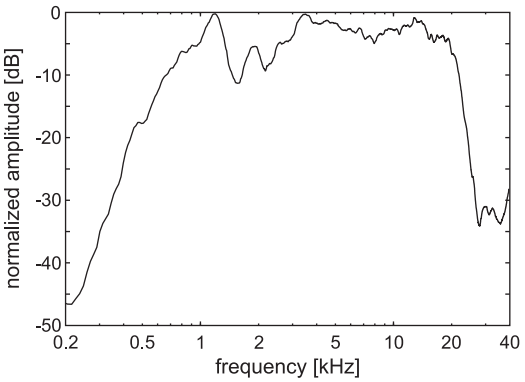

Fig. 1. Spectrum of the noise used for noise exposure.

2.3.1. Measurement of acoustic startle reflex

The ASR to 2, 4, 8, and 16 kHz tone pips and to 1.5–45 kHz broad-band noise (50 ms duration, 5 ms rise/fall times, varying levels) was recorded. Each test session contained 7 trial types: startle stimuli of different intensities (70, 80, 90, 100, 110, and 120 dB SPL) and a baseline trial without the startle stimulus, presented in a random order. Each trial type was presented ten times. The average inter-trial interval varied from 15 to 40 s. The mean ASR amplitude of each trial type was calculated as an average of all the ASR amplitudes for that given trial type with the highest and the lowest ASR amplitudes excluded. A trial was considered to have evoked a startle reaction if the mean ASR amplitude for that trial exceeded the average amplitude of the baseline trial (0.03 ± 0.008 V) by more than twice the standard deviation (i.e., it was more than 0.05 V). Thereafter, the ASR "threshold" was determined as the minimum startle intensity at which there was a startle reaction for at least 50% of the trials.

2.3.2. Measurement of prepulse inhibition of ASR

In the prepulse inhibition procedure, 10 different trial types were used: acoustic startle pulse alone (white noise at 110 dB SPL, 50 ms, 5 ms rise/fall times), 8 combinations of the startle pulse and prepulse tones (50 ms duration, 5 ms rise/fall time) at different intensities (10, 20, 30, 40, 50, 60, 70, and 80 dB SPL), and a baseline trial (without acoustic stimulus). The inter-stimulus interval between the prepulse and startle stimulus was set to 50 ms. Each of the ten trial types was presented ten times. The average inter-trial interval varied from 15 to

40 s. The PPI of ASR was measured for tonal prepulses at 2, 4, 8, and 16 kHz. The efficacy of the PPI of ASR was expressed as:

$$\text{PPI} = (\text{amplitude of ASR inhibited by prepulse tone}) \div (\text{amplitude of ASR alone}) \times 100\%.$$

2.4. Measurement of ABR hearing thresholds

In order to assess the hearing threshold in adult exposed and control rats, the auditory brainstem responses (ABR) to tonal stimuli (3 ms duration, 1 ms rise/fall times, frequency range 2–40 kHz) were recorded. The conditions of the stimulation and recording of the auditory brainstem responses were described in detail previously [27]. Briefly, the recording was performed in animals lightly sedated with an intramuscular injection of 0.03 mg/kg of medetomidin hydro-chloride (Domitor, Farmos). ABRs were recorded with subcutaneous needle electrodes placed at the vertex (active electrode) and inside neck muscles (reference electrode); the signal was processed with a TDT system III setup using BioSig software. The threshold at each frequency was determined as the minimal tone intensity that still evoked a visually noticeable potential peak in the expected time window of the recorded signal.

2.5. Statistical analysis

To determine whether the mean values of the ASR amplitude differed for different stimuli within a given experimental group and to test the differences between the mean values of ASR to a given stimulus and to compare the efficacy of the prepulse inhibition in the exposed and control groups, analysis of variance (ANOVA) with the post-hoc Newman–Keuls test was used. The difference of slopes of the PPI functions was estimated using a t-test or linear regression analysis.

3. Results

3.1. Hearing thresholds in adult exposed and control rats

Hearing thresholds in the range of 2–40 kHz in adult exposed and control rats were not significantly different (Fig. 1 in the Supplementary material).

3.2. Acoustic startle reflex

For both experimental groups, the mean values of ASR amplitudes in response to tone pips at 2, 4, 8 and 16 kHz and to white noise pulses at different stimulus intensities are shown in Fig. 2. The ASR thresholds in the exposed and control animals were similar: approximately 100 dB SPL for 2 kHz, 80–90 dB SPL for 4–16 kHz, and 70 dB SPL for white noise. The ASR amplitudes near the ASR threshold were also similar in both groups; in contrast, the magnitudes of the ASR responses to high stimulus levels (110–120 dB SPL) were markedly lower in the exposed animals (except for the 2 kHz tone, Fig. 2). In both groups, the ASR magnitude exhibited a decreasing trend with increasing stimulus frequency: the high frequency tones evoked considerably lower ASR amplitudes than the low frequency stimuli (Fig. 2). In the controls, a significant decrease of ASR amplitude started at 16 kHz, whereas in exposed rats the pronounced decrease appeared already at 8 kHz ($p<0.05$) (Fig. 3). It should be noted that the startle responses at 16 kHz were easily detected: the ASR amplitudes at the threshold level in response to stimuli of 16 kHz were approximately seven times higher than the average amplitude of the baseline trial. This value corresponds to more than a 15 dB signal-to-noise ratio.

3.3. Prepulse inhibition of the acoustic startle reflex

The efficacy of the prepulse inhibition of ASR was measured using 2, 4, 8, and 16 kHz tonal prepulses at various intensities. Fig. 4 shows

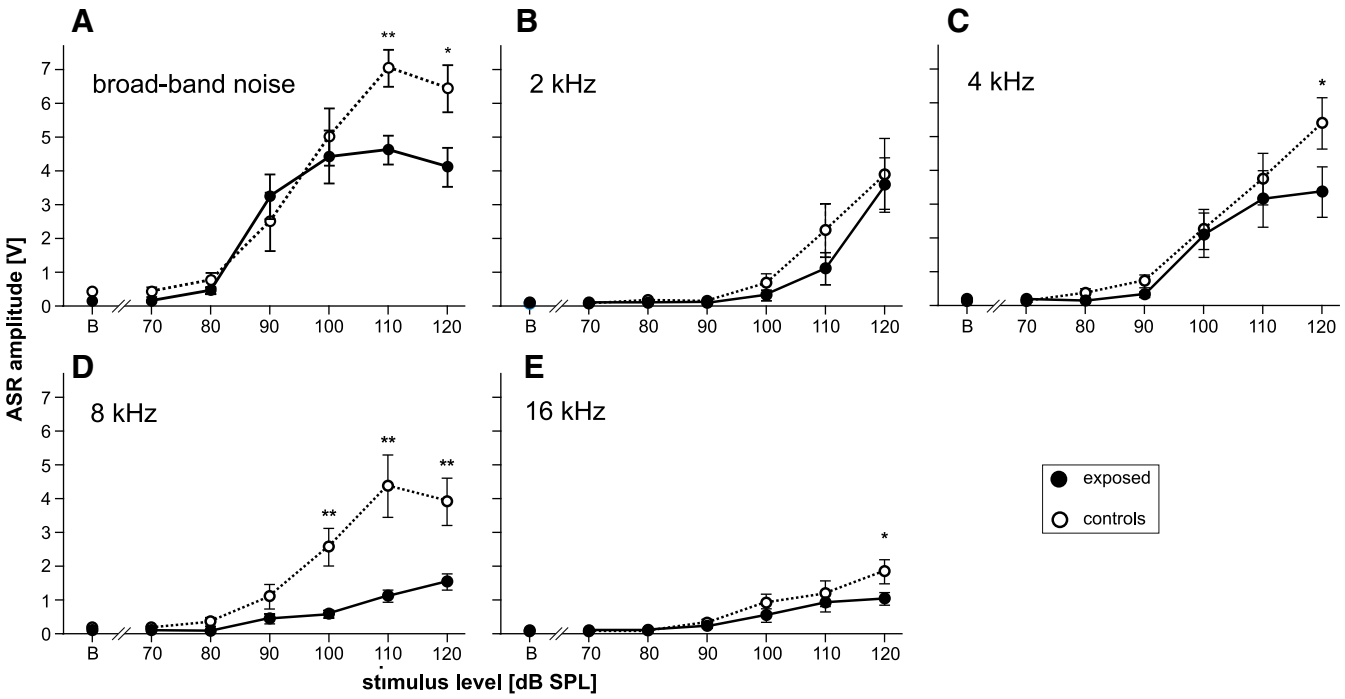

Fig. 2. Amplitude-intensity functions of the acoustic startle reflex in response to noise pulses (A) and tone pips of different frequencies (B, C, D, and E); "B"— baseline trial, error bars — SEM. *$p<0.05$; **$p<0.01$, ANOVA with the post-hoc Newman–Keuls test.

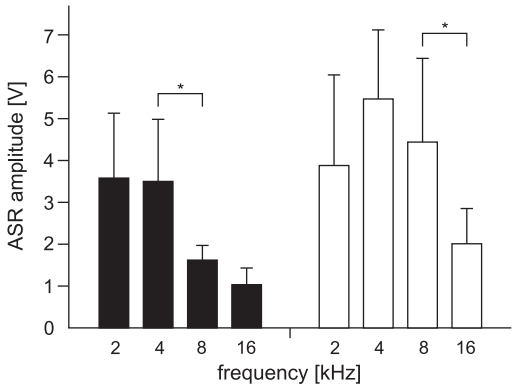

Fig. 3. Amplitude of the ASR (mean values expressed in V and SEM) in response to tones of 120 dB SPL for different frequencies in exposed (filled bars) and control (open bars) rats; *p<0.05; ANOVA with the post-hoc Newman–Keuls test.

the average relative ASR amplitudes in dependence on the prepulse intensity (PPI function); 100% corresponds to the amplitude of an uninhibited ASR (a value marked with "S" on the abscissa). It is apparent that the PPI functions for the exposed and control animals have different shapes. In the controls, the PPI functions were characterized by a steady linear decrease, which at 2 kHz was preceded by an initial plateau (lack of PPI of ASR at low intensities). In the exposed rats, the PPI functions were characterized by a steep decrease in ASR amplitude (i.e., a steep increase of the inhibitory efficacy) at lower prepulse intensities (20–30 dB SPL), followed by a phase of a very slow decrease of ASR amplitude (prepulse levels from 20–30 dB SPL to 60–70 dB SPL), where an increase of the prepulse intensity resulted in only a minor change of ASR magnitude. Significant differences between the average values of the ASR amplitudes for control and exposed animals were found at the following prepulse intensities: 20 and 30 dB at 2 kHz and 4 kHz, 20 dB at 8 kHz and 30 dB at 16 kHz.

With respect to the shapes of the exposed PPI functions, three phases of the PPI functions were identified for all tested frequencies. Phase 1 (a fast decrease of ASR amplitude) begins at the lowest prepulse level for which the ASR is not significantly different from 100% and ends at the so called transition point defined as follows: compared with the ASR at the transition point, the prepulse intensity that is 10 dB below the transition point evokes a significantly higher ASR and the prepulse intensity that is 10 dB above the transition point does not evoke a significantly lower ASR. Phase 2 (a slow decrease of ASR amplitude) begins at the transition point and spans a 40 dB range of prepulse intensities (the range in which, in most cases, a 10 dB prepulse intensity increment causes no significant increase in the PPI efficacy, see Table 1 of the Supplementary material). Phase 3 is the residual part of the PPI function where the values of PPI of ASR in the exposed rats were similar to those of controls. In the quantitative analysis, the first and second phases of the PPI function were compared, as these were the parts of the PPI function where the exposed animals differed most from the controls. For all prepulse frequencies, the slope of phase 1 of the PPI function in exposed rats was significantly larger than the slope of the corresponding part of the control PPI function (Fig. 5, upper panels). In contrast to this, the slope of phase 2 was significantly smaller in exposed animals than in controls (Fig. 5, bottom panels). Additional statistical analysis of the differences between PPI of ASR in exposed and control animals, based on ANOVA with the post-hoc Newman–Keuls test, is presented in Table 1 in the Supplementary material.

4. Discussion

The results of the present study demonstrate that a brief noise exposure of rat pups during the critical period of their development that produces only a temporary threshold shift [16] results in altered behavioral responses to sounds in adulthood, reflecting anomalies in the processing of sound intensity and loudness perception.

Our previous experiments revealed that noise exposure (8 min, 125 dB SPL) on P14, which was also used in this study, produced an immediate elevation of hearing thresholds. The ABR hearing thresholds in control rats at P14 ranged from 60 to 80 dB SPL, while the ABR hearing thresholds in noise exposed animals were elevated by a further 15–20 dB over the whole frequency range [17]. While the hearing thresholds in control animals approached adult values within the next several days, in the exposed rats, the hearing thresholds converged slowly to the adult values, fully recovering within the subsequent two or three weeks [17]. Reversible hearing loss in rat pups could be related to cochlear injuries induced by stereocilia lesions and/or glutamate excitotoxicity, which is manifested by the swelling of the afferent nerve terminals under the inner hair cells

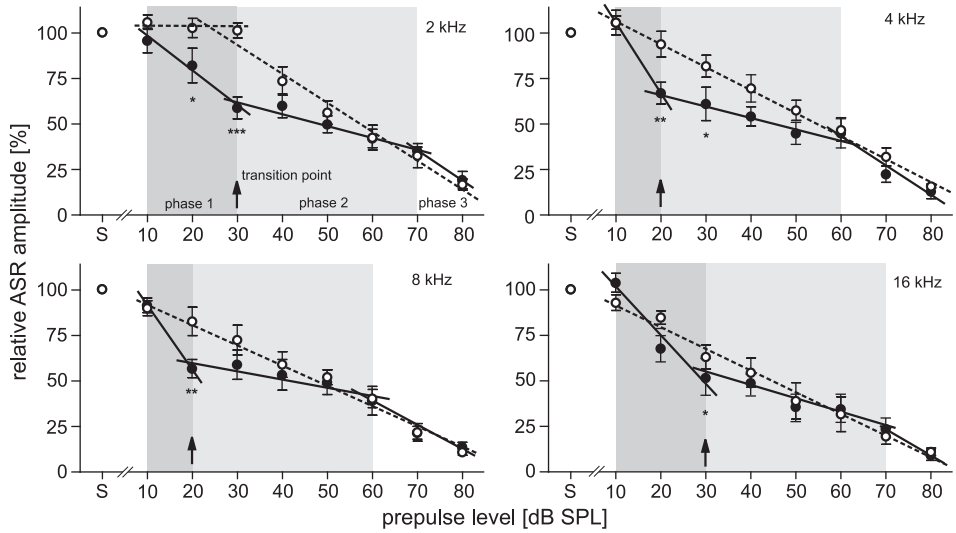

Fig. 4. Efficacy of the prepulse inhibition: dependence of the mean relative ASR amplitude on the prepulse intensity; 100% corresponds to the amplitude of an uninhibited ASR (startle response without a prepulse tone, marked as "S" on the abscissa). Dashed lines: linear regression curves for data obtained in control rats; solid lines: linear regression curves for data obtained in exposed rats. The first and second phases of the exposed PPI function are marked by gray shading. *p<0.05; **p<0.01; ***p<0.001, ANOVA with the post-hoc Newman–Keuls test.

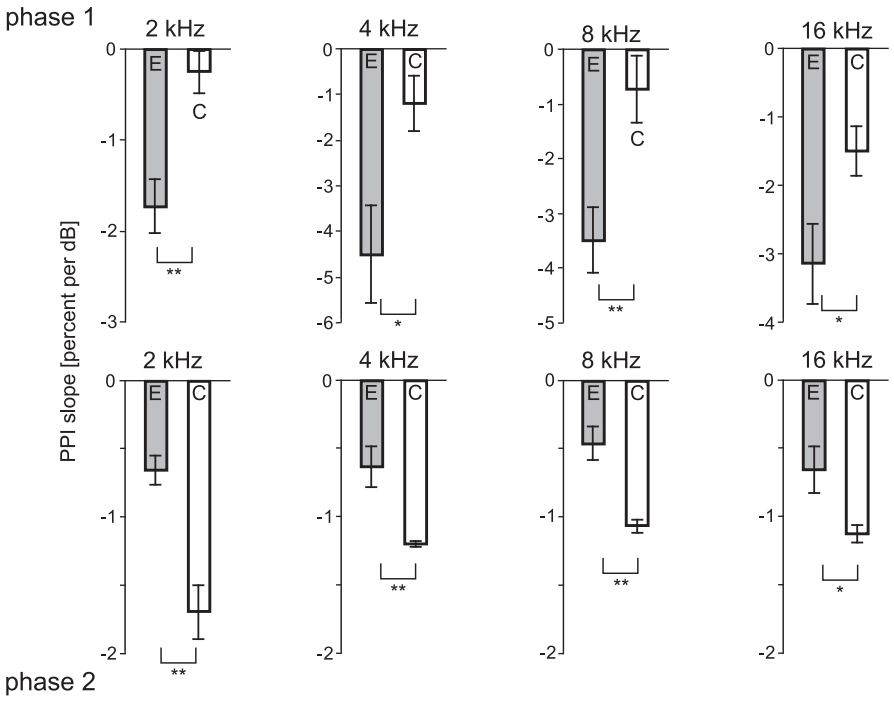

Fig. 5. Slope of the PPI function (filled bars: exposed rats; open bars: controls). Upper panel: phase 1; lower panel: phase 2. The difference between slopes was quantified using an unpaired t-test (phase 1), and linear regression analysis (phase 2); *$p<0.05$; **$p<0.01$.

(type 1 afferent dendrites) as a result of a brief noise exposure [28–31]. Such hearing loss may result in a reduction of the neural input (i.e., sensory deprivation) to the central auditory system, which leads to pronounced changes in the auditory function of these animals as demonstrated previously [8,16,32,33].

While both the ABR hearing thresholds and the ASR thresholds obtained in the present study were similar in adult animals exposed to noise on P14 and controls, a reduced strength of the startle reflex in response to intense stimuli in exposed rats was observed in the frequency range 4–16 kHz in comparison with controls. The decreased ASR amplitudes could be a behavioral consequence of the reduced neuronal excitability detected in our electrophysiological study in the IC of the rats exposed under the same conditions [18], where lower maximum response magnitudes, a narrower dynamic range of rate-intensity functions, and a decreased number of monotonically responding neurons were found.

Our findings are in accordance with several previous studies [25,34,35] demonstrating that high frequency tones evoke considerably lower ASR amplitudes than do low-frequency stimuli. The possible mechanism underlying this phenomenon can be related to the shape of the tuning curves of auditory neurons: neurons in the cochlear nucleus are not only sensitive to their characteristic frequencies, but they also respond to loud low frequency stimuli [36]. Large ASR amplitudes in response to low frequency stimuli may be attributed to the behavioral meaning of the acoustical stimuli [35]. Even though rats are more sensitive to high frequencies and communicate largely using ultrasonic vocalizations, they perceive signals over a broader frequency range and, moreover, low frequency audible vocalizations represent important components of their pain-related behavior [37]. Thus, a large ASR to low frequency sounds can help the rats to survive in their natural environment.

Although the ASR magnitude showed a decreasing trend with increasing stimulus frequency in both groups of animals, the most pronounced decrease of ASR amplitudes was observed at 16 kHz in control rats, while in exposed rats, the most pronounced decrease of ASR amplitude occurred already at 8 kHz. Thus, despite the absence of any change in the auditory thresholds and ASR thresholds, the ASR in rats exposed to noise was more affected at higher frequencies. Similar results were observed in C57BL mice with a genetically determined progressive age-related high-frequency hearing loss [38]. In this species, the decrease in the ASR amplitude occurred during the first year of life in the presence of normal hearing thresholds for frequencies 4–16 kHz. The authors explained this phenomenon as a reduced potency of the central neural excitation that drives the ASR.

Pierson and Snyder-Keller [4] demonstrated that in rats at P14, the regions of the auditory system devoted to the processing of high frequencies are less mature than the structures responsible for the processing of low frequency sounds. The acoustic trauma thus affects mostly those parts of the system where the development is in progress at the time of the trauma, while the regions that are already mature remain almost unaffected. Several findings have indicated that the immature auditory system generally exhibits reduced excitability compared with the adult state [39–41], hence the suppressed ASR amplitudes for high frequency sounds observed in the present study may be regarded as an indication of the noise-evoked underdevelopment of the high frequency regions of the auditory system, which retained the characteristics of the immature circuitry.

An analysis of the suppression of the ASR by preceding stimulation revealed a number of anomalies in PPI function in the noise-exposed animals. In comparison with control rats, in which an increase of prepulse intensity was accompanied by a consistent increase of PPI efficacy, PPI functions in exposed rats had a different shape with three distinguishable phases. A significantly stronger ASR inhibition observed at lower levels of prepulse intensities (20–30 dB SPL) in the exposed rats (phase 1) may reflect an abnormal sensitivity to sound (recruitment) at suprathreshold levels. A small and insignificant change of the inhibitory efficacy during a further increase of the prepulse intensity up to 60–70 dB SPL (phase 2) indicates a similar salience of these sounds and thus they are probably perceived as having similar loudness.

The increased PPI efficacy of low-intensity tones at middle frequencies was also described in rats after ototoxic treatment with neomycin [22] and in C57BL mice during young adulthood [25,38]. This phenomenon was considered by the authors [25] to be a

manifestation of the increased salience of certain sounds based on the hearing-loss-induced plasticity of the central auditory system [16,42,43].

The specifics of PPI in exposed rats observed in our study evidently reflect experience-dependent plasticity in the central auditory system caused by noise exposure in the early postnatal period and may be regarded as a behavioral consequence of anomalous sound level coding. Although the brain mechanisms underlying PPI are not completely understood, most authors agree that the effect of a prepulse on the startle circuit involves the inferior colliculus, superior colliculus and other central auditory structures including the auditory cortex [21,24,25]. In this respect, it may be assumed that the observed anomalies of PPI function primarily reflect changes in the central auditory system. Our previous electrophysiological study of the changes in intensity coding at the level of the IC in exposed rats with the same noise exposure paradigm [17] identified a number of analogies with the results of the present behavioral study. It was shown that while the thresholds of response of IC neurons were comparable in exposed and control animals, the maximum response magnitudes were lower in the exposed rats and the neuronal rate-intensity functions in exposed rats reached saturation at lower stimulus intensities, which corresponds to a narrower dynamic range and a steeper initial slope of the rate-intensity functions. Cumulative rate-intensity functions showed a fast change of firing rates for stimulus intensities within the first 30 dB above the threshold, while for higher sound levels, the flat or even non-monotonic shape of the cumulative functions indicated a worsened level-discrimination ability. According to these electrophysiological data and the results of the immunohistochemical study by Pierson and Snyder-Keller [4], we can conclude that the behavioral changes observed using ASR and PPI of ASR are associated with changes in acoustical signal processing at the IC level. We cannot exclude minor residual pathological changes in the cochlea and auditory nerve caused by noise exposure in the sensitive developmental period. However, normal DPOAEs, indicating the preservation of outer hair cell function (17), normal ABR thresholds and unchanged ABR amplitude-intensity functions (17), indicating no changes in the processing of acoustical stimuli at the brainstem level, suggest that the noise exposure of juvenile rats did not result in any evident damage of the peripheral auditory system in adult rats, but rather produced alterations in the central auditory system.

Acknowledgments

The study was supported by grants AV0Z50390512, GACR 309/07/1336, GACR 309/08/H079, and LC 554.

Appendix A. Supplementary data

Supplementary data to this article can be found online at doi:10.1016/j.physbeh.2010.12.010.

References

[1] Blakemore C, Cooper GF. Development of the brain depends on the visual environment. Nature 1970;228:477–8.
[2] Hubel DH, Wiesel TN. The period of susceptibility to the physiological effects of unilateral eye closure in kittens. J Physiol 1970;206:419–36.
[3] Moore DR. Postnatal development of the mammalian central auditory system and the neural consequences of auditory deprivation: a review. Acta Otolaryngol Suppl 1985;421:19–30.
[4] Pierson M, Snyder-Keller A. Development of frequency-selective domains in inferior colliculus of normal and neonatally noise-exposed rats. Brain Res 1994;636:55–67.
[5] Syka J. Plastic changes in the central auditory system after hearing loss, restoration of function, and during learning. Physiol Rev 2002;82:601–36.
[6] Chang EF, Merzenich MM. Environmental noise retards auditory cortical development. Science 2003;300:498–502.
[7] Lenoir M, Bock GR, Pujol R. Supra-normal susceptibility to acoustic trauma of the rat pup cochlea. J Physiol Paris 1979;75:521–4.
[8] Saunders JC, Chen Ch-S. Sensitive periods of susceptibility to auditory trauma in mammals. Environ Health Perspect 1982;44:63–6.
[9] Rybalko N, Syka J. Susceptibility to noise exposure during postnatal development in rats. Hear Res 2001;155:32–40.
[10] Iwasa H, Potsic WP. Maturational change of early, middle, and late components of the auditory evoked responses in rats. Otolaryngol Head Neck Surg 1982;90:95–102.
[11] Roth B, Bruns V. Postnatal development of the rat organ of Corti. II. Hair cell receptors and their supporting elements. Anat Embryol 1992;185:571–81.
[12] Geal-Dor M, Freeman S, Li G, Sohmer H. Development of hearing in neonatal rats: air and bone conducted ABR thresholds. Hear Res 1993;69:236–42.
[13] Poon PW, Chen XY, Hwang JC. Altered sensitivities of auditory neurons in the rat midbrain following early postnatal exposure to patterned sounds. Brain Res 1990;524:327–30.
[14] Zhang LI, Bao S, Merzenich MM. Disruption of primary auditory cortex by synchronous auditory inputs during a critical period. Proc Natl Acad Sci USA 2002;99:2309–14.
[15] Gao F, Zhang J, Sun X, Chen L. The effect of postnatal exposure to noise on sound level processing by auditory cortex neurons of rats in adulthood. Physiol Behav 2009;97:369–73.
[16] Salvi RJ, Wang J, Ding D. Auditory plasticity and hyperactivity following cochlear damage. Hear Res 2000;147:261–74.
[17] Grécová J, Bureš Z, Popelář J, Šuta D, Syka J. Brief exposure of juvenile rats to noise impairs the development of the response properties of inferior colliculus neurons. Eur J Neurosci 2009;29:1921–30.
[18] Bureš Z, Grécová J, Popelář J, Syka J. Brief noise exposure of juvenile rats impairs the processing of sound intensity in the inferior colliculus of adult animals. Eur J Neurosci 2010;32:155–64.
[19] Davis M. The mammalian startle response. In: Eaton RC, editor. Neural mechanisms of startle behavior. New York: Plenum Press; 1984. p. p287–351.
[20] Koch M. The neurobiology of startle. Prog Neurobiol 1999;59:107–28.
[21] Ison JR, Hammond GR. Modification of the startle reflex in the rat by changes in the auditory and visual environments. J Comp Physiol Psychol 1971;75:435–52.
[22] Young JS, Fechter LD. Reflex inhibition procedures for animal audiometry: a technique for assessing ototoxicity. J Acoust Soc Am 1983;73:1686–93.
[23] Fitch RH, Threlkeld SW, McClure MM, Peiffer AM. Use of a modified prepulse inhibition paradigm to assess complex auditory discrimination in rodents. Brain Res Bull 2008;76:1–7.
[24] Swerdlow NR, Geyer MA, Braff DL. Neural circuit regulation of prepulse inhibition of startle in the rat, current knowledge and future challenges. Psychopharmacology (Berl) 2001;156:194–215.
[25] Carlson S, Willott JF. The behavioral salience of tones as indicated by prepulse inhibition of the startle response: relationship to hearing loss and central neural plasticity in C57BL/6J mice. Hear Res 1996;99:168–75.
[26] Ison JR, Allen PD. Low-frequency tone pips elicit exaggerated startle reflexes in C57BL/6J mice with hearing loss. J Assoc Res Otolaryngol 2003;4:495–504.
[27] Popelář J, Grécová J, Rybalko N, Syka J. Comparison of noise-induced changes of auditory brainstem and middle latency response amplitudes in rats. Hear Res 2008;245:82–91.
[28] Robertson D. Functional significance of dendritic swelling after loud sounds in the guinea pig cochlea. Hear Res 1983;9:263–78.
[29] Canlon B, Miller J, Flock A, Borg E. Pure tone overstimulation changes the micromechanical properties of the inner hair cell stereocilia. Hear Res 1987;30:65–72.
[30] Puel JL, d'Aldin C, Ruel J, Pujol R. Noise-induced hearing loss: current physiological investigations. In: Prasher D, Luxon L, editors. Advances in noise research. Vol. 1: biological effects of noise. London: Whurr Publishers Ltd; 1998. p. 17–21.
[31] Pujol R, Puel JL. Excitotoxicity, synaptic repair, and functional recovery in the mammalian cochlea: a review of recent findings. Ann NY Acad Sci 1999;884:249–54.
[32] Henry KR. Pinna reflex thresholds and audiogenic seizures: developmental changes after acoustic priming. J Comp Physiol Psychol 1972;79:77–81.
[33] Chen CS. Acoustic trauma-induced developmental change in the acoustic startle response and audiogenic seizures in mice. Exp Neurol 1978;60:400–3.
[34] Pilz PK, Schnitzler HU, Menne D. Acoustic startle threshold of the albino rat (*Rattus norvegicus*). J Comp Psychol 1987;101:67–72.
[35] Błaszczyk JW, Tajchert K. Effect of acoustic stimulus characteristics on the startle response in hooded rats. Acta Neurobiol Exp (Wars) 1997;57:315–21.
[36] Evans EF. Cochlear nerve and cochlear nucleus. In: Keidel WD, Neff WD, editors. Handbook of sensory physiology. Berlin, Heidelberg, New York: Springer-Verlag; 1975. vol. V/2; p1–108.
[37] Jourdan D, Ardid D, Chapuy E, Eschalier A, Le Bars D. Audible and ultrasonic vocalization elicited by single electrical nociceptive stimuli to the tail in the rat. Pain 1995;63:237–49.
[38] Parham K, Willott JF. Acoustic startle response in young and aging C57BL/6J and CBA/J mice. Behav Neurosci 1988;102:881–6.
[39] Moore DR, Irvine DR. Development of binaural input, response patterns, and discharge rate in single units of the cat inferior colliculus. Exp Brain Res 1980;38:103–8.
[40] Mysliveček J. Development of the auditory evoked responses in the auditory cortex in mammals. In: Romand R, editor. Development of auditory and vestibular system. New York, London, Paris, Tokyo, Toronto: Academic Press; 1983. p. 167–207.
[41] Brugge JF, O'Connor TA. Postnatal functional development of the dorsal and posteroventral cochlear nuclei of the cat. J Acoust Soc Am 1984;75:1548–62.
[42] Kaas JH. Plasticity of sensory and motor maps in adult mammals: a review. Annu Rev Neurosci 1991;14:137–67.
[43] Popelář J, Erre JP, Aran JM, Cazals Y. Plastic changes in ipsi-contralateral differences of auditory cortex and inferior colliculus evoked potentials after injury to one ear in the adult guinea pig. Hear Res 1994;72:125–34.